NAT'L INST. OF STAND & TECH R.I.C.
A11104 489507

NIST
PUBLICATIONS

NISTIR 5550

Workshop Summary Report: Industrial Applications of Scanned Probe Microscopy

A Workshop co-sponsored by NIST, SEMATECH, ASTM, E42.14, and the American Vacuum Society

held at the
NIST, Gaithersburg, MD 20899

on
March 24-25, 1994

J. A. Dagata
National Institute of Standards
and Technology

A. C. Diebold
SEMATECH

C. K. Shih
University of Texas-Austin

R. J. Colton
Naval Research Laboratory

U.S. DEPARTMENT OF COMMERCE
Technology Administration
National Institute of Standards
and Technology
Manufacturing Engineering Laboratory
Gaithersburg, MD 20899

QC
100
.U56
1994
NO.5550

NIST

NISTIR 5550

Workshop Summary Report: Industrial Applications of Scanned Probe Microscopy

A Workshop co-sponsored by NIST, SEMATECH, ASTM, E42.14, and the American Vacuum Society

held at the NIST, Gaithersburg, MD 20899

on March 24-25, 1994

J. A. Dagata
National Institute of Standards
and Technology

A. C. Diebold
SEMATECH

C. K. Shih
University of Texas-Austin

R. J. Colton
Naval Research Laboratory

U.S. DEPARTMENT OF COMMERCE
Technology Administration
National Institute of Standards
and Technology
Manufacturing Engineering Laboratory
Gaithersburg, MD 20899

December 1994

U.S. DEPARTMENT OF COMMERCE
Ronald H. Brown, Secretary

TECHNOLOGY ADMINISTRATION
Mary L. Good, Under Secretary for Technology

NATIONAL INSTITUTE OF STANDARDS
AND TECHNOLOGY
Arati Prabhakar, Director

EXECUTIVE SUMMARY

An Industrial Applications of Scanned Probe Microscopy (SPM) workshop was held at NIST Gaithersburg on March 24-25 1994. The meeting, co-sponsored by NIST, SEMATECH, ASTM E42.14, and the American Vacuum Society, was attended by over one hundred SPM users, suppliers, researchers and program managers from industry, government, and academia. The enthusiastic response to the workshop announcement, especially from the industry users and SPM vendors who made up 60% of the participants, indicates a willingness on the part of the applied SPM community to work together on the critical developmental issues facing this emerging community. The workshop fostered a common understanding of the roles of each of the constituent groups in the evolution of applied SPM by focusing on three objectives: Determine development and standardization requirements within industry for scanning probe microscopy measurements; Develop a consensus and publish a National View and Timetable for SPM requirements; and, Restrict the workshop to Industrial Applications of Microroughness, Dimensional Metrology, and Electrical Characterization.

Relying on the needs expressed by the Semiconductor Industry Association in its 1992 and draft 1994 National Technology Roadmap for Semiconductors, workshop presentations reviewed the standard of performance for SPM-based measurements required by industry over the next decade and the status of SPM research in each of the three areas listed above. The presentations were followed by facilitated discussions on SPM developments needs in each area. This report summarizes the outcome of these discussions: the standardization and development needs required for acceptance of quantitative SPM-based measurements within industry.

A broadly shared view of the field which emerged from the discussions was that rather definite efforts must be initiated in the near term in order for there to be rational and efficient progress towards routine quantitative measurements with SPM-based tools. Briefly, the most immediate SPM standardization requirements identified by the discussion groups were the need for:

- **the timely publication of standard methods and practices for obtaining and reporting experimental data,**

- **the development and widespread availability of suitable standardized roughness and step-height calibration samples, and**

- **probe tip characterization.**

It was generally concluded that until these elements become integrated into an accepted protocol which can be widely adopted, reliance of industry on SPM data for process control or quality assurance will be slow.

The discussion groups also identified many of the specific advances in instrumentation, standardization, and research & development which will represent important milestones along the evolutionary path of SPM development. For example, some of the most frequently cited milestones were:

- **the universal availability of linearized piezo-scanners over the entire SPM product line,**

- **automated sampling for statistical process control,**

- **improved probe characteristics including tip-shape and wear properties, and**

- **a more complete understanding of the underlying physical and chemical interactions which affect sensitivity and image contrast.**

This report also evaluates the effectiveness of the workshop format and recommends that another workshop take place at NIST in May 1995. A successful element of the first workshop was the focus of presentations on a small number of narrowly defined, and clearly expressed, industry needs, together with the SPM developments which are now underway to address these needs. Future workshops should retain the narrowly defined focus of the first workshop, although specific session topics may include a broader view of industrial applications. Another important element of the workshop was the generous amount of time available for discussion, both informal and as part of the facilitated discussion sessions which followed each overview session. These formal discussions proved to be a valuable source of information, once the responses for all sessions were compiled. We believe that facilitated discussions can be an effective means for soliciting input and developing a consensus on issues critical for the growth of the applied SPM community. Refinement and better preparation of the discussion format of future workshops will allow the participants in subsequent discussions to consider SPM developments in more substantive detail. Finally, the need to engage the SPM suppliers in shaping the agenda of future workshops has been recognized. Without their active participation in the process, the goal of an accurate timetable for quantitative SPM instrumentation cannot be achieved.

Additional copies of this report are available as NISTIR #5550 from the National Technical Information Service (NTIS, Springfield VA 22161), or by contacting the authors directly:

John A. Dagata
NIST
220-A117
Gaithersburg MD 20899
ph: 301-975-3597
fax: 301-869-0822
email: dagata@enh.nist.gov

C. K. Ken Shih
Department of Physics
University of Texas
RLM 5.208
Austin TX 78712
ph: 512-471-6603
fax: 512-471-1005
email: shih@utaphy.ph.utexas.edu

Alain C. Diebold
SEMATECH
2703 Montopolis Road
Austin TX 78714
ph: 512-356-3146
fax: 512-356-3083
email: alain_diebold@sematech.org

Richard J. Colton
Code 6177
Naval Research Laboratory
Washington DC 20375
ph: 202-767-0801
fax: 202-7673321
email: rcolton@stm2.nrl.navy.mil

ABSTRACT

An Industrial Applications of Scanned Probe Microscopy (SPM) workshop was held at NIST Gaithersburg on March 24-25 1994. The meeting, co-sponsored by NIST, SEMATECH, ASTM E42.14, and the American Vacuum Society, was attended by over one hundred SPM users, suppliers, researchers and program managers from industry, government, and academia. The workshop aimed to develop a consensus view on standard practices for SPM-based measurements, and to establish the basic features required of future generations of commercially available SPMs required for quantitative measurement. Workshop discussions identified three critical standardization requirements: the timely publication of standard methods and practices for obtaining and reporting experimental data, the development and widespread availability of suitable standardized roughness and step-height calibration samples, and probe tip characterization. The discussions also identified several critical areas needed to advance the SPM as a quantitative measurement tool: the universal availability of linearized piezo-scanners over the entire SPM product line, automated sampling for statistical process control, improved probe characteristics including tip-shape and wear properties, and a more complete understanding of the underlying physical and chemical interactions which affect sensitivity and image contrast were among the most often cited discussion topics. This report assesses the effectiveness of the workshop format and concludes with specific recommendations for a second, follow-up workshop.

TABLE OF CONTENTS

EXECUTIVE SUMMARY p. iii
ABSTRACT p. vii

PART I: WORKSHOP SUMMARY REPORT

A. INTRODUCTION p. 3
  1. Workshop Motivation
  2. Objectives of the Workshop
  3. Purpose of the Workshop

B. REVIEW OF INDUSTRY NEEDS p. 7
  1. Microroughness
  2. Critical Dimension Metrology
  3. Electrical Characterization

C. OUTCOME OF THE FACILITATED DISCUSSIONS p. 9
  1. SPM Standardization Requirements
  2. Consensus View on SPM Developments
  3. Timetable for SPM Developments

D. EVALUATION OF THE WORKSHOP FORMAT p. 17

E. CONCLUSIONS AND RECOMMENDATIONS p. 19

F. ACKNOWLEDGMENTS p. 20

PART II: TECHNICAL PROGRAM (REPRINT)

A. AGENDA p. 23

B. EXTENDED ABSTRACTS p. 31

C. LIST OF PARTICIPANTS p. 121

PART I: WORKSHOP SUMMARY REPORT

A. INTRODUCTION

An Industrial Applications of Scanned Probe Microscopy (SPM) workshop was held at the National Institute of Standards and Technology (NIST) Gaithersburg on March 24-25 1994. The meeting, co-sponsored by NIST, SEMATECH, the American Society for Testing and Materials (ASTM) E42.14, and the American Vacuum Society (AVS), was attended by over one hundred SPM users, suppliers, researchers and program managers from industry, government, and academia. The enthusiastic response to the workshop announcement, especially from the industry users and SPM vendors who made up 60% of the participants, indicates a willingness on the part of the applied SPM community to work together on the critical developmental issues facing this emerging community.

1. Workshop Motivation

The motivation for this workshop arose from the recognition that there are special circumstances which will have a determining effect on the evolutionary course of SPM development, particularly in the realization of the scanned probe for dedicated process control and inspection in advanced manufacturing[1]. There are several reasons for this:

> First, SPM technology has spread extremely rapidly in the past decade because, once the basic principles were discovered, it was quickly realized that the SPM is a rather simple electromechanical system. Because of low cost and ready availability, new and more powerful SPM-based techniques have progressed from laboratory demonstration to widespread commercially availability before there has been time for construction of a broad scientific knowledge base. Without this knowledge, it will be difficult to provide an acceptable basis for truly quantitative SPM-based measurements.
>
> Second, the rationale for government support of basic research and development (R&D) is changing[2], leading to a shift away from single investigator researcher to more comprehensive collaborations. From the standpoint of SPM-based tool development, the chief feature of this shift is to make R&D an aspect of instrument development. This means that new and more effective means of communication between SPM tool developers, i.e., the suppliers, and the research personnel in university and government laboratories need to be established.

---

[1] D. A. Swyt,"Metrological Issues in Precision Tolerance Manufacturing: A Report of a NIST Industry-needs Workshop", *J. Res. NIST* **98** 245 (1993).

[2] L. Geppert, "Industrial R&D: The New Priorities", *IEEE Spectrum*, 31 30 (1994).

Third, the nature of advanced manufacturing is changing[3]. Development of processes and fabrication tools is now recognized as an incremental activity. Also, the focus of corporate R&D has moved towards short-term goals. Therefore, it is more difficult for R&D outside the specific manufacturing environment to be relevant. On the other hand, it is some of these questions where in-situ nanoscale process control can be expected to have the greatest impact, thereby establishing SPM's role in advanced manufacturing.

Taken together, these forces are bringing about novel R&D alliances. As the leading tool of nanotechnology, the ultimate success of SPM-based methods will be greatly influenced by the acceptance of these methods by industry.

2. Workshop Objectives

The objectives of this workshop, as stated in the Technical Program, were:

- **Determine development and standardization requirements within industry for scanning probe microscopy measurements.**

- **Develop a consensus and publish a National View and Timetable for SPM requirements.**

- **Restrict this workshop to Industrial Applications of Microroughness, Dimensional Metrology, and Electrical Characterization.**

3. Purpose of the Workshop

The purpose of the workshop was to foster a common understanding of the roles which industry users, SPM suppliers, and government and university researchers play in the future of quantitative SPM-based methods. The workshop format was structured in such a way that each of these groups could readily identify with these roles. Furthermore, the narrowly defined workshop objectives, expressed in terms of industry needs, provided a structure for reviewing rapid developments taking place in this field and for the technical discussions of SPM development needs which followed. Because of the narrow focus of this workshop, information exchange between users, researchers, and vendors was considerably more selective than at general purpose conferences such as the AVS National Symposium. Workshops which provide the SPM community with an opportunity to focus on specific development needs are, in this sense, very much complementary to other forms of information exchange.

---

[3] G. W. Rubloff and M. Liehr,"Overview: Manufacturing Challenges and the Role of Research", *A Key to Competitiveness: The Science and Technology of Manufacturing* (American Vacuum Society, NY, 1993), p. 21.

This report summarizes the conclusions of the participants which arose during the workshop discussions. These conclusions reflect the current state-of-the-field for SPM and attempt to identify some of the specific requirements in the areas of standardization and instrument development if SPMs are to play a significant role in industrial applications, particularly in the semiconductor industry.

B. REVIEW OF INDUSTRY NEEDS

Introduction of scanned probe techniques into advanced manufacturing depends critically on developments in two broad areas: The first relates to general issues of quantitative measurement, and fundamental understanding of probe-sample interactions lies at the heart of this. The second relates to issues involving the integration of the scanned probe concept into dedicated, high-throughput tools which will have a well-defined impact on the manufacturing process. The Semiconductor Industry Association's (SIA's) 1992 Semiconductor Technology Roadmap is an effort by a US industry group to articulate its needs for such tools. (The 1992 Roadmap will be replaced by the SIA's 1994 National Technology Roadmap for Semiconductors.) Inasmuch as the roadmap identifies three key areas where SPMs may have a significant impact in this industry over the next decade, we believe that the SIA document serves as a point of reference for specific SPM developments which will allow scanned probe tools to become competitive with other techniques.

1. Microroughness

Howard Huff of SEMATECH presented specifications for silicon materials. This information provided a basis for discussion of silicon semiconductor characterization requirements for the SPM community. The SIA 1994 National Technology Roadmap for Semiconductors (formerly the SIA Roadmap) was under development at the time of this meeting. A draft version of the starting materials roadmap was used as the source of the silicon specifications. His talk covered two areas: silicon materials and surface preparation, and standards and characterization requirements. There is a dependency between silicon material parameters and the properties of devices and IC yield. The control of surface and bulk contamination and particulate levels, and wafer flatness were considered important to future IC manufacture. In particular, the use of SPM to measure and specify silicon microroughness was discussed[4]. Final requirements for silicon materials can be found in the November 1994 version of the National Technology Roadmap for Semiconductors.

2. Critical Dimension Metrology

Rob Hershey of SEMATECH presented the second overview of the 1992 and draft 1994 SIA Roadmap concerned with the anticipated needs of the semiconductor industry for critical dimension (CD) metrology over the next decade. The measurement and automation requirements anticipated by the roadmap for both mask-level and wafer-level control of feature size and placement accuracy at the 10% tolerance (3-σ reproducibility) were emphasized.

---

[4] Y. E. Strausser, B. Doris, A. C. Diebold, and H. R. Huff, "Measurement of Silicon Surface Microroughness by AFM", 185th Meeting of the Electrochemical Society, May 22-27, 1994, San Francisco CA.

The technical drivers for measurement are well understood from the experience with SEM and optical methods: pattern placement and fidelity along with metrology issues are defined with respect to the 0.25 - 0.18 μm design rules in the SIA Roadmap. These issues vary somewhat for traditional mask, x-ray mask, and phase-shift mask approaches since the mask-level aspect ratios determine the significance of sidewall metrology. Considerable effort is being directed among several groups, especially IBM and AT&T Bell Labs, towards addressing the SPM-specific solutions to sorting out how proximal probe tools can provide the proper information here.

The technical drivers for automated wafer and mask inspection are largely decoupled from the more fundamental measurement questions. The significant investment of IBM and Veeco Instruments into an SPM-based wafer inspection station represents the only significant exploration of this issue to-date. Potential funding sources for industrial R&D, such as SEMATECH or NIST's ATP program, may provide for collaborations on a scale which would allow definite answers to be obtained. In any case, if the SIA Roadmap, as it currently stands, is in any way realistic regarding SPM tool development for CD inspection, there is much progress that must be made in the understanding of SPM measurement as well as in automation.

3. Electrical Characterization

Larry Larson of SEMATECH presented an overview of semiconductor industry needs in the area of electrical characterization anticipated by the draft 1994 Roadmap. His talk emphasized two aspects of this area for which the currently available tools do not provide sufficiently accurate or local nanometer-scale information of dopant distributions: process monitoring for implantation, the 1-dimensional (1-D) profiling case, and process design and analysis, 2-D profiling for technical computer-aided-design (T-CAD) validation. Larry raised a particularly salient point for this workshop, that a novel technique such as SPM must offer the user the promise of meeting or exceeding the existing standard of performance to be considered for replacement. For process monitoring this standard is $\pm$ 5% in 3-σ repeatability.

Needs for 1-D profiling arise because of the tolerances required for 0.25-μm and 0.18-μm gate-length technologies. The critical need is to characterize the dose/energy relationship of the implant process to $\pm$5% accuracy for source/drain. Uniform and repeatable doping and dimensional control becomes crucial for doping in the 10^{19-20} cm^{-3} range and junction depths of only 50 nm.

Process design and analysis through accurate modeling of complete device characteristics by T-CAD software is becoming a significant strategy in implementing the decreasing design rules envisioned in the SIA Roadmap. Software models must be verified for 0.25-μm gate length technology and below. Experimental data on dopant distributions at the source and drain as well as within the channel region, so-called 2-D profiling, is essential input for this program. Since the needs of the T-CAD program are inherently off-line, they represent a great opportunity for SPM contributions to the semiconductor industry over the next decade.

C. OUTCOME OF THE FACILITATED DISCUSSIONS

The delivery of a concise statement of standardization and development needs for quantitative SPM-based measurements was a major goal of the workshop. The facilitated discussions which followed each of the three overview sessions on Microroughness, Critical Dimension Metrology, and Electrical Characterization, gathered input from the workshop participants on all aspects of SPM instrumentation, standardization, and R&D. The discussions focused on specific targets given in the 1992 SIA Roadmap, and some information from the draft 1994 Roadmap, in order to define the standard of performance required for SPM tools over the next decade. Defining a standard of performance for applied SPM implies that it will be possible to verify measurement accuracy according to accepted standards and that future generations of commercially available SPMs possess the requisite hardware and software capabilities. Industry-user, SPM-supplier, and Government/ University-researcher groups were charged with generating critical needs lists in each of the three overview areas. This section summarizes the outcome of these discussions.

1. SPM Standardization Requirements

Critical needs for quantitative SPM measurement were considered by each discussion group within the context of microroughness, critical dimension metrology, and electrical characterization measurement criteria. Specific topics which were viewed as requiring emphasis on the part of the applied SPM community over the next three years are summarized in Table I, with a mark given to indicate that the strongest needs were expressed during these particular discussions. All groups identified the publication of standardized practices and procedures, the availability of and guidance on standard reference materials, and the availability of tip characterization structures and software prominently on their lists.

(a) Microroughness

During the microroughness sessions it was universally recommended that tips must be characterized with regard to their size, shape, uniformity, and durability. Furthermore, the tip dimensions must be traceable, perhaps to the wavelength of light. Several structures were discussed as potential tip characterizers, including monodispersed gold or polystyrene spheres, metal clusters, and microfabricated silicon structures. A number of data analysis procedures were also presented from which the tip shape could be deduced using the standard structures. At present, there is no standard tip in use for microroughness measurements. Tip sharpness and aspect ratio, which must be controlled so that surface features are a factor of ten larger than the tip radius, must be specified before a roughness value can be accepted. In addition, other parameters including tip orientation, rigidity, durability, composition, and chemical properties may need to be specified as well.

Roughness calibration standards utilizing atom-based or lithographically defined step heights were also considered to be of extreme importance by all groups. The stability and

TABLE I. Topics identified during the facilitated discussions as having significant impact on standardization of practices and procedures for obtaining and reporting SPM data. The Table summarizes the responses of three groups of the workshop participants representing the viewpoints of industry users, SPM suppliers, and government/university researchers. A discussion session was held following each of the overview presentations on Microroughness, Critical Dimension Metrology, and Electrical Characterization. A mark indicates that the topic was cited as one of the "top three" items of importance for that session or was discussed extensively by the group when no rankings appeared on facilitated discussion charts for that session .

GROUP/Session

TOPICS	SPM Suppliers	Industry Users			Researchers		
	Single Session	Microroughness	Critical Dimension	Electrical Characterization	Microroughness	Critical Dimension	Electrical Characterization
Tip Characterization							
uniform tip shape		■			■	■	■
durable materials		■	■		■		
certifiable geometry	■		■	■	■	■	
novel properties		■	■	■			■
Standard Reference Materials							
atom-based roughness stds.	■	■			■	■	
< 10-nm step height and linewidth stds.			■			■	
1-D, 2-D electrical test structures				■			■
Standard Practices and Procedures							
data analysis		■	■	■	■		
tip characterization structures and software	■	■	■	■	■		

TABLE II. Topics identified during the facilitated discussions as having significant impact on the development of instrumentation required for quantitative applications of SPM-based techniques in industry. The Table summarizes the responses of three groups of the workshop participants representing the viewpoints of industry users, SPM suppliers, and government/university researchers. A discussion session was held following each of the overview presentations on Microroughness, Critical Dimension Metrology, and Electrical Characterization. A mark indicates that the topic was cited as one of the "top three" items of importance for that session or that it had been discussed extensively by the group when no rankings appeared on facilitated discussion charts for that session.

	GROUP/Session						
	SPM Suppliers	Industry Users			Researchers		
TOPICS	Single Session	Microroughness	Critical Dimension	Electrical Characterization	Microroughness	Critical Dimension	Electrical Characterization
Instrumentation:							
linearized scanners	■			■		■	■
closed-loop control		■	■		■		
tip registration		■	■				
automation	■		■			■	■
sample tilt		■	■				
correlation with other techniques	■			■	■		
Standardization:							
definitions	■						
data analysis software	■		■	■			
data format	■		■		■		
other industry needs				■			
Research and Development:							
improved tip properties		■	■		■	■	■
physical and chemical sensing tips		■		■			■
environmental control	■					■	
sample preparation requirements				■			
power spectral density analysis		■					
contact- vs. noncontact mode SPM	■						

traceability issues related to such structures below the 10-nm range are not at all resolved at the present time, and guidance on this is needed.

Present microroughness measurements rely exclusively on the procedures, methods, and algorithms developed by the surface profilometry community. These data usually appear as 1-dimensional line profiles. However, SPM data usually appear as 2-dimensional image data files. Reliable algorithms and data-taking procedures optimized for SPM use and developed in conjunction with standardized test data sets, must be made available.

(b) Critical Dimension Metrology

Design rules for next-generation semiconductor device requirements are specified in the 1992 SIA Roadmap, and draft 1994 version. Suitable probe tip geometries and appropriate lateral and vertical calibration standards are needed to ensure the performance of SPM-based tools for each successive device generation. High-aspect ratio and re-entrant probe tips for sidewall inspection were discussed by the groups, with concerns expressed about uncovering measurement problems unique to special tip shapes. Widespread availability and guidance on traceable calibration standards with multiple pitch lengths over a range of 10 nm to 1 μm were called for.

(c) Electrical Characterization

Electrically active standards, including both 1-dimensional and 2-dimensional silicon test structures with graded and abrupt layers, are needed by researchers who are presently investigating various SPM-based methods for profiling active dopant regions in silicon devices. These methods include scanning tunneling, scanning capacitance, and other novel techniques. Highly local measurements of ultrashallow dopant distributions are required for verifying computer models used in scaling advanced devices as well as for failure analysis. Comparisons among various probe-based methods for spatial resolution, doping accuracy and range, sensitivity, and measurement speed will rely on the availability of such structures.

2. Consensus View on SPM Developments

(a) Instrumentation

A broader view of the development needs over the next decade for the applied SPM community is presented in Table II. The list of topics is expanded to include the full range of discussion topics and are organized into three categories: Instrumentation, Standardization, and Research and Development. A look at Table II makes it clear that advances and acceptance of standard practices and procedures, for example, is strongly dependent on the availability of these features in commercial products. The major instrumentation developments that were discussed concerned the improvements in scanning operations and tip registry, especially the universal availability of closed loop control and accurate tip replacement. The issues related to the automation of SPM measurements, throughput, mechanical stability, and environmental compatibility with fabline in the case of CD metrology was also deemed important. The correlation of SPM data with that obtained by other techniques, especially industry standard methods was mentioned.

(b) Data Format and Software Standardization

Standardization of data formats, definitions of experimental quantities, and consideration of other industry needs were brought up during the discussions. A standardized data format among SPM suppliers, for example, would be important for integrating SPMs into automated inspection stations. In addition, the acceptance of standard practices and procedures would be enhanced if advanced data analysis routines such as power spectral density routines could be easily installed within all vendor-supplied data analysis environments. Already there are indications that third-party sources for image analysis software and tip deconvolution routines may provide an additional mechanism for establishing standard practices. Finally, specialized data sampling software for dopant profiling or sidewall imaging must be implemented as part of routine sampling strategies when the issues of throughput become significant. Ease of implementing third-party software routines at a number of R&D locations may prove highly desirable in the near future.

(c) Research and Development

Research leading toward a better understanding of the environmental controls which are required for microroughness and CD measurements on various surfaces was considered to be quite important for the acceptance of SPM measurements in industry. Other specific items noted for study over the short-term were more detailed treatment of power spectral density applications in microroughness, sample preparation, and a general description of contact-mode vs. non-contact-mode force microscopy. A better understanding of tip properties and the fabrication and widespread availability of tips which can discriminate physical properties and chemical identities on the nanoscale was considered to be very important.

Finally, Table II also notes particular comments which were recorded during the sessions which are worth noting: The SPM suppliers specifically noted the need for an accurate roadmap for SPM development. One of the objectives of this workshop was to initiate the dialogue which will lead to such a roadmap. The consensus on where we are and what we need to do is only just emerging. Further efforts to engage the applied SPM community will be necessary to see this work be accomplished.

3. View on a Timetable for SPM Developments

Before enumerating the challenges which lie ahead for the applied SPM community, it is worthwhile to recall that the reason there can be an industrial applications workshop today is, in large measure, due to the extremely rapid commercialization of the technology. The current situation is one in which SPM suppliers are rapidly improving designs and capabilities of their instruments; many industrial R&D labs around the world have already purchased SPMs, while many more are considering seriously their purchase. However, the SPM suppliers have outrun the capacity of the scientific community to fully understand much of the basic phenomena which comes into play at the nanoscale. This is a fairly unusual situation, but not without precedent. For example, semiconductor metrology using scanning electron microscopes becomes problematic because electron scattering within the sample volume, virtually ignored by the field until recently, has still not been adequately addressed.

A specific timetable for the SPM development needs listed in Table II did not emerge from the facilitated discussions. Indeed, whether or not we tie an "SPM Roadmap" to the targets indicated in the SIA's 1994 National Technology Roadmap for Semiconductors, it was premature, at least at the time of the workshop, to examine the elements listed in Table II and consider the consequences of progress or the lack of it on the future development of the applied SPM field. There were many comments from the participants which were recorded which can help to shape our thinking and set the stage for further discussion. For example, we emphasize that an accurate roadmap, as suggested above, is not possible without there being a way to lay out in some rational fashion the SPM development steps. These steps will be shaped by technical considerations and by the industrial advantages which industrial users can expect to realize from them.

D. EVALUATION OF THE WORKSHOP FORMAT

A workshop summary and outcome statement of the facilitated discussion have been given above, indicating that the first steps have now been taken towards meeting the workshop objectives. This has been achieved through the participation of the key groups which have a stake in the sustained progress of industrial applications of SPM and its growth into new areas. The meeting offered participants an awareness hopefully of other concerns and other efforts now in progress to push SPM development. It is perhaps useful at this point to analyze briefly the more and less successful elements of the workshop format. In doing so we can reach some conclusions about improving the targeting of future efforts for national support of this field.

The more clearly successful elements of the workshop format were the focus of the sessions on a small number of themes with a clear statement of industry needs. Given these expressed needs, it becomes possible to have a reference point for assessing the current relevance of SPM research towards addressing those needs. In this regard, we were extremely fortunate to have the specific targets laid out in SIA Roadmap and the essential support of SEMATECH to provide speakers who could articulate the relationship between the need for accurate measurements and performance.

The requirements that came out of the microroughness, critical dimension, and electrical characterization presentations were meant to provide specific targets for the facilitated discussions. They are in our opinion largely generic issues for implementing SPMs into the manufacturing environment. The heavy emphasis on how to make SPM measurements quantitative, rather than organizing the workshop around specific applications in a variety of industries was intentional to provide the strong focus which would appeal to industry. There are emerging application areas where substantial progress using SPMs has occurred besides the semiconductor electronics industry. Magnetic disc technology and polymers and coating industries are fields which are deserving of focused sessions at a future workshop.

We have several comments to make about the facilitated discussions. First, the use of a rather formalized structure for evoking a consensus, although familiar in industry settings, was something of a risk to attempt with researchers and suppliers. In our view these groups struggled with format and produced valuable responses to the question of SPM requirements needed to meet the targets specified in the SIA Roadmap. Some of the difficulty arose certainly because the group as a whole did not have sufficient familiarity with the specific numbers contained in the roadmap. The format of the overview and SPM-related talks were intended to put everyone on an equal level regarding the roadmap targets. This was somewhat too ambitious. Additional preparation of specific questions relating the roadmap targets and particular SPM developments would have allowed the discussion to progress beyond where it did. Our conclusion is that carefully prepared facilitated discussions can be an effective means for soliciting input within the applied SPM community.

The role of SPM suppliers as an active participant in current and future SPM development is becoming recognized. This comes in part because of the rapid pace of development of the commercial market which is outrunning research in some aspects as well as privatization of research, as practiced by SEMATECH and NIST's ATP wherein R&D costs become part of the cost of product development. Effective communication will be essential between suppliers and researchers to ensure that this happens. It is crucial that SPM suppliers are actively involved in helping to shape the agenda of future workshops.

E. CONCLUSIONS AND RECOMMENDATIONS

The main conclusions of this summary outcome statement for the first Industrial Applications workshop are:

- **The applied SPM community has validated, by their active participation in this workshop, that the format was useful for addressing the critical development issues for quantitative SPM applications. Each of the constituent groups, industry users, SPM suppliers, and government/academic researchers, were better able to see their role in the evolution of SPM-based tools and techniques for industrial applications as a result of attending the workshop;**

- **Participants were able to reach a consensus during the discussion sessions on SPM standardization needs and instrument development needs. Their responses are summarized in Tables I and II;**

- **The task of defining the standard of performance for SPM-based tools and articulating a realistic timetable for full development remains unfinished; and,**

- **Given the interest in and importance of this task, plans for a second workshop should be proposed as a follow-up to the first.**

Therefore, we recommend that a second workshop be held at NIST-Gaithersburg, on May 2-3, 1995. The workshop format should retain a focus on well-defined objectives, which contributed to the success of the first. However, it is important that we broaden the format to include industry focus sessions on some new topics: Magnetic Data Storage Technology, Coatings & Polymers, as well as on Semiconductors - those subjects covered here, as well as overlay and feature placement. As before, the purpose of the presentations will be to make all participants familiar with specific industry needs and the current SPM research which is specifically targeted to these needs.

The workshop format should further develop the facilitated discussion sessions, particularly to build on the consensus themes which feature prominently in this summary report for the first workshop. Key topics include a specific timetable for probe tip/calibration artifact/data standardization and construction of future generations of quantitative SPMs. For instance, we believe that all participants would benefit from discussions which make the SPM community more aware of how groups and institutions such as ASTM and NIST actually "produce" standard practices and materials. Also, the role of SPM suppliers in providing verifiable performance in commercially available SPMs should be explored. The elements of this effort arise from sources spread out across the SPM community, industry users, SPM suppliers, and government/university researchers. The various pieces must be constructed largely during a period in the US characterized by changing or uncertain national and corporate support of basic scientific exploration. Workshops such as this one must learn to effectively assist the dynamics of the industry user/researcher collaborations. Initial successes of these alliances for specific industrial applications will be inherently small-scale problem -solving. As such, they are not likely to benefit from commercialization support. However, they are likely to be extremely important in providing the basis for industry use of quantitative SPM data. This means that rapid refinement and wide acceptance of the standardization requirements for procedures, samples, and probes will be crucial.

SPM tool evolution will be dictated by market demands, in the sense that there is no publically funded initiatives for long-term SPM development, per se. If we anticipate reasonable progress in standards issues, applied SPM R&D, outsourced to university or government researchers by SPM suppliers, will become increasingly linked to tool development as the demand for dedicated inspection and process control matures. For this reason, it is becoming clear that future industrial applications workshops focus on and assist the dynamics of the supplier - researcher relationship as well. This can be done by refining the timetable for SPM developments, In particular, the mutual understanding of the "upgrade rate" for the "baseline" software and hardware features could provide a more sustained development path for SPM-based tool evolution.

F. ACKNOWLEDGEMENTS

The authors/organizers wish to thank **Clayton Teague** (NIST), **Ivan Amato** (NIST, **Yale Strausser** (Digital Instruments), **Andy Gilicinski** (Air Products and Chemicals), and **Joe Griffith** (AT&T Bell Labs) for reading this summary report prior to publication. The workshop would not have been possible without organizational and financial support from the management of NIST and SEMATECH which allowed us to bring together a uniformly excellent group of speakers who were able to articulate both industry needs and those of the SPM community. We acknowledge, in particular: **Dennis Swyt**, Division Chief of the Precision Engineering Division, for providing secretarial and financial support; SEMATECH, for making possible the SIA Roadmap overviews by **Howard Huff**, **Rob Hershey**, and **Larry Larson**, and for **Lisa Duncan**'s help in organizing the facilitated discussions; and, the NIST Conference Planning Office for considerable assistance and advice with arrangements.

PART II: TECHNICAL PROGRAM (REPRINT)

INDUSTRIAL APPLICATIONS OF SCANNED PROBE MICROSCOPY

March 24 - 25 1994

NATIONAL INSTITUTE OF STANDARDS AND TECHNOLOGY
Gaithersburg MD 20899

AGENDA

THURSDAY MARCH 24 1994

8:00 - 8:10 OPENING REMARKS AND WELCOME,
John Dagata, *NIST-Gaithersburg*

Session I: MICROROUGHNESS MEASUREMENT

SESSION CHAIR: **Alain Diebold**, *SEMATECH*

Overview of Industry Needs

8:10 - 8:40 200-mm Silicon Wafer Specifications: A critical examination vis-a-vis the National Semiconductor Technology Roadmap,
Howard Huff, *SEMATECH*

Probe Tip Shape and Probe-Sample Interactions

8:40 - 9:00 Options for Describing Probe Shape and Orientation,
Joe Griffith, *AT&T Bell Labs*

9:00 - 9:20 Analysis of Probe Microscope Images,
Dave Keller, *University of New Mexico*

9:20 - 9:40 Lateral and Vertical Measurement Issues for SPMs: Requirements, State-of-the-art, and Standards Needs,
Gopal Pingali and Dave Martin, *University of Michigan*

9:40 - 10:00 Interfacial Force Microscopy: New Opportunities with a Stable Force Sensor,
Jack Houston, *Sandia National Labs*

10:00 - 11:30 BREAK and POSTER SESSION

Surface Microroughness

11:30 - 11:45 Surface Roughness: Figures of Merit,
Leigh Ann Files-Sesler, *Texas Instruments*

11:45 - 12:00 Roughness Measurement in Semiconductor Processing,
Yale Strausser, *Digital Instruments*

Power Spectral Density vs. Average Numbers (Ra, RMS):

12:00 - 12:15 Power Spectral Density Calculation,
Yale Strausser, *Digital Instruments*

12:15 - 12:30 Comparison of AFM and Angle-resolved Scattering,
Dan Hirleman, *Arizona State University*

12:30 - 1:15 LUNCH

1:15 - 2:30 FACILITATED DISCUSSION: Determination of Consensus Set of Development Needs, Facilitator: **Lisa Duncan,** *SEMATECH*

2:30 - 2:45 BREAK

Session II: DIMENSIONAL MEASUREMENT

SESSION CHAIR: **Clayton Teague**, *NIST-Gaithersburg*

Overview of Industry Needs

2:45 - 3:10 Overview of Dimensional Measurements and Comparison with Other Technology,
Rob Hershey, *SEMATECH/Motorola*

Critical Dimension Measurement

3:10- 3:30 Dimensional Measurement by Scanned Probe Microscopy,
Yves Martin, *IBM-Yorktown*

3:30 - 3:50 Critical Dimension Measurement: Test Structures, Metrology Instrument Correlations, and Calibration Techniques,
Herschel Marchman, *AT&T Bell Labs*

3:50 - 5:00 BREAK and POSTER SESSION

5:00 - 6:00 FACILITATED DISCUSSION: Determination of Consensus Set of Development Needs, Facilitator: **Lisa Duncan,** *SEMATECH*

FRIDAY MARCH 25 1994

Session III: ELECTRICAL CHARACTERIZATION

SESSION CHAIR: **Randall Feenstra,** *IBM-Yorktown*

Overview of Industry Needs

8:00 - 8:20 Overview of Industrial Needs for Local Electrical Characterization
Larry Larson and Mike Duane, *SEMATECH*

Two-dimensional Dopant Profiling

8:20 - 8:40 Junction and Dopant Profiling Using Scanning Tunneling Microscopy and Spectroscopy,
Ken Shih, *University of Texas-Austin*

8:40 - 9:00 AFM Characterization of VLSI Devices,
Gabi Neubauer, *Intel Corp*

9:00 - 9:20 Quantitative Inversion of Scanning Probe C-V Data for 2D Impurity Dopant Profiling,
Clayton Williams, *University of Utah*

9:20 - 9:40 Scanning Capacitance Microscopy for Profiling pn-junctions in Silicon,
Joe Kopanski, *NIST-Gaithersburg*

9:40 - 10:30 BREAK and POSTER SESSION

10:30 - 10:50 Spreading Resistance Microprobe,
Bob Marcus, *NJIT*

10:50 - 11:10 Structural Studies of the SiO_2/Si System,
Eric Garfunkel, *Rutgers University*

11:10 - 12:30 FACILITATED DISCUSSION: Determination of Consensus Set of Development

Needs, Facilitator: **Lisa Duncan**, *SEMATECH*

12:30 - 1:30 LUNCH

Session IV: NEW DEVELOPMENTS IN INSTRUMENTATION AND PROCESS CONTROL

SESSION CHAIR: **Rich Colton**, *Naval Research Lab*

Overview of Future Industry Needs

1:30 - 1:40 Feature Placement Accuracy,
Clayton Teague, *NIST-Gaithersburg*

New Developments and Opportunities

1:40 - 1:45 Pitch Standards via Laser-focused Deposition,
Jabez McClelland, *NIST-Gaithersburg*

1:45 - 2:00 Sensors and Actuators in Scanned Probe Microscopy,
Steve Hues, *Naval Research Lab*

2:00 - 2:15 Probe Microscope Tip Fabrication,
Herschel Marchman, *AT&T Bell Labs*

2:15 - 2:30 Overview of NIST's Advanced Technology Program,
Thomas Leedy, *NIST-Gaithersburg*

2:30 - 3:00 BREAK

SPM VENDORS' PERSPECTIVE

3:00 - 3:15	Topometrix	**Paul West**
3:15 - 3:30	Digital Instruments	**Virgil Elings**
3:30 - 3:45	Park Scientific: Advances in Instrumentation for SPMs used in Dimensional Metrology,	**Michael Kirk and Lindsey Mitobe**
3:45 - 4:00	Burleigh Instruments	**David Henderson**
4:00 - 4:15	Veeco	**Thomas Jay**

4:15 - 4:30 FACILITATED DISCUSSION SUMMARY,

Lisa Duncan, Alain Diebold, *SEMATECH*, and **John Dagata**, *NIST-Gaithersburg*

4:30 - 4:45 CLOSING REMARKS

4:45 ADJOURN

POSTER PRESENTATIONS

1. Polished Silicon as an SPC Sample,
   Robert H. Brigham, *Charles Evans & Associates*

2. Roughness of SiGe Films Studied by AFM and STM,
   M. A. Lutz and R. M. Feenstra, *IBM-Yorktown*

3. Evaluation of Wafer Micro-roughness with sub-Angstrom Resolution on the AFM: Results of an AMD-sponsored Round Robin,
   Ruby Raheem and Ercan Adem, *Advanced Micro Devices*

4. Using Cluster Materials for High Resolution Tools in AFM,
   Donald A. Chernoff, *Advanced Surface Microscopy*

5. ISO Methodology for Determining and Reporting Uncertainty in Measurement for Surface Topography Standards,
   J. Jerry Prochazka, *VLSI Standards*

6. Use of Tip Standards in AFM Studies of Silicon Surface Roughness and Polymer Coating Morphology,
   Rebecca M. Rynders, James R. Stets, and Andrew G. Gilicinski, *Air Products*

7. The Effect of AFM Tip Radius on Imaging Thin Film Surfaces,
   K. L. Westra and D. J. Thomson, *University of Manitoba*

8. Electrical Characterization of Semiconductors by STM: Tip-induced Band-bending and Pinned vs. Unpinned Surfaces,
   R. M. Feenstra and M. A. Lutz, *IBM-Yorktown*

9. Cross-sectional Scanning Probe Microscopy of Semiconductor Structures,
   M. Johnson, H. Salemink, and E. Druet, *IBM-Zurich*

10. Air and Vacuum STM/S of Bulk-doped GaAs and pn Junctions,
    R. M. Silver, J. A. Dagata, and W. Tseng, *NIST-Gaithersburg*

11. Progress Towards Contact Mode Scanning Potentiometry,
    John Moreland, *NIST-Boulder*, and **Craig Prater**, *Digital Instruments*

12. 2-Dimensional Delineation of Semiconductor Doping by Scanning Resistance Microscopy,
    C. Shafai and D. J. Thomson, *Univ of Manitoba*

13. High-precision Calibration and Drift Estimation of Scanning Probe Microscopes by Fourier Analysis,
Jan Jorgensen, *Danish Institute of Fundamental Metrology*

14. A Calibrated Atomic Force Microscope,
Thomas H. McWaid and Jason Schneir, *NIST-Gaithersburg*

15. Effect of Overlayer Thickness on the Nanoindentation of SiO_2/Si,
Charles Draper, *Vanderbilt University*, **Richard J. Colton and Steven M. Hues**, *Naval Research Lab*

16. Scanning Near Field Optical Microscopy for Gene Mapping,
Raul Fainchtein, *Johns Hopkins University*

17. Measuring Biomolecular Recognition Insertions with the Atomic Force Microscope,
G. U. Lee, D. A. Kidwell, and R. J. Colton, *Naval Research Lab*

18. Phases of Alkanethiol Self-assembled Monolayers on Au(111),
G. E. Poirier, H. E. Rushmeier, and M. J. Tarlov, *NIST-Gaithersburg*

19. Chemical Profiling of Sub-surface Semiconductor Structures by Magnetic Resonance Force Microscopy,
P. C. Hammel and G. J. Moore, *Los Alamos*, and **M. L. Roukes**, *Caltech* .

20. Magnetic Force Microscopy of Thin-film Recording Heads,
Paul Rice and John Moreland, *NIST-Boulder*

21. SPM Imaging of Thin Film Morphologies,
Alexana Roshko, *NIST-Boulder*

22. Surface Modification of YBCO Thin Films using the Scanning Tunneling Microscope,
R. E. Thomson, John Moreland, and A. Roshko, *NIST-Boulder*

23. Nanometer-scale Electronic Properties of Organic Insulators, and
High-resolution Force Transducers for Smart Sensor Arrays,
Robb White, *Columbia University*

V. EXTENDED ABSTRACTS

Oral Presentations	pages 33 - 79
Poster Presentations	pages 81 - 119

200 MM SILICON WAFER SPECIFICATIONS: A CRITICAL EXAMINATION VIS-A-VIS THE NATIONAL SEMICONDUCTOR TECHNOLOGY ROADMAP[1]

Howard R. Huff
SEMATECH, Inc.
2706 Montopolis Drive, Austin, Texas 78741

The Semiconductor Industry Association (SIA) has recently noted that "semiconductor technology offers the potential for rapid, continued progress in electronics performance and functionality. The advances (in semiconductor technology) are the driving force for the information age (1)." Crystalline silicon and silicon-based materials such as silicon-germanium, related hetero-junctions and, more recently, silicon on insulator (SOI) continue to be the premier materials driving the ultra large scale integration (ULSI) microelectronics revolution. Decreasing IC design rules and vertical dimensions along with increasing die size are driving improvements in silicon materials. Improved control of the magnitude, tolerance and uniformity of Czochralski silicon wafer characteristics–coupled with an improved understanding of the inter-relationships among silicon material characteristics, IC fabrication processes and IC performance–continues to be the key to superior IC product performance, reliability and yield in the mega-IC era (2).

The implications on cost-performance of selectively scaling device geometries and miniaturizing components, even as the die size increases, will become more important as 200 mm wafers proliferate the industry and 300 mm and larger wafers are selectively introduced. The technical significance of silicon wafers and representative examples of surface contaminants (particles, surface microroughness and metals), bulk impurities (oxygen and carbon), surface topography (wafer flatness) and epitaxial structures required for the mega-IC era will be reviewed in the context of the SIA report for the 64 Mbit, 256 Mbit and 1 Gbit DRAM. We will discuss the relevance and viability of several of these silicon wafer goals in the context of a recent assessment of 2500 polished 200 mm wafers from several global silicon suppliers.

Rather than discuss specifications (4-11) extensively, however, we will emphasize evolutionary and significantly improved characterization techniques envisioned for 200 mm and larger wafers (12,13). Standards, diagnostics and metrology have become as significant as the wafer specification goals since these goals are approaching the measurement precision. The days of "off-the-shelf" measurements for the semiconductor industry are surely past (14). In situ and non-destructive metrology have become limiting factors in virtually all wafer preparation and IC process technologies (15). These procedures will become increasingly important, along with real-time feedback control, as we approach the giga-IC era (16). Indeed, measurement technology has become immeasurably important (17).

---

[1] Published in "Proceedings of The Fourth International Symposium on ULSI Science and Technology," (edited by G.K. Celler, E. Middlesworth and K. Hoh) p. 103-132 (1993) ECS

REFERENCES

(1) Semiconductor Industry Association, San Jose (March, 1993)

(2) H.R. Huff in *Symposium on Advanced Science and Technology of Silicon Materials*, (edited by M. Umeno), 140-154, 25-29 Nov., 1991 Kona, Hawaii

(3) H.R. Huff in *Fourth International Symposium on ULSI Science and Technology*, (edited by E. Middlesworth and G. Cellar), 1993 p.103-132 (1993) ECS

(4) L.T. Gallinger and L.A. Kieny in *SEMICON/JAPAN Technical Proceedings 1991*, 182-184, 6-7 Dec., 1991

(5) S. Takasu, H. Terauchi and T. Araki in *Symposium on Advanced Science and Technology of Silicon Materials*, (edited by M. Umeno), 171-179, 25-29 Nov., 1991 Kona

(6) P.O. Hahn in *Symposium on Advanced Science and Technology of Silicon Materials*, (edited by M. Umeno), 180-188, 25-29 Nov., 1991 Kona, Hawaii

(7) M. Watanabe, Solid State Technology, March 69-73 (1991) and April, 133-142 (1991)

(8) T. Takenaka in *SEMICON/JAPAN Technical Proceedings 1991*, 144-147, 6-7 Dec.'91

(9) H.R. Huff in *Concise Encyclopedia of Semiconducting Materials and Related Technologies* (edited by S. Mahajan and L.C. Kimerling), 478-492 (1992), Pergamon

(10) W.M. Bullis and W.C. O'Mara, *Solid State Tech.* April, 1993 p. 59-65

11) W.M. Bullis and H.R. Huff in *Encyclopedia of Advanced Materials*, (edited by S. Mahajan), (To Be Published), Pergamon Press

(12) Y.E. Strausser, B. Davis, A.C. Diebold and H.R. Huff, *ECS Extended Abstracts*, 94-1, (To be published, 1994)

(13) W.M. Bullis in "Semiconductor Silicon/94," (edited by H.R. Huff, W. Bergholz and K. Sumino) (To be published, 1994) ECS

(14) *Proceedings of the International Workshop on Silicon Materials for Mega-IC Applications*, (edited by H.R. Huff, W.M. Bullis, R. Scace, W. Baylies & W. Brown), Sponsored by SEMATECH, SEMI, NIST, and ASTM (1991)

(15) H.R. Huff and W.M. Bullis, *STEP/Large Diameter Wafers*, SEMICON/WEST '90, 25 May 1990

(16) H.R. Huff, ECS Ext. Abstracts, 93-1, Abstract #660, p. 943-944 (1993)

(17) R. M. White, *Physics Today*, April, p. 55-57 (1993)

Options for Describing Probe Shape and Orientation

J. E. Griffith, AT&T Bell Laboratories
Murray Hill, NJ 07974-0636

Probe tip shape and orientation are two of the most important attributes determining the performance limits of a profilometer or scanning probe microscope[1]. Methods for accurately and efficiently describing probe shape are therefore essential for portraying the quality of data in a given scan. The ASTM Subcommittee E42.14 on STM/AFM is presently developing standards for reporting probe shape. This presentation will describe some of the options that the subcommittee is considering.

Even in the profilometry of flat surfaces, specification of a single tip radius at the apex is not necessarily sufficient to describe the behavior of the instrument[2]. In probe microscopy of high-aspect-ratio structures, regions of the probe far from the apex can come into contact with the surface. These probes often have complicated and even reentrant shapes, so the number of parameters required to characterize them can be surprisingly large. Stylus shapes have mainly been described in terms of simple geometrical forms: pyramids, cones, cylinders, paraboloids, spheres, etc. This approach to probe specification has two problems. First, with the advent of probes with flared ends or with lateral spikes, the possible shapes are proliferating to an unmanageable number. Second, real probe tips often do not exactly conform to a simple shape. This can be caused by design, by variability in the probe manufacture, or by wear of the probe during use. The possibility that the probe shape is not symmetrical about the probe axis is especially troublesome.

With the advent of probe tip characterizers and software to extract the tip shape from the characterizer scan[3,4], it will soon be possible to measure actual probe shapes with the probe microscope. The software being developed naturally describes the probe in the same manner that scanned surfaces are depicted, as measured heights on a rectangular grid. In these programs, it is neither necessary nor particularly desirable to describe the probe as an idealized geometrical form. This representation does have some difficulties of its own. The flared probe in the figure, for instance, does not have a single-valued representation. It is likely that for especially simple shapes, such as a nearly perfect cylinder, the user will continue to express the probe shape in terms of a few parameters, while for more complicated shapes an image of the probe surface generated from appropriate software will be necessary.

Beyond the shape itself, there are several characteristic lengths, illustrated in the figure, that must be specified. The first is the *probe length*, which is the distance between the apex and the shank or cantilever holding the probe. The probe length is especially important when the probe is slender enough to flex under lateral forces. The second is the *active length*, which subtends the area of the probe that may come into contact with the surface. The active length depends on the surface scanned. The final length is the *characterized length*, which is the length of the probe that has been measured with a probe tip characterizer. Clearly, the characterized length should be greater than or equal to the active length.

The orientation of the probe also affects its ability to reach recessed areas of a sample. For instance, a slender probe attempting to descend into a deep, narrow hole will not reach the bottom if it's orientation deviates significantly from the axis of the hole. In addition, the orientation of an asymmetric probe about its axis affects its interaction with the surface. If the probe is measured by scanning a probe tip characterizer, then the orientation of the characterizer relative to the sample is the dominant concern. In general, the sample normal vector should coincide with the characterizer normal vector. If the probe tip is removed from the probe microscope during probe characterization, then as many as three angles (Euler angles, for instance) may be needed to specify the orientation of the probe relative to the sample.

REFERENCES

1. J. E. Griffith and D. A. Grigg, "Dimensional metrology with scanning probe microscopes", J. Appl. Phys. **74**, R83 (1993).
2. J. F. Song and T. V. Vorburger, "Stylus profiling at high resolution and low force", Appl. Opt. **30**, 42 (1991).
3. G. S. Pingali and R. Jain, "Surface recovery in scanning probe microscopy", Proc. SPIE **1823**, 151 (1992).
4. D. J. Keller and F. S. Franke, "Envelope reconstruction of probe microscope images", Surf. Sci. **294**, 409 (1993).

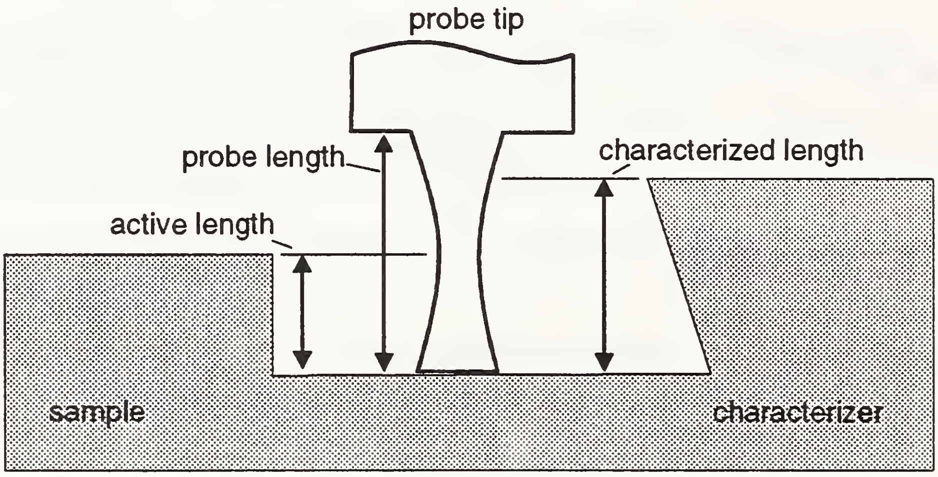

Figure. Depiction of probe length, characterized length and active length.

Analysis of Probe Microscope Images

David Keller, Fransiska Franke, and Ke Luo

Department of Chemistry, University of New Mexico
Albuquerque, NM 87131

Probe microscope images always contain distortions caused by the finite size and shape of the probe tip. These distortions affect the lateral dimensions, the apparent depths, and the overall shape of image features. It is important that they be understood and minimized in all applications of probe microscopy, especially for applications to metrology. We will describe two basic theories of image formation for probe microscopes: the Legendre Transform method and the Envelope method. Both theories can be shown to be equivalent mathematically, but are quite different in their view of the problem, in the ease with which they can be manipulated to reach general conclusions, and especially in the way they are implemented in practical applications.

Envelope Image Analysis

The envelope approach is most simply understood by thinking of the sample surface as a series of very sharp, closely spaced spikes. By varying the height of each spike, and by placing them very close together, any surface can the generated. The probe microscope image of the surface will then be a series of probe microscope images of sharp spikes. But the probe microscope image of a spike is just an inverted image of the probe tip itself. Therefore, the probe microscope image of the entire surface can be thought of as being composed of a large number of inverted tip surfaces (see figure 1). In fact, the new, image surface is the *envelope* formed by all the inverted tip surfaces. In a similar way it is possible to show that the original, undistorted *sample* surface can be reconstructed from an a probe microscope image by forming the envelope of a series of *tip* surfaces. Finally, if a probe microscope image of a known sample is taken, the *tip shape* can be found by forming the envelope of a series of *sample* surfaces.

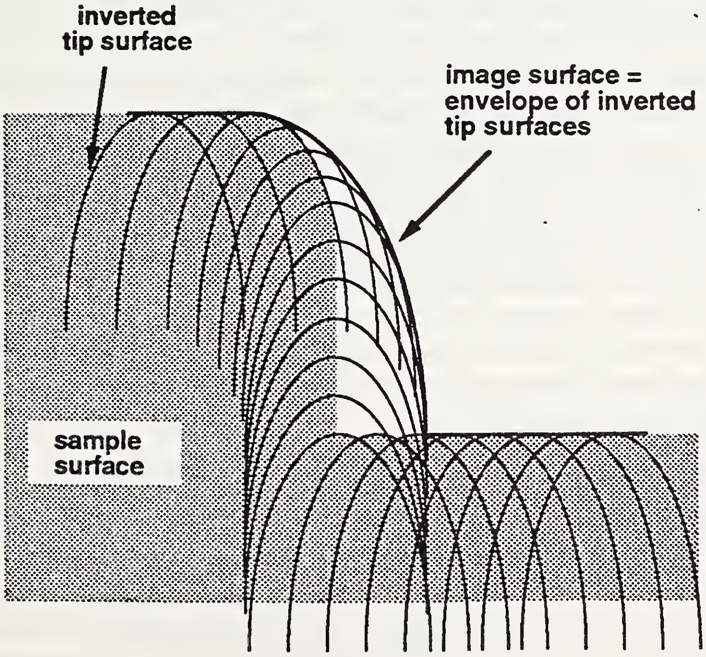

Figure 1 Probe image as envelope of tips

The envelope method for analyzing probe microscope images is difficult to express mathematically in a convenient way, but it is easy to implement as a stable, well defined computer algorithm. All practical image analysis algorithms that we are aware of use some variant of the envelope method.

The envelope approach can also be used to prove three fundamental theorems concerning probe microscope images. The *reciprocity theorem* states that an image of sample made with a certain tip shape is the same as the image of a tip made with the sample. The reverse image theorem states that the reconstructed sample surface is the same as the the surface generated by imaging the *underside* of the *image* surface with an inverted tip. The reverse image theorem then implies the *noise clipping theorem*, which says that certain types of noise in probe microscope images can be *a priori* identified as inconsistent with any possible image surface, and so can be rejected. This last theorem is obviously the basis for a noise filtering technique.

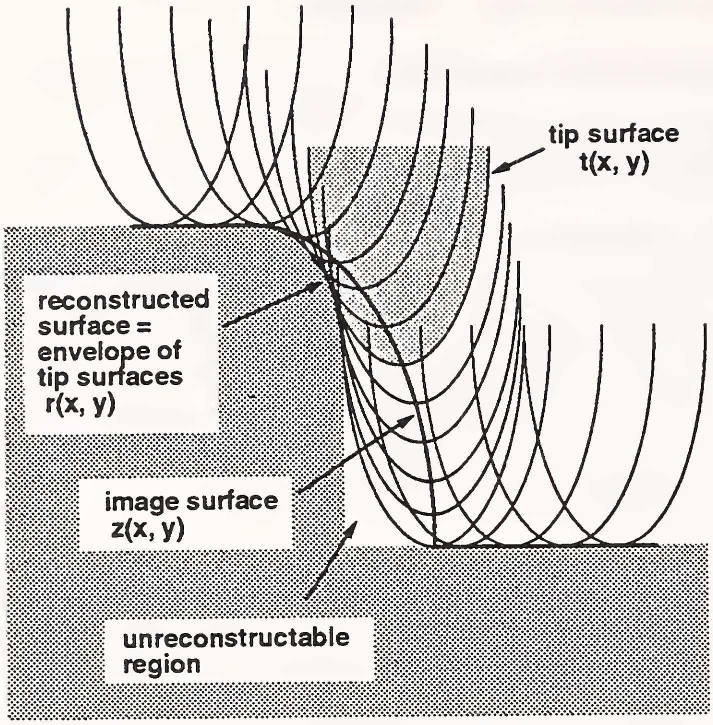

Figure 2 Reconstruction of distorted image

Legendre Transform Image Analysis

The Legendre transform approach is based on the observation that the Legendre transforms of the image, the tip, and the sample surfaces are related to each other in a simple way. It is much harder to implement for use on real data than the envelope methods, but has the advantage that it is expressed in familiar analytical notation, and so can be used to prove certain theorems that would be impossible to prove by envelope methods alone. Let i(x,y) be the image surface, t(x,y) be the tip surface, and s(x, y) be the sample surface, and let L[i(x, y)], L[t(x, y)], and L[s(x, y)] be the corresponding Legendre transforms of these surfaces. Then the *Legendre transform rule* is

$$L[s(x, y)] = L[i(x, y)] + L[t(x, y)]. \tag{1}$$

In other words, the Legendre transform of the sample surface is the sum of the Legendre transforms of the image and tip surfaces. This is as simple a rule as could be hoped for, and is reminiscent of the convolution theorem for lens-based microscopes, which says that the Fourier transform of the image is the product of the Fourier transforms of the sample and the transfer function (which represents the lens). One way to look at the difference between probe and optical microscopy therefore, is that the Legendre transform is a local, non-linear transform, while the Fourier transform is a non-local, linear transform. Since the Legendre transform can be inverted, that is, there is a back-transform that recovers the original function, equation 1 says that if any two surfaces are known the third can be found. As with the envelope approach therefore, it is possible to find either the sample surface, the tip surface, or the image surface by performing appropriate operations on the other two surfaces.

The Legendre transform rule (and other, equivalent, formulations of the Legendre transform method) can be used to prove the curvature theorem, which says that at any point on the sample the radius of curvature (that is, the inverse of the second derivative) of the sample, R_s, is the sum of the radii of curvature of the image, R_i, and the tip, R_t:

$$R_s = R_i + R_t. \tag{2}$$

The curvature theorem means, among other things, that a bump on the sample surface can never appear in a probe microscope image to be sharper (i. e., have a smaller radius of curvature) than the tip.

The envelope and Legendre transform methods have been used to reconstruct distorted images, to create artificial images of models (for comparison to experimental data), and to find the shapes of probe tips. These examples, together with the general theories, will be presented. Special attention will be given to how the envelope method works in the case of re-entrant structures and tip shapes.

Lateral and Vertical Measurements Issues for SPMs: Requirements, State-of-the-art, and Standards Needs

Gopal S. Pingali, Ramesh Jain and David C. Martin
University of Michigan, Ann Arbor, MI 48109, USA

Lateral and vertical measurements in Scanning Probe Microscopes (SPMs) are critically affected by the non-linear geometric interactions between the scanning probe and the scanned sample. Probe-sample interactions can result in faulty measurements of critical dimensions and microroughness, and distortion of true surface topography. Several images taken in the nanometer to micrometer range are presented to indicate the severity of this problem. An imaging model that allows prediction of probe-induced artifacts on a sample is presented. The model is in terms of gray scale morphological dilation and expresses the image I as

$$I = S \oplus P^{\wedge} \tag{1}$$

where S represents true surface topography, $P^{\wedge}$ the probe shape reflected about the origin and $\oplus$ gray scale morphological dilation. Image analysis and restoration techniques are outlined to obtain a better estimate of true surface topography and to indicate which regions in an SPM image represent reliable data. A calibration technique is developed to automatically recover the three-dimensional shape and orientation of the scanning probe from the image of a calibration structure. It is pointed out that sample and probe orientations are important parameters in SPM imaging. A better estimate of true sample topography can be obtained by imaging the sample at several orientations, applying appropriate orientation compensation techniques to each image, and combining information from multiple images. This work suggests and brings out the need for several standards for SPM imaging as outlined below.

- **Image analysis and restoration standards:** SPM images cannot be accepted at face value. Image analysis and restoration techniques are an essential complement to SPMs. Such techniques give a better estimate of true surface topography and indicate the reliability of image data. The application of such techniques to SPM images should be made a standard. We suggest some techniques for this purpose.
- **Probe shape calibration software standards:** The three-dimensional shape of the probe is an essential input to the image analysis and restoration techniques discussed above. Hence, techniques for determining the shape of the probe and means for specifying the shape should be part of the SPM imaging standard. We suggest software techniques to automatically recover the shape of the probe from the image of a known calibration structure. The probe shape should be calibrated at several different resolutions using appropriate calibration structures.
- **Probe shape calibration sample standards:** Standards need to be set for structures used in probe shape calibration. We present results with an undercut cylindrical structure. Our work indicates that a range of calibration structures may be required corresponding to imaging at different resolutions, and that a single calibration structure

is not suitable for all probe shapes. Therefore, a calibration structure should be accompanied with specifications regarding the range of measurements for which it should be used and the probe shapes for which it is valid. Besides, calibration structures should be widely available, reproducible and accurate.

- **Sample and probe orientation calibration standards:** Sample and probe orientations are important parameters in SPM imaging. It is crucial to separate the background orientation of the sample from true surface topography. A calibration area with known topography is required for determining the background orientation of the sample. We suggest the use of planar calibration areas for determining sample orientation. The probe shape calibration structure can then be used to obtain both the probe shape and probe orientation.

- **Orientation compensation software standards:** Currently, background plane subtraction is commonly used in the SPM community to correct for the orientation of the sample. This distorts features especially in samples such as semiconductor wafers. Background plane orientation should be used to correct for sample orientation. This should be made a part of the SPM imaging standard.

- **Instrumentation standards for manipulating sample and probe orientations:** Current SPMs do not provide a mechanism for varying sample and probe orientations. We present results indicating that undercut sidewalls can be imaged by taking advantage of sample orientation. SPMs should allow variation of sample and probe orientations. Samples can be scanned at different orientations and the resulting images combined to yield a better estimate of the true surface topography. Future research needs to address the development of probe microscopes which allow the user to program in appropriate scan strategies instead of using just the raster scan.

- **SPM imaging simulation standards:** Tools for simulating SPM imaging can be invaluable for the SPM designer and the SPM user. Users can determine the suitability of an SPM for samples of interest. Designers can visualize the effect of different parameters such as probe shape and sample and probe orientations and can accordingly modify the design of the instrument. We present such a simulation tool and suggest that standards should be set for SPM image simulation.

- **Image format standards:** Much of the information related to the different standards should be incorporated into an SPM image. Thus, the image should include information regarding the shape of the probe used for scanning, the orientation compensation mechanism used, if any, and so on. Standardizing the image format would mean that this information is available with every SPM image and is consistent across instruments from different vendors.

References

[1] Gopal Sarma Pingali, "Image Modeling and Restoration for Scanning Probe Microscopy," *Ph.D. Dissertation*, University of Michigan, January 1994.

Interfacial Force Microscopy: New Opportunities with a Stable Force Sensor

J. E. Houston, P. Tangyanyung, R. C. Thomas, T. A. Michalske
Sandia National Laboratories, Albuquerque, NM
and
R. M. Crooks
Texas A&M University, College Station, TX

Scanning probe techniques have shown dramatic growth over the last several years and are presently making significant impact on surface and interfacial problems in material science. The most widely used of these techniques is atomic force microscopy (AFM) which can measure interfacial forces down to the atomic level and which is applicable to virtually all materials. In its present embodiment, however, the AFM is limited in applicability by its use of a deflection force sensor which is mechanically unstable under rapidly varying interfacial forces. In contrast, interfacial force microscopy (IFM) utilizes a self balancing force sensor which eliminates the instability and permits operation in both the attractive and repulsive modes. In addition, the sensor has a zero effective compliance which means that subtle interfacial interactions (for example, bond rupture) are not dominated by the energy stored in the sensor itself.

In this presentation we show results demonstrating the enhanced capabilities of the IFM in applications ranging from studies of the mechanical properties of single monolayers on metal surfaces to measurements of the electrostatic component of the adhesive bond between monolayer films having end groups with differing electric dipole moments. In the first of these examples, we demonstrated that single monolayers of *n*-alkanethiol molecules passivate the strong bonding interaction between a metal probe and substrate and permit quantitative determinations of the elastic modulus and shear-stress threshold for plastic deformation of single nanometer size grains in polycrystalline films. These capabilities are illustrated in the figure below, which shows the loading curve and post-loading image of a single 200 nm grain in a 200 nm thick Au film grown on glass.

The loading curve of fig. (a) shows an initial Hertzian behavior (solid line) indicating an elastic deformation. The plastic threshold occurs when the curve deviates from Hertzian. The sudden drops in load represent "stick-slip" events during the plastic deformation probably due to the formation of slip bands, as evidence by the trigonal nature of the indentation shown in fig. (b).

In the second example, force measurements of the electrostatic interaction of polar surfaces is shown to open the capability of surface potential mapping and the delineation of morphology and surface potential. These results, and others, will be discussed in terms of potential applications to a broad range of materials and processing studies.

This work was supported by the US Department of Energy, Office of Basic Energy Sciences, Division of Material Sciences under contract DE-AC04-76DP00789.

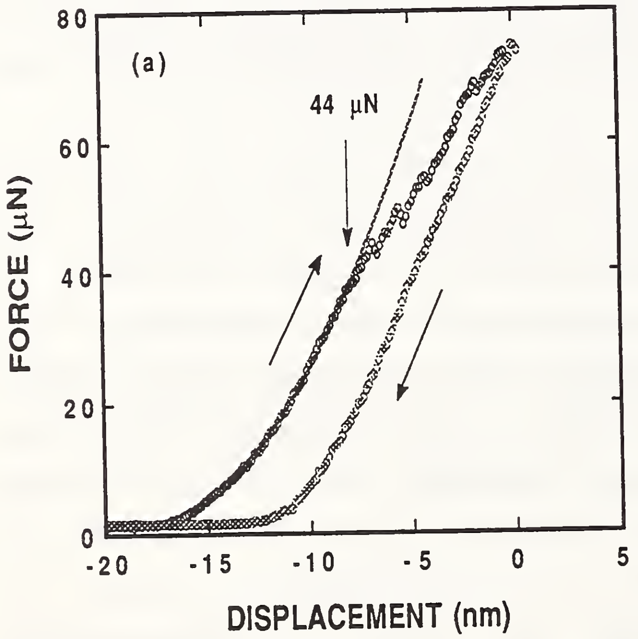

(b)

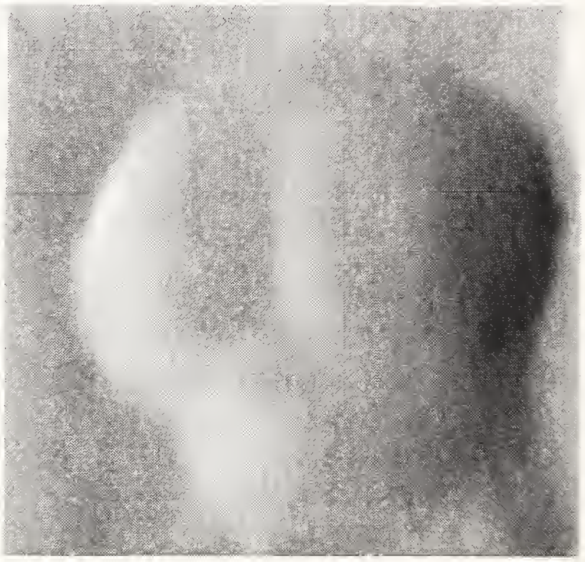

Surface Roughness: Figures of Merit

Leigh Ann Files-Sesler
Texas Instrument, Inc.

Typically when one seeks to describe surface roughness numerical values are of primary interest. Pictures may paint a thousand words, but unfortunately neither pictures nor words fit well in statistical process control charts. Ironically, often understanding pictures is intuitively simple, but distilling them down to a meaningful number or set of numbers may not be simple at all.

In the semiconductor industry one is often trying to correlate surface structure with device properties. Properties of interest might include bondability, reflectivity, capacitance, adhesion, friction, and understanding mechanisms of defect formation.

In our research we have shown correlations between reduction in root-mean-squre, RMS, roughness and increased bondability. We have also related low average roughness, Ra, values to increased reflectivity. Other researchers have demonstrated a correlation between reduction in fractal dimension with enhanced ability to remove particles from surfaces. In other industries, bearing ratio calculations have been used for determining frictional properties of materials.

A recent area of interest is correlation of surface roughness with gate oxide integrity. The question is what figure of merit is appropriate for this analysis. One might argue that the actual property which one wants to measure is the minimum thickness of the dielectric layer at any given point within an actual device contact area, or if yield is the primary concern the area of a wafer over which the oxide is below a minimum thickness, or perhaps for reliability the distribution of thickness over the wafer or over an average of typical device areas. As you can see choosing any one value to correlate with device electrical properties is not an easy matter, and in this case one would be looking at a secondary measurement (i.e. one might assume a flat substrate and measure an average thickness, perhaps by ellipsometry, and then relate variations in height on the oxide surface to variations in oxide thickness).

Currently we are investigating the use of surface area calculations for evaluating materials being considered for use in capacitors. Once again the interest of the customer might be related to a specific area correlating to a device structure size, analysis of a wide range of areas to determine variability and yield, or perhaps best case senarios for initial investigations.

If one is concerned about shorting between metal layers which are separated by a thin dielectric then hillocks in the base metal layer may be of primary concern. In this case the maximum peak height within a given area might be the most relevant figure of merit, or the number of hillocks in a given area.

The appropriate number or set of numbers required to describe a surface depends upon the specific property and depth of detail necessary for a given application (often a relative or "go /no go" measurement is sufficient). Therefore, this talk will refer to a variety of examples where different figures of merit correlate well with the property of interest. Of course it is also critical that the relevant spatial frequencies and limitations be reported any time these values are used.

Roughness Measurement in Semiconductor Processing

Yale E. Strausser
Digital Instruments, Inc.
Santa Barbara, CA 93103

There are many steps in semiconductor processing which benefit from roughness measurement. These steps range from the specification of the original silicon wafer surface, through the growth or deposition of various films, monitoring the surface morphological changes in grain growth, following the efficacy of each of the cleans, examining the residues left from etching and resist strips, to the planarization steps using reflow, spin-on-dielectrics, or CMP. There are important benefits throughout the process flow. All of these steps involve roughness on one scale or another.

To specify the roughness of a surface requires the determination of two quantities. These are the size perpendicular to the surface (amplitude of the roughness) and the size in the plane of the surface (wavelength of the roughness). The wavelength may be only one quantity if the roughness distribution on the surface is isotropic, or it may need to be specified in two or more directions . As SPMs are measurement tools, once the surface of interest is measured all of this information is available in the data. A particularly useful method for displaying all of this information is a graph of the power spectral density (PSD). The PSD of a surface is essentially just a plot of the amplitude of the roughness of the surface as a function of its spatial frequency.

To accurately measure the roughness on a surface requires a measuring probe which has high spatial resolution and a high aspect ratio at the end. It also requires a measurement technology which allows it to sense the surface at a high resolution without changing the surface. Presently, the best solution for this combination is the use of etched Si probes in the TappingMode™ of AFM operation. Traditional contact AFM interacts too strongly with many of the surfaces which need to be measured in semiconductor processing resulting in the modification of the surface during the measurement. Non-contact AFM lacks the spatial resolution required to measure the true surface roughness.

TappingMode operation provides a good combination of low vertical force, no lateral or frictional force, but yet operation in the repulsive region of the interatomic potential to retain the high spatial resolution that contact AFM offers. The etched single crystal silicon tips have a radius of curvature at the end which is something less than 5 nm and an overall included sidewall angle of 35 degrees, with some sharpening on the last 100 nm. Used in conjunction, the etched single crystal tips operated in TappingMode, provide the ability to measure features over the spatial wavelength bandpass of 4 nm to tens of microns. This provides some overlap with optical techniques on the long roughness wavelength end and extends to near atomic dimensions at the short wavelength end.

An important concern when measuring roughness on this scale is the condition of the tip. It is certainly possible to wear down or break off the end of a tip made of a brittle material such as silicon, or to pick up a particle attached to any type of tip. Tip characterization schemes are thus important considerations. One such scheme which is currently in use is the application of colloidal gold spheres to monitoring tip shapes. Imaging of the tip before and after measuring microroughness is a good check on its' condition. These spheres are available in diameters which cover the roughness amplitude range found, for example on silicon wafers, and therefore image the part of the tip which is being used in that application. Another useful indication of tip condition is a PSD plot from the data taken with the tip. If the tip has become flattened the high frequency information will be reduced in amplitude. On very hard surfaces repetitive measurements of the same area will show decreasing RMS roughness or a change in slope of the PSD curve to indicate a flattening of the tip. On soft surfaces this will indicate a modification of the surface.

As semiconductor integrated circuit technology moves to smaller and smaller dimensions on a lateral scale, it is also necessary to utilize thinner films with correspondingly smoother interfaces. This results in the need to monitor the roughness of smoother surfaces. As a result SPM systems which are intended for this application must have a very low noise floor. For example, the measurement of the roughness of todays typical incoming silicon wafers requires a noise floor on the order of 0.03 nm RMS over a 4 nm to 1 µm spatial wavelength bandpass. Over that bandpass typical incoming polished wafers show an RMS roughness of 0.04 to 0.08 nm.

Operation in ambient means that there is a surface oxide present on nearly all semiconductor related samples measured in these systems. Since there is a significant difference in the volume occupied by a silicon film and the oxide film it produces, it is likely that roughness measurements on silicon surfaces are not completely representative of the silicon surface before exposure to atmosphere. On the other hand, measurements of epitaxial silicon films grown on vicinal silicon (100) surfaces show very clearly the single (SL) and double (DL) atomic layer step heights and the smooth atomic terraces expected of these surfaces and seen in in-situ STM measurements of silicon homoepitaxy. While the AFM does not see the silicon dimer rows, both S_A and S_B type terrace edges are clearly seen and identified. These observations of the single layer step heights (0.14 nm high) and the sharp resolution of the meandering of the S_B terrace edges is evidence that the native oxide film is thin and conformal.

In GaAs homoepitaxy by MBE defects have been monitored and island growth has been observed in competition with step flow. In the heteroepitaxial deposition of compound films misfit dislocations are frequently formed at the interface between films with high interface stress resulting from abrupt changes in the lattice constants. These dislocations produce an effect on surface morphology of the growing film which is retained to significant thickness. The cross hatched pattern of these features has been observed at the surface of films of Si_xGe_{1-x} epitaxially grown on Si; at the surface of films of InAlAs grown on GaAs; and at the surface of InGaAs films grown on GaAs.

In the area of film growth or deposition, grain size and surface morphology have been measured on films of aluminum, polysilicon, TiN, various silicides, tungsten, and a variety of dielectric films. These films have been monitored through various processing steps and changes in grain size and/or surface morphology have been monitored. In many cases these measurements have been correlated with TEM and given consistent results.

Measurements after etching have shown irregularities in the form of stringers, blobs of material (probably polymer), and non-flat trench bottoms. AFM has been a good tool for monitoring etch process parameters and to guard against etch irregularities.

Planarization measurements are a natural for AFM since it is the only tool which can measure the small angles involved without sacrificing the sample. Very small angles can be measured over very small areas in glass reflow or SOG, or roughness over large areas can be monitored in CMP.

Power Spectral Density Calculation

Yale E. Strausser
Digital Instruments, Inc.
Santa Barbara, CA 93103

When applied to a data set of measured z(x,y) values the power spectral density function gives the spatial frequency spectrum of the surface roughness. This function provides a convenient representation of the amplitude of a surfaces' roughness as a function of the spatial frequency of the roughness. Here by spatial frequency we mean just the inverse of the in-plane spatial wavelength of the roughness features.

The PSDs are defined and calculated as follows:

$$PSD_{1D} = 1/l \, [\, \pi/2 \int e^{i(px)} z(x)\, dx \,]^2$$

$$PSD_{2D} = 1/A \, [\, \pi/2 \iint e^{i(px+qy)} z(x,y)\, dx\, dy \,]^2$$

Where l is the length of a one dimensional scan which acquired the data set, A is the area of a two dimensional scan which acquired the data set, p is the spatial frequency in the x direction, and q is the spatial frequency in the y direction.

The one dimensional PSD (PSD_{1D}), which results from a line measurement of z(x) such as would be obtained from a stylus profilometer, has units of length^3 and is typically presented as a graph of log of the PSD_{1D} on the y scale versus log of the spatial frequency on the x scale. The two dimensional PSD (PSD_{2D})which results from an area measurement of z(x,y) such as is obtained from a SPM, has units of length^4. The PSD_{2D} is either presented as a three dimensional plot or, in many cases, is angle averaged to provide a two dimensional plot of log PSD_{2D} versus log of the spatial frequency.

In a data set the spatial frequency bandpass is determined by:

1) the dimensions of the scanned area
    -this gives the lowest spatial frequency

2) the number of data points in a line
    -this gives the highest spatial frequency from the spacing between 3 successive points

3) there is also an instrument response function applied to the data which may selectively attenuate certain frequencies

  -e.g., a high radius, low aspect ratio tip will attenuate higher frequencies

The PSD is related to many of the other representations of surface roughness. The RMS value corresponding to a certain spatial frequency bandpass can be obtained by taking the square root of the integral of the PSD over that bandpass. The autocorrelation function and the PSD are a Fourier transform pair. This means that they are just different ways of expressing the same information and each can be calculated from the other. Some surfaces produce straight-line PSDs on log-log plots where the slop of the straight line is related to the fractal dimension of the surface. The PSD can also be calculated from the fractal representation of the surface.

The benefits to be gained from using PSD to report or specify roughness are in at least four areas. First of all it completely describes the roughness, describing the distribution of its' amplitude and of its' in-plane dimension (or wavelength). Second it brings to your attention any prominent roughness wavelengths. Next it points out the spatial wavelength bandpass of the measurement data. It is also a valuable estimator of instrument performance. Vibration frequencies creeping into the SPMs' operation show up as peaks in the PSD, any frequency selective filtering of the data will show up as a roll-off in amplitude at that frequency, etc. Single numerical value representations of surface roughness do not do these things. At the very least an RMS roughness value should have its' associated bandwidth reported along with it.

CORRELATION OF SURFACE STATISTICS BY AFM AND ANGLE-RESOLVED SCATTERING FROM SEMICONDUCTOR SUBSTRATES

E. Dan Hirleman
Mechanical and Aerospace Engineering Department
Arizona State University

Introduction:

The continuing decrease in characteristic feature size of integrated circuits is projected in the SIA Roadmap to reach 0.18 µm in the year 2001. Given the industry rule-of-thumb that contamination of the order of 1/4 the feature size and greater may be killer defects, in-line methods for *detection* of contaminant particles down to about 0.04 µm will be needed by that time. While the push to ever-smaller particles is clearly important, there will also be a need for rapid, in-line *identification* of relatively large particles and defects as a means of predicting the effects and determining the source of the contamination. These relatively large particles (larger than the characteristic feature size) have a very high probability of killing a chip and are therefore of considerable importance as well. A primary candidate technology for this problem will be wafer scanners based on optical scattering. Here the scattering signature (scattered light properties as a function of observation direction for given incident beam focus spot size, wavelength, angle, and polarization) will be measured using photodetector arrays, and contaminants will be detected and identified using pattern recognition schemes. However, with decreasing particle sizes the scattering signature of the contaminant/defect will become increasingly difficult to distinguish from the background scattering of the surface (IC pattern and/or microroughness). In that context then, a complete understanding of light scattering by the contaminant- and defect-free surface is a crucial component in any attempt to 1) predict lower size detectability limits, and 2) develop algorithms for optical detector array configurations in advanced instruments, and 3) support development of accurate defect identification as opposed to only detection. For most semiconductor surfaces there are wavelengths where surface topography unambiguously determines the background scattering signature. Since AFM measures, in theory, the surface topography, we are interested in AFM as an independent check on our measurement of the properties of substrate scatter. In this presentation, recent ASU efforts toward correlating AFM measurements with angle-resolved scatter (ARS) data will be discussed. The presentation will be based on results reported in Bawolek (1992) and Bawolek et al. (1993).

Summary:

The atomic force microscope (AFM) used in this study was a commercially-available unit. The probe that traced the sample was a pyramidal silicon nitride tip on the end of a silicon nitride cantilever bonded to a glass support. SEM micrographs of the tip shown in Bawolek et al. (1993) were used to estimate the tip diameter as 50 nm. The AFM measurements were taken on 400 x 400 grids with scan steps of 2.5, 5.0, and 25 nm. The vertical range of the instrument was set to 100, 200, 300, 400, or 500 nm depending on the sample. Because the AFM does not directly provide 2-D z(x,y) data (adjacent scan lines have some vertical offset that must be compensated thereby introducing additional experimental uncertainty), we computed 2-D power spectral densities (PSD) from 1-D versions. The 1-D PSD were obtained by taking the Fourier transform of the 1-D autocorrelation function calculated by summing all traces. The autocorrelation function was then fit with a parametric model (ABC model), and then a closed form analytical expression for the 2-D PSD was obtained. Also, we used fractal analysis to estimate the PSD and determine fractal dimensions for the samples.

In this research we concentrated on three samples each of two types of substrates common in the integrated circuit industry -- polysilicon and aluminum. For the polysilicon samples (deposited on thermal oxide by chemical vapor deposition), rms roughness values of 42, 18, and 3 nm with 1/e correlation lengths determined from AFM autocorrelation functions of 100, 85, and 25 nm, respectively, were used. The aluminum samples had rms roughness values of 17, 3.8, and 3.2 nm with 1/e correlation lengths of 200, 40, and 35 nm, respectively.

The light scattering measurements were made on the ASU scattering apparatus discussed in detail by Bawolek et al. (1993). HeNe and Ar lasers were used to illuminate the samples with 632.8 and 488 nm radiation. The laser beams were focused to nominally 10 μm diameter spots ($1/e^2$ irradiance) and scanned across the surface. The scattered light was collected using a photodetector array consisting of 32 rings and 32 wedge-shaped elements. The detector was centered on the specular beam (45 degree incidence for 632.8 and 76.3 degrees for 488 nm), and subtended a conical region with nominally 60 degree half-angle. Measurements of surface scatter were taken by scanning a 2 mm x 2 mm area in 10 μm steps, and averaging the detector outputs obtained at each step. The polarization of the incident beam could be rotated, and we report measurements for both S and P incident beam polarization states. Because of the ring shaped detectors, we measure both in-plane and out-of-plane scatter and therefore do not use polarization analyzers at the detector.

After calculating the 2-D PSD for the surfaces from AFM measurements, we then used vector scattering theory to predict the angle-resolved scattering-signature, both mean value and variations with position on the surface. Some results showing the best agreement between theory and experiment for mean scattering signatures are presented in Fig. 1 along with measured rms variations in Fig. 2. The qualitative agreement in Fig. 1 is reasonable, including prediction of the cross-over angle of the scattering signature from S and P incident polarization states. We attribute the quantitative discrepancies to internal scatter in our instrument due to a very small sample-to-detector distance as is optimal for particle scattering studies. We are in the process of modifying the instrument to reduce this effect.

References:

E. J. Bawolek (1993). "Light scattering by spherical particles on semiconductor surfaces," Ph.D. dissertation (Arizona State University, Tempe AZ)

E. J. Bawolek, J. B. Mohr, E. D. Hirleman, and A. Majumdar (1993), "Light Scatter from Polysilicon and Aluminum Surfaces and Comparison with Roughness Statistics by AFM," *Applied Optics*, V. 32, pp. 3377-3400.

Acknowledgments:

Major contributions of Dr. E. J. Bawolek of Intel and Dr. J. B. Mohr of Motorola are gratefully acknowledged. Research supporting this presentation was partially funded by the Semiconductor Research Corp. under contract 91-MJ-153.

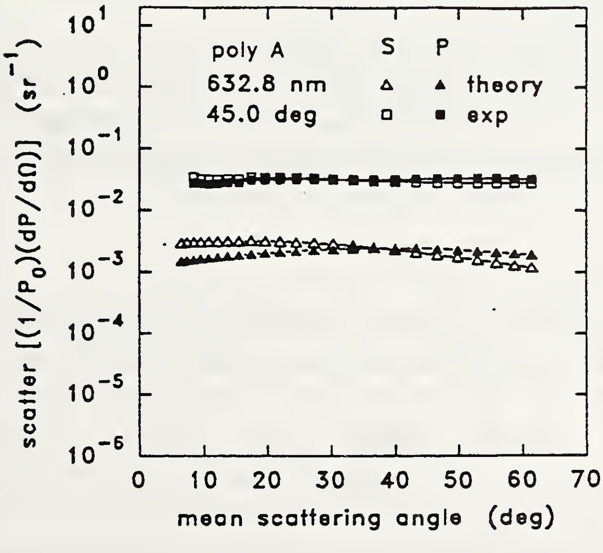

Fig. 1. Surface-averaged optical scatter from polysilicon sample A (42 nm rms roughness, 100 nm 1/e lateral autocorrelation length) for 632.8 nm illumination at 45 deg incident angle with a nominal 10 μm focus spot. Angles correspond to mean of ASU ring detectors.

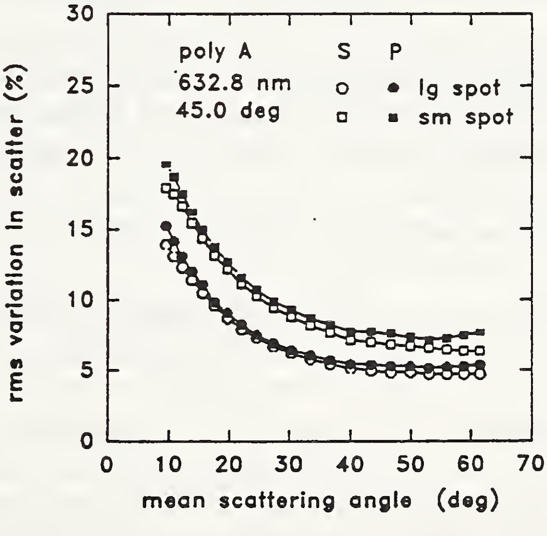

Fig. 2. Measured rms variation in optical scatter for the experimental conditions of Fig. 1. The small and large spot sizes (diameter at $1/e^2$ irradiance points) were nominally 10 μm and 20 μm, respectively.

Overview of Dimensional Measurements and Comparison with Other Technology

Robert R. Hershey
SEMATECH/Motorola, Inc.

Dimensional Metrology in the Semiconductor Industry typically centers around photolithography and is driven by feature size and feature placement. The primary dimensional features of interest are lines, spaces and holes as well as their relative placement to one another both within the current layer and between subsequent layers of processing. Since all modern semiconductor manufacturing is done using step-and-repeat wafer exposure systems, these features must be measured both on the wafer and on the mask used to generate the wafer.

There are three major differences between wafer and mask metrology. First, wafer features are either the same size or up to 5X smaller than on the mask. (Within the next 10 years, wafer critical dimensions are expected to shrink to 120nm.) Second, feature aspect ratios on wafers are rapidly approaching 8:1 which contrasts sharply with the 1:1 or lower aspect ratios observed on masks. Finally, masks, unlike wafers, are used in transmission thus simplifying the metrology somewhat.

The requirement to measure features both on the wafer and on the mask used to generate the wafer divides dimensional metrology into two broad categories, namely wafer-level metrology and mask-level metrology.

Wafer-level metrology will continue to be driven by the critical dimension (CD) and overlay requirements of advanced Litho Processes. Currently output metrology based on scanning electron microscope images for CD and "box-in-box" brightfield optical overlay measurement systems are used almost exclusively for 0.5um process control and are expected to dominate at 0.35um design rules.

For overlay, brightfield optical metrology is expected to be the technique of choice through 0.12um design rules provided process integration issues do not preclude the use of features large enough to be reliably detected by this technique. Successful overlay control will hinge on the industries ability to develop targets which exhibit reduced sensitivity to processing. Key process issues to be addressed are target asymmetries associated with resist coat over topography, radial asymmetry of metal and dielectric films deposited on the wafer and the design of measurement structures which are more robust to chemical mechanical polish (CMP).

At present, CD SEM measurement capability is marginally capable at 0.5um design rules. At 0.35um and below, the use of high throughput CD SEMs is expected to bridge the gap between marginal measurement capability and advanced process control requirements by improving estimates of process characteristics through averaging and measurement of actual circuit features. At 0.25um it will be necessary to begin driving CD control through the use of input metrology. These control methods will require the development of new sensor technologies to monitor resist coat thickness and uniformity, photo-active compound (PAC) / photo-acid generator (PAG) and solvent concentration, pre/post bake temperature and uniformity, develop uniformity and 100% sampling of wafers following develop to determine within lot and within wafer variation of CDs. The driver behind this proliferation of sensors is the realization that complex interactions between the incoming wafer, coat, bake, expose and develop frequently can not be corrected by subsequent processing without adversely effecting device performance characteristics. In addition, there is strong pull from industry to develop a more accurate and precise method of measuring resist and final CDs for estimating process biases.

Mask-level metrology is currently making extensive use of confocal optical measurements for CD and faces its biggest challenge in obtaining statistically significant amounts of data to better understand systematic errors in the manufacturing process. The mask industry is poised and ready to turn to scanning electron microscopes or scanning probe microscopes should better capability be required; however, widespread use of SEM and AFM is not expected for at least 5 years.

Mask-level feature placement metrology is expected to continue to rely on interferometric stage techniques through the end of the decade. Some research is currently underway to develop better closed-loop control of the mask writing equipment which may make separate pattern placement metrology less critical.

Streamlining the flow of large amounts of data from highly automated CD and overlay instrumentation is another major impediment to easy and efficient implementation of measurement systems. Standardization on a GEM messaging set for use with CD, overlay and mask metrology equipment is required to address this issue.

Dimensional Measurement by Scanning Probe Microscopy

BY

Yves Martin
IBM Research Division
T.J. Watson Research Center
P.O.Box 218
Yorktown Heights, NY 10598

Abstract

Scanning Tunneling Microscopy and Atomic Force Microscopy have demonstrated unique capabilities for measuring dimensions of features in the nanometer regime. Measurement of height of small lines and trenches, or of width for very shallow features, can be accomplished with an accuracy of the order of the nanometer, in air, and without special sample preparation.

However, tip shape often restricts measurements when a sample possesses structures with large vertical to horizontal aspects ratios, or near-vertical sidewalls {1}. The topography or profile of structures is not mapped by a single point of the tip any more, even if the tip is thin and long. Software deconvolution algorithms seldom restore the true sample profile from the measured data. And most important, the accuracy achieved for **width** measurement is very limited.

New methods {2-4} have been proposed, that allow sensing and profiling of vertical sidewalls, using different tip shapes and new tip control servo systems. The new two-dimensional servo-control system inherent to these new methods suggests the acronym 2D-STM or 2D-AFM to designate them. They may ultimately deliver capabilities that compete with Critical-Dimension Scanning-Electron-Microscopy (CD-SEM). Our own activities have revealed that repeatability in measuring width of a line or trench by 2D-AFM can approach one nanometer. Furthermore, line or trench width is obtained as a function of height. Among other unique capabilities, the measurement of sidewall angles and the mapping of small sidewall undercuts is made possible in a non-destructive way, in contrast to traditional cross-sectional SEM measurements, where the sample needs to be sliced to permit side observations.

References

1. H.Yamada, T.Fujii and K.Nakayama, "Linewidth measurement by a new STM", Jap.J.Appl.Phys. 28, 2402 (1989)
2. A. Sato, Y. Tsukamoto, M. Baba and S. Matsui, "Measurement of sidewall roughness by scanning tunneling microscope", Jap. J. of Appl. Phys. 30, 11B, 3298 (1991).
3. D. Nyyssonen, L. Landstein, and E. Coombs, "Two-dimensional atomic force microprobe trench metrology system", J. Vac. Sci. Technol. B9, 6, 3612 (1991)
4. Y. Martin and H.K.Wickramasinghe, "Method for imaging side-walls by Atomic-Force-Microscopy", submitted to Appl.Phys.Lett. Nov.1993

CD–SXM imaging & metrology

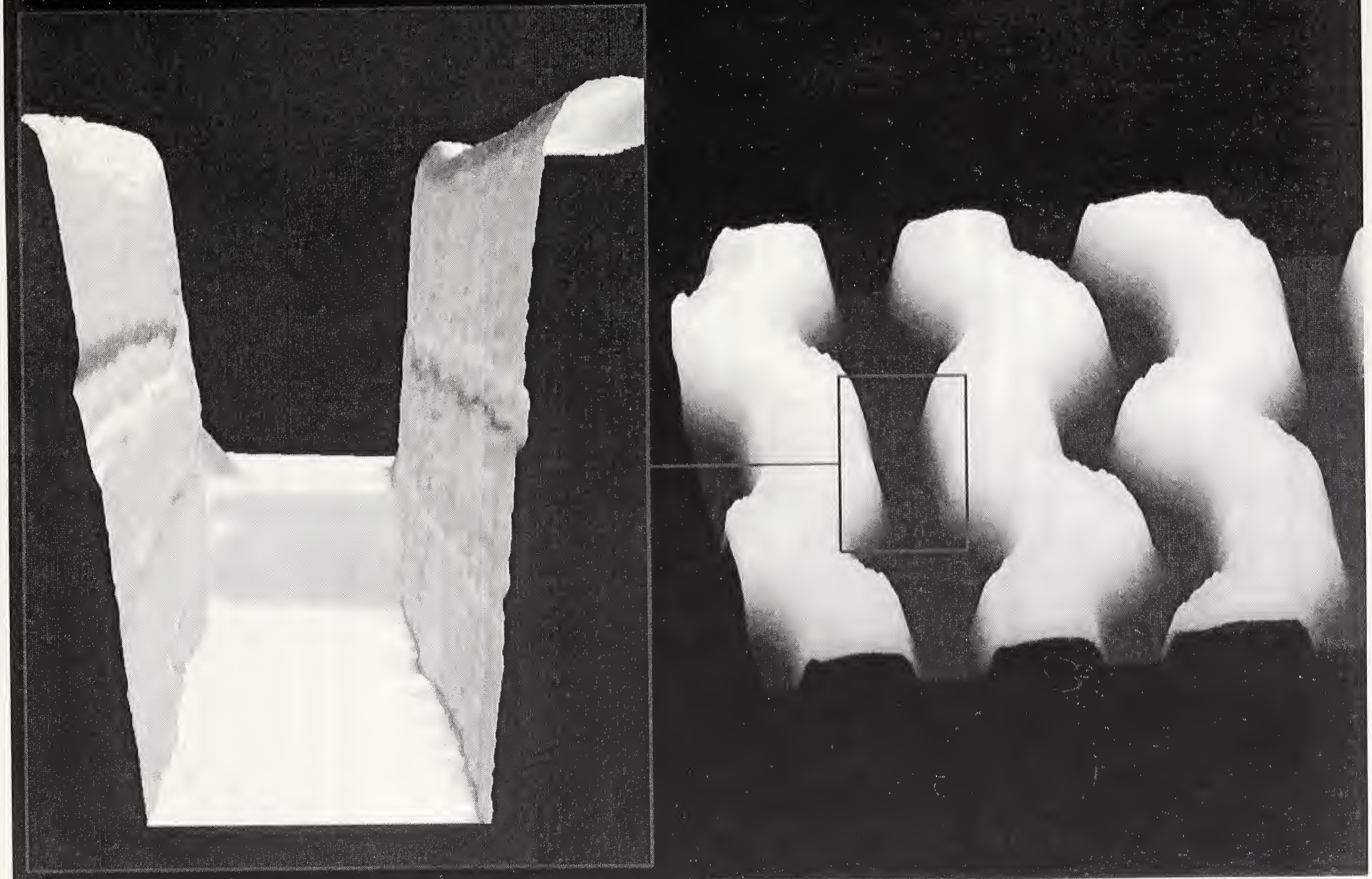

RIE lines height=1μm ; bottom width=0.45 μm

IBM Research Y. Martin, H.K. Wickramasinghe

Critical Dimensional Measurements: Test Structures, Metrology Instrument Correlations, and Calibration Techniques.

Herschel Marchman
AT&T Bell Laboratories, 600 mountain Ave., Murray Hill, NJ 07974

The ability to perform accurate dimensional measurements is key to the development of new submicron device fabrication processes and the monitoring of existing ones. To improve measurement accuracy, standard reference materials for each type of feature pattern are needed in order to calibrate metrology instruments. Unfortunately, traceable standard reference materials do not yet exist for submicrometer critical dimension (CD) metrology. To help initiate progress in this area, a set of test reticles (see Figure 1) has been fabricated to study the physical phenomena affecting accuracy and precision of three-dimensional measurements on the nanometer scale and to serve as in-house calibration standards.

The first member of the set, known as the Lateral Resolution Tester, was made with relatively flat chromium features having linewidths as narrow as 200 nm to assess the lateral resolution of each instrument. The PSM Feature Tester contains many types of three-dimensional features often encountered on advanced optical masks and is used for determining the effect of structure topography and composition on resolution and accuracy. The Herschel Tester possesses periodic apertures having different depths and widths for exploring the effect of feature width on depth measurement and depth on lateral CD measurement. All of these test structures have been brought together to produce a new calibration/test vehicle known as the Round Robin Reticle (RRR). This reticle will be used for a round robin comparison of measurements taken with various metrology tools at different laboratories across the nation.

A comparison of currently available metrology systems will be made using experimental data obtained from the test reticles. These current techniques include conventional optical, scanning confocal, coherence probe, scanning electron, and atomic force microscopes. Improvements to current CD metrology techniques using an atomic force microscope and a new generation of imaging probes developed in-house will also be presented.

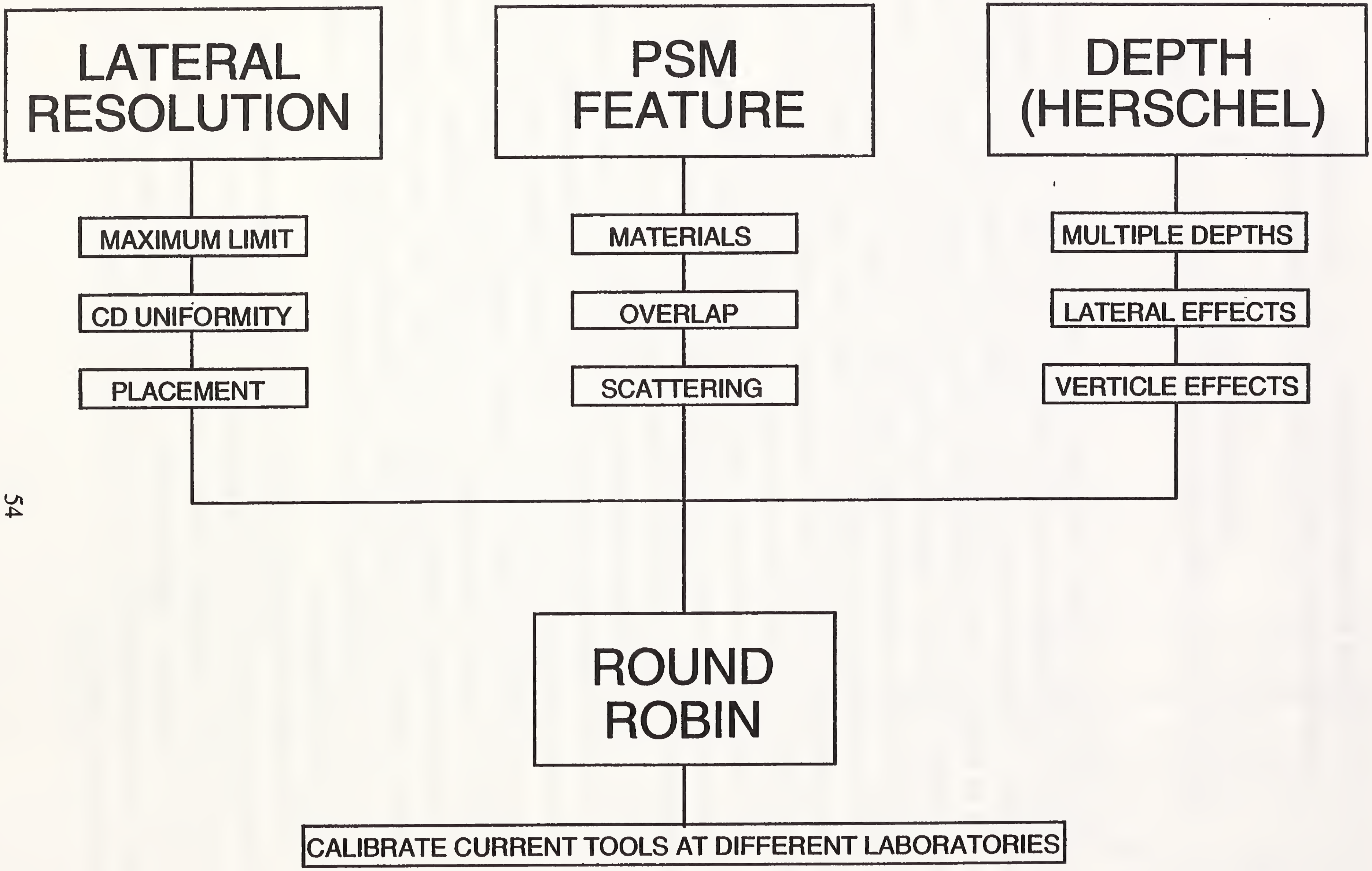
LATERAL RESOLUTION
MAXIMUM LIMIT
CD UNIFORMITY
PLACEMENT
PSM FEATURE
MATERIALS
OVERLAP
SCATTERING
DEPTH (HERSCHEL)
MULTIPLE DEPTHS
LATERAL EFFECTS
VERTICLE EFFECTS
ROUND ROBIN
CALIBRATE CURRENT TOOLS AT DIFFERENT LABORATORIES

Figure 1 - Organizational chart of the reticle set.

Overview of Industrial Needs for Local Electrical Characterization

Larry Larson
Implant Program Manager

Michael Duane
Phase 5/6 Integration

SEMATECH, 2706 Montopolis Drive, Austin TX 78741

512-356-7145
Larry.Larson@SEMATECH.org

512-356-7827
Michael.Duane@SEMATECH.org

This joint discussion will give an overview of present and future electrical characterization needs as a function of the needs of the user.

Characterization for process control is generally one parameter sampled in multiple sites over a single test wafer. This test is driven by quick turnaround and sensitivity. The measure of sensitivity is driven by both competitive standards and by precision/tolerance ratios for the specific process. For relatively high doping levels the standard is competitive, where within wafer uniformities less than 0.5% are achieved and wafer-wafer repeatability stays less than 1%. For low dose characterization, the precision/tolerance ratio is marginal and there is a need for a fast-turnaround (15-30 minutes/wafer) method for precise characterization.

One-dimensional characterization, perhaps as a sub-set of two dimensional characterization, is driven by the needs of the development users, both those responsible for producing the shallow junctions and those planning the devices which use the layers. The National Roadmap details our expectations of the doping levels and depths to be met. A copy of the Doping Requirements as defined in 1993 is the page following this text. The Implant Program has a project in place to achieve the 0.18 micron technology S/D junction depth of 40nm. This means that on a research level, we have a need to be able to measure a 40 nm junction to an accuracy on the order of 10%. The profile of that layer will need to be measured to the accuracy needs of the TCAD modelers. This will be demonstrated on early results profiles which show that level of process achievement. Both of these dimensional requirements are research needs at SEMATECH right now, and are expected to be routine for development efforts in 1998.

Two dimensional profiling has exactly the same needs for depth and profile accuracy. These are convoluted with the spatial dimensions of the devices that are to be developed. The targeted devices for 0.18 micron will be discussed and the measurement needs for developing those devices will be derived from those feature sizes. The second page following this is the draft metrology roadmap for doping. The timelines and numbers on this roadmap follow from this type of discussion. These plans are being analyzed for a improved National Roadmap planned for the end of this year.

DOPING REQUIREMENTS

	1992	1995	1998	2001	2004	2007
Physical Gate Length (µm)	0.35	0.25	0.18	0.12	0.10	?????
Equiv DRAM	64Mb	256Mb	1Gb			
S/D Characteristics						
S/D Junction Depth nm	100	60	40	25	10	
Structure	"LDD"	"LDD"	HCS	HCS	HCS or Si Based Hetero-junction	Note 1
Surface Concentration (cm^{-3})	10^{18}	10^{18}	7–10x 10^{17}	5–10x 10^{17}	—>	Note 2
Away from Channel (cm^{-3})	$\geq 10^{20}$					Note 2
Channel Doping (cm^{-3})	mid 10^{17}	6x 10^{17}	8x 10^{17}	10^{18}	10^{18}	Note 3
Retrograde Well						
Peak Concentration (cm^{-3})	4x 10^{17}	6x 10^{17}	8x 10^{17}			
Peak Depth (nm)	800	500	350			
Crystal Defects (cm^{-2})	0.032	0.017	0.001			
Junction Leakage		1 fA/µm				

1. LDD - Lightly Doped Drain structure
   HCS – Hot Carrier Suppressed (elevated source/drain).
2. Peak concentrations for S/D and channel at surface.
3. High channel concentration may degrade carrier mobility. May need more complex structure Aoki et. al 1990 IEDM), or Gel[2].

T-CAD + Materials and Bulk Processes
2-D Profiling Metrology

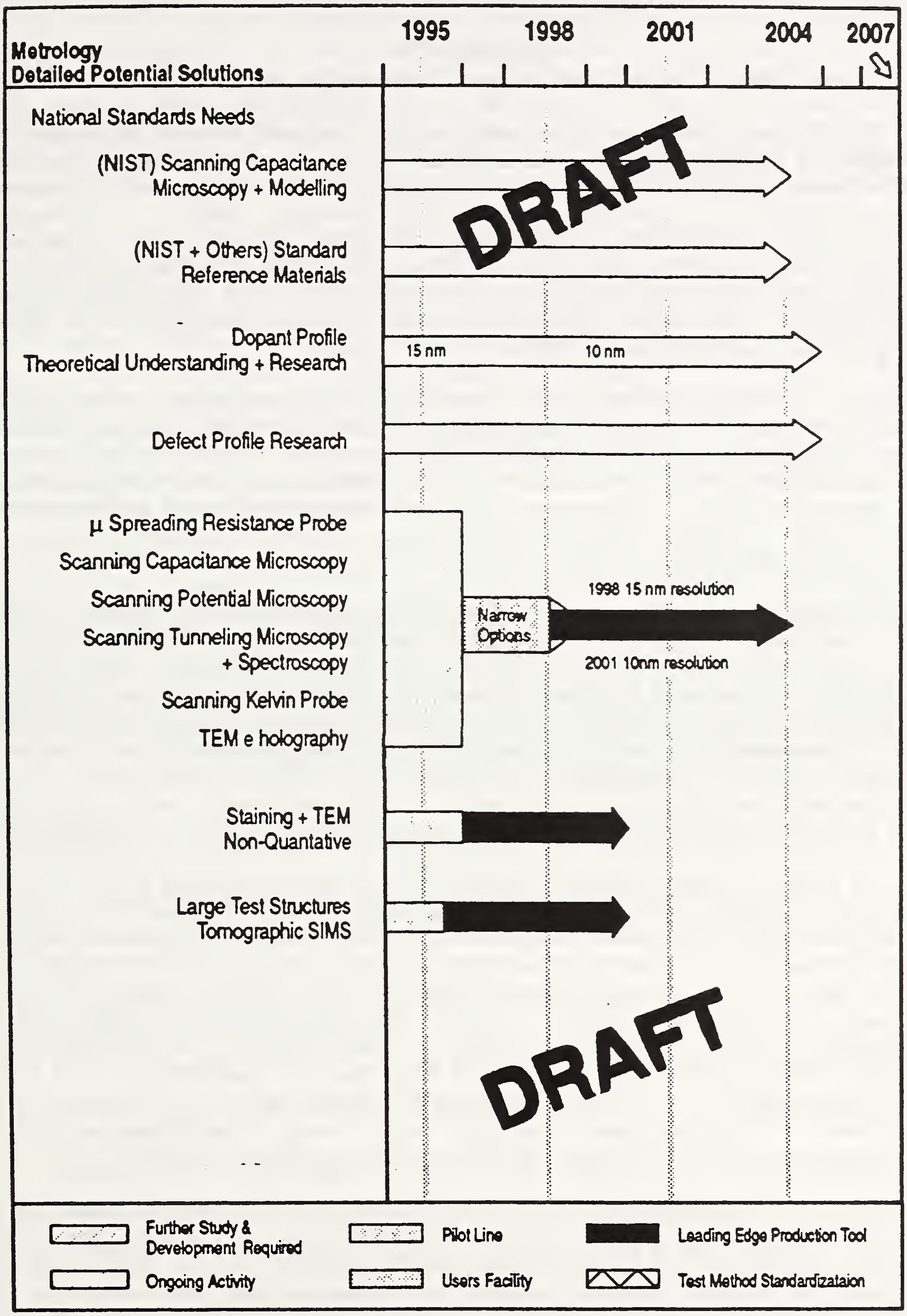

DRAFT
DRAFT

Junction and Dopant Profiling Using Scanning Tunneling Microscopy and Spectroscopy

C.K. Shih
Department of Physics, University of Texas, Austin, Texas 78712

As the trend in device *miniaturization* in microelectronics continues, accurate information of junction location and doping density in *all dimensions* has become most critical for the future development of faster and higher density devices. Conventional characterization methods such as Capacitance-Voltage (C-V), Secondary Ion Mass Spectroscopy (SIMS), and Spreading Resistance Probe (SRP) provide only one-dimensional information with a resolution on the order of 5 nm or larger. Such unfulfilled needs have stimulated much research in the scanning probe microscopy community aimed at providing nanometer-scale resolution in dopant profiling both laterally and vertically. This paper focuses on the current effort in the junction and dopant profiling using scanning tunneling microscopy and spectroscopy.

I will first provide a brief review of the current status-of-the-field from which I wish to identify key factors underlying the most important characteristics for dopant profiling - spatial resolution, dynamic range, and activated versus total dopants. Furthermore, I will try to provide a personal view of the roadmap from where we stand now to the ultimate goal: precise delineation of junction and dopant profiling in all dimensions with nanometer resolution and a high dynamic range in *real* devices. Hopefully, this will stimulate more detailed discussions and lead to a collective view of the roadmap.

In reviewing the current status of the field, I arbitrarily separate the general issue of dopant profiling into two steps: (1) precise delineation of the *pn* junction, and (2) quantitative determination of the doping density. In terms of the *pn* junction delineation, the progress during the past three years has been very significant. Precise delineation of pn-junctions including a clear identification of the depletion region has been demonstrated in both Si [1,2] and GaAs [3-6] model devices. There appears to be no fundamental difficulty in applying this to real-devices as long as the sample surface can be appropriately prepared. This ability should allow one to obtain zeroth order information regarding the junction profile for ultra-small devices, such as the a clear delineation of the lightly-doped-drain (LDD) boundary in the channel region of a MOSFET.

However, such a zeroth order information, is not sufficient for future industrial needs. The real challenge lies in the quantitative determination of local dopant density as a function of position with high spatial resolution and dynamic range. I will review the current progress according to three different approaches: (1) dopant-selective-etching, (2) direct dopant counting using STM, and (3) indirect determination of dopant concentration from local tunneling characteristics. In the first approach, the dopant concentration is deduced from the etched-depth based on a very carefully calibrated concentration-dependent etch rate. A similar approach has been used in the TEM community. Although STM researchers at NTT have claimed a spatial resolution of 10 nm and a dynamic range of $1 \times 10^{16} / \mathrm{cm}^3$ to $1 \times 10^{19} / \mathrm{cm}^3$ [7], similar performance has never been reported elsewhere. On the other hand, it has been found in most of the TEM studies that a quantitative determination of concentration $< 1 \times 10^{17} / \mathrm{cm}^3$ is very difficult to achieve [8].

The second approach, direct counting of each individual dopant, has been demonstrated in modulation-doped GaAs devices by researchers at the IBM-Zurich lab when the dopant concentration is $1 \times 10^{18} / \mathrm{cm}^3$ or above [9]. *However*, this approach is not applicable to Si-devices. In the UHV-cleaved GaAs(110) surface, the intrinsic surface states are outside the bulk band-gap. Therefore, they will not mask the observation of the effects of ionized dopants. Unfortunately such an ideal situation hardly exists in Si. Nevertheless, this work did reveal a clear correlation between the apparent topographic height and the local dopant concentration. Thus, it is presumed that the local tunneling characteristics depend on the local doping density. This leads to the third approach which has been undertaken in my own group at UT.

By using MBE-grown, modulation-doped GaAs samples, we have also observed a definitive correlation between the apparent topographic height and the doping level: abrupt change from $5x10^{18}$ to $5x10^{17}$ was observed to within 5 nm and from $5x10^{17}$ to $5x10^{16}$ to within 10 nm [10]. The sample surface was prepared by ex-situ cleave followed by sulfur-passivation. The underlying mechanism for observation of the correlation between the apparent topographic height and the doping density remains an open question. Nevertheless, this approach appears promising. The issue now is whether or not one can obtain similar result in Si-devices.

For development of any new characterization method for dopant profiling, it is very important to clearly identify the key factors which determine the spatial resolution and the dynamic range. STM is intrinsically a high spatial resolution method since the tunneling current is localized within 1-2 nm. Depending on how STM is applied, other factors may also play important roles. For a method utilizing the change in the local tunneling characteristics to deduce the dopant concentration, these include the surface Fermi-level pinning, the tip-induced band bending effect, and the Debye-length. In terms of the dopant-selective etching approach, careful calibration of the etch-rate is the first critical factor. In addition, the deeper the etching, the more the probe tip shape will cause the deterioration of the spatial resolution. Furthermore, since the concentration-dependent etch-rate is a manifestation of the local electrochemical potential, the Debye-length may also affect the spatial resolution.

It appears that all the methods that I have reviewed probe only the activated dopant concentration. A search for methods which probe the total dopant concentration should be pursued in order to have important impact in the modeling of doping processes. Furthermore, all the methods discussed here have been applied only to model devices which were designed specifically for demonstration purposes. The sample preparation procedure may or may not be applicable to studies of real-devices. In the development of a new characterization method, it is necessary to corroborate results with those of other techniques in order to establish quantitative standards. In addition, ambiguity and complexity in the data interpretation must be minimized. Finally, ease-of-use and quick-turn-around are important considerations in an industrial setting.

REFERENCES

[1] S. Kordic, E.J. van Loenen, and A.J. Walker, IEEE Electronic Device Lett. **12**, 422 (1991).

[2] E.T. Yu, M.B. Johnson, and J.-M. Halbout, Appl. Phys. Lett. **61**, 201, (1992).

[3] R.M. Feenstra, E.T. Yu, J.M. Woodall, P.D. Kirchner, C.L. Lin, and G.D. Pettit, Appl. Phys. Lett. **61**, 795 (1992)

[4] J.A. Dagata, W. Tseng, J. Bennett, J schneir, and H.H. Harary, Appl. Phys. Lett. **59**, 3288 (1991); Ultramicroscopy **42**, 1288 (1922).

[5] S. Gwo, A.R. Smith, C.K. Shih, K. Sadra, and B.G. Streetman, Appl. Phys. Lett. **61**, 1104 (1992).

[6] A.R. Smith, S. Gwo, A. Shih, K. Sadra, B.G. Streetman, and C.K. Shih, Proceedings of PCSI-21, to appear in J. Vac. Sci. and Technol.

[7] T. Takigami and M. Tanimoto, Appl. Phys. Lett. **58**, 2288 (1991).

[8] J. Liu, M.L.A. Dass, R. Gronsky, J. Vac. Sci. and Technol. B **12**, 353 (1994).

[9] M.B. Johnson, H.P. Meier, and H.W.M. Salemink, Appl. Phys. Lett. **63**, 3636 (1993).

[10] A.R. Smith, A. Shih, B.G. Streetman, and C.K. Shih, unpublished.

AFM Characterization of VLSI Devices

Gabi Neubauer and Andrew Erickson*
Intel Corporation, Materials Technology Dept., Santa Clara, CA 95052
*University of Utah, Dept. f. Electr. Engineering, Salt Lake City, UT 84105

Introduction

Over the last years, an increasing need has been identified for a direct two-dimensional measurement scheme for dopant concentrations in semiconductor devices to provide accurate knowledge especially for calibration of process modeling. Up to now, quantitative 2-D information could only be inferred from one-dimensional dopant level measurements via SIMS and SRP. A large variety of different approaches have been taken to close this gap experimentally (1): these include developments of different staining or etching procedures which are sensitive to concentration and type of electrically active dopants; development of SIMS methods, such as angle lapping and employment of tomography techniques, for measuring chemical dopant distributions; and methods to measure electrical properties, such as capacitance, contact resistance and others. This last area has largely benefited from the development of the scanning probe technology over the last decade, and derivatives of both of the principal scanning probe techniques, i.e., Scanning Tunneling (STM) and Atomic Force Microscopy (AFM), have been applied. We have extended our earlier application of AFM imaging of VLSI cross sections and are reporting here our first results on characterization of electrical, i.e., capacitance, properties on implanted annealed silicon wafers.

Experimental Setup

Our experiments were conducted on a Digital Instruments Nanoscope III Large-Stage AFM, operated in air. A feedback network ensures scanning of the probe tip under constant repulsive force and provides the topography information for the sample surface. Sample preparation was similar to standard metallographic SEM cross section preparation: A glass cover slide was attached to the specimen to protect the top layers; grinding and polishing involved using increasingly higher grades of polishing papers and finished with a final polishing step with Syton for 30 seconds. Tip and part of the cantilever substrate were coated with ~300-500 Å of Cr. A thin native oxide layer, forming on the cross section due to the operation in air serves as a thin insulator between coated tip and sample. Capacitance measurements were accomplished by an RCA capacitance sensor circuitry which was originally designed for the RCA Video disk player. It's operation is based on a 915 MHz oscillator driving a resonant circuit, which is tuned in part by the external capacitance to be measured. As the resonant frequency is moved off the oscillator frequency by the external capacitance, the amplitude of oscillation is decreased. The peak oscillation of the resonant circuit is detected and, rectified into a DC voltage, forms the sensor's output. An AC bias is applied to the sample (probe tip at ground) and alternately depletes and accumulates the surface region, thus modulating the surface capacitance under the tip at the bias frequency.

The RCA sensor output is then fed through a lock-in into the auxiliary channel of the AFM, and topography and capacitance data are recorded simultaneously. With the AC bias at >100kHz and ±10V, our technique scans the entire C-V curve and certainly does not extract the quality of information provided by full C-V curves. However, we believe that our results should be less dependent on shifts in the flat band voltage due to oxide or surface charges.

Results

Our work presented here is an extension of our AFM applications on imaging of VLSI cross sections. In that earlier work we concentrated on imaging of cross sections for line width and thickness measurements and also attempted junction delineation by chemical staining. Both these results will be briefly discussed in the presentation. Our work on capacitance measurements has concentrated on a feasibility study of our AFM large stage setup and dealt with measurements on cross sections of blanket implanted and annealed Si wafers. Results will be presented on capacitance data of several B, As, and P implants, which were acquired simultaneously with topography data.

Discussion and Outlook

All of our results obtained so far are qualitative only. Comparison of the micrographs show a clear correlation between topographical features, such as the glue/Si interface, and capacitance signals. As expected, the capacitance signal decreases in the highly doped region of the silicon and has a sharp increase at the glue edge. In addition, the obtained one-dimensional sections through our capacitance scans show a good agreement of total dopant implant depths with those obtained from SIMS depth profiles. Further work on this project will have to address several limitations of our setup: The three-dimensional geometry between probe tip and surface region is not addressed at all and extensive modeling will have to be introduced. Also, nonlinear responses can be expected from the RCA sensor for large ΔC, thus limiting the dynamic range of capacitance changes, and dopant concentrations, which can be measured. Several approaches are planned for the future: for the capacitance setup, we want to measure a variety of blanket implanted wafers with no junctions, which differ in dopant dose, implant energy and annealing temperature; we also want to employ the tapping/ pseudoattractive mode setup to enable capacitive force, rather than capacitance measurements. In a parallel approach, we are planning to revisit our experiments with etch delineation. Finally, we will try to explore other quantitative measurement schemes, if time permits, through cooperation with other research groups.

Acknowledgments

We would like to thank Joe Kopanski (NIST) and Clayton Williams (Univ. of Utah) for their advice and assistance in bringing our project up to date.

References

(1) R. Subrahmanyan, J. Vac. Sci. Tech. **B 10** (1), 358 (1992).

Quantitative Inversion of Scanning Probe C-V Data for 2D Impurity Dopant Profiling

Y. Huang and C.C. Williams
Department of Physics, University of Utah
Salt Lake City, Utah 84112

The Scanning Capacitance Microscope (SCM) has been applied to the problem of measuring 2D dopant profiles near the surface of silicon. By performing "local" capacitance-voltage (C-V) measurements with a nanometer scale tip near a sample surface, a characteristic C-V curve is obtained which may be related to the "local" dopant density. The inversion of the C-V data to dopant profile is a challenge due to several factors. These factors include the fact that the magnitude of the measured capacitance is very small (typically less than one attofarad). While such capacitances can be measured, such sensitivity cannot be reached with millivolt probing voltages. The measured C-V curves cannot therefore be considered as true differential capacitance curves. Modeling of the measurement is also challenged by the fact that the depletion region below the tip is three dimensional, and the exact tip shape, size and charge state are, in general, unknown.

In spite of these and other challenges, it has been demonstrated that SCM C-V measurements scale monotonically with dopant density. Furthermore, the local C-V measurements can be performed with good repeatability. This repeatability condition is very significant, since measurements on unknown samples may be directly compared with measurements on known samples (with the same tip). Recently, we have made a first attempt at quantitatively inverting the local capacitance data acquired on a real VLSI test structure to obtain a lateral dopant profile. On the particular test structure analyzed in this study, the dopant density varies by approximately 4 orders of magnitude over a distance of 200 nanometers. Since absolute capacitances cannot be measured on this small scale, the dopant profile obtained by the SCM in the lightly doped region is constrained to the known value of the dopant density in that region. If this constraint is used, the rest of the measured profile matches the simulated profile to first order. A discussion of these results and the models used to invert the SCM data to dopant profile will be discussed.

*This work is supported by the Semiconductor Research Corporation

Scanning Capacitance Microscopy For Profiling PN-Junctions in Silicon

Joseph J. Kopanski, Jay F. Marchiando, Jeremiah R. Lowney and David G. Seiler

Semiconductor Electronics Division
National Institute of Standards and Technology
Gaithersburg, MD 20899

The NIST scanning capacitance microscope (SCM) combines an atomic force microscope (AFM) with a high sensitivity capacitance measurement. A metallized AFM tip, separated by an air gap and oxide layer from a semiconductor, is used to form a metal-insulator-semiconductor (MIS) capacitor. As the cantilever tip of the AFM is scanned over a semiconductor surface, topography and capacitance are measured simultaneously, permitting capacitance measurements limited in spatial resolution by the tip radius. The RCA videodisc sensor is used for capacitance detection.

Our ultimate goal is to use SCM to profile pn junctions in silicon with 20 nm spatial resolution. The Semiconductor Industry Association Technology Roadmap has identified junction dopant profiling on this scale as an essential metrology for the development of future generation integrated circuits by providing feedback for process development and control, and for TCAD models. Other potential applications of SCM include mapping and manipulation of the charge distributions on insulators, and mapping of the native and process-induced lateral variations in the electrical properties of bulk and layered semiconductor materials. The emphasis of our program is to develop the measurement techniques, capacitance sensor calibrations, and theoretical interpretation that are essential for SCM to become a practical method of junction profiling by the semiconductor industry. In keeping with this goal, we have modified an existing commercial AFM to simultaneously operate as a SCM in air. Metallized commercial AFM cantilevered tips are used. Our early work has concentrated on data acquisition techniques and interface of the sensor to the AFM with high sensitivity and low noise.

Equally important as the SCM measurements to obtaining highly accurate junction profiles, is the modeling and interpretation of the measured data. SCM measures the capacitance between a nominally hemispherical SCM probe and the planar semiconductor surface, and involves the charge distribution within the semiconductor as well as on the surfaces. Thus, the conventional one-dimensional parallel plate model for C-V profiling of semiconductors is not appropriate and a numerical solution of a nonlinear Poisson equation in three-dimensions is necessary. The research problem is to provide the optimal convergence techniques that are needed when iterating to self-consistency. The output of the model, from a given dopant profile in silicon (Fig. 1a), is the corresponding potential distribution (Fig. 1b), from which the differential capacitance may be determined.

Initial measurements with SCM have been made on silicon with a periodic structure consisting of highly p-type doped, 4.8-μm-wide, lines covered with 10 nm of oxide alternating with lightly n-type doped lines covered by a slightly thicker oxide. An AFM image of the test structure, Fig. 2a, shows the steps in the oxide at the junction to be about 6 nm high. A differential capacitance image, Fig. 2b, was acquired simultaneously with the AFM image. The differential capacitance image was generated from the response of the sensor to a 2 V_{pp} 80 kHz signal plus a dc voltage offset applied to the silicon. The transition in differential capacitance at the junction is less sharp than the corresponding AFM topography. The capacitance-voltage response of the capacitor formed between the tip and the test structure, measured when the motion of the AFM/SCM tip is stopped, is shown in Fig. 3. Our next objective is to calibrate the SCM using a series of well-defined test structures. Collaborators, including SEMATECH and INTEL, have provided additional test structures with dimensions relevant to commercial devices.

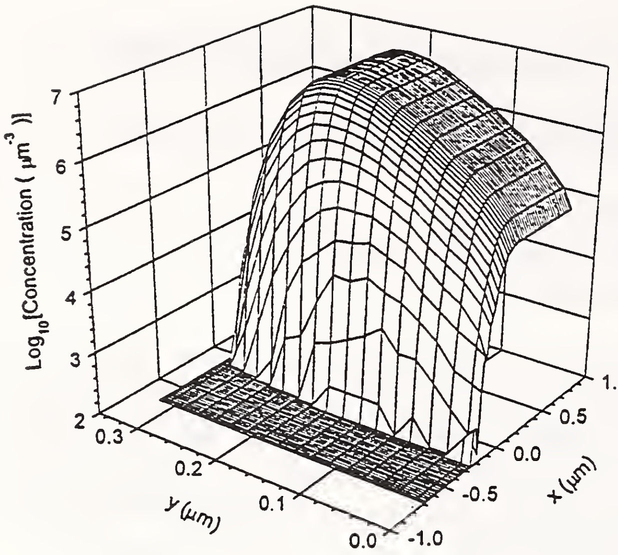

Fig. 1a Profile of B implanted into silicon at 50 keV and a dose of 10^{14} cm^{-2}.

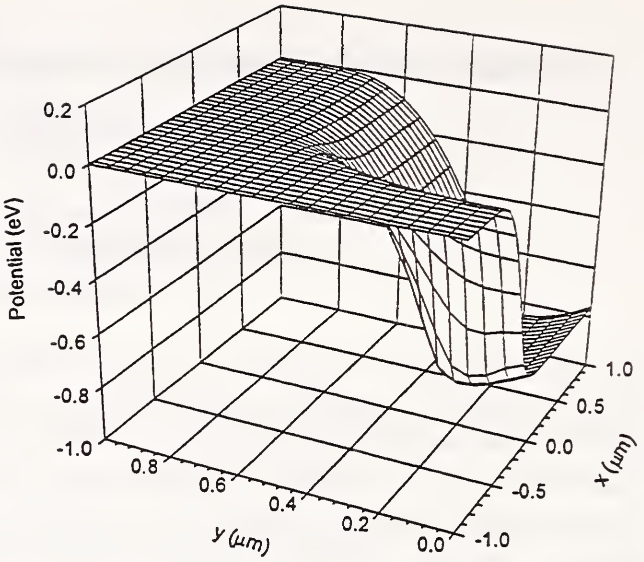

Fig. 1b Potential distribution from a simplified solution of the Poisson equation for the profile in Fig. 1a.

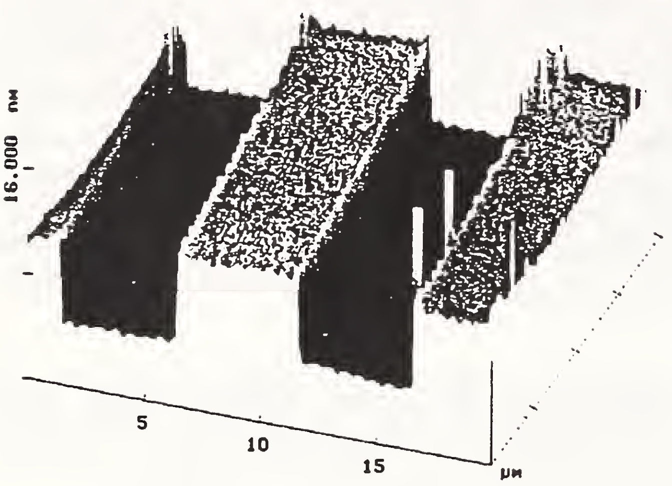

Fig. 2a AFM image of lateral junction test pattern.

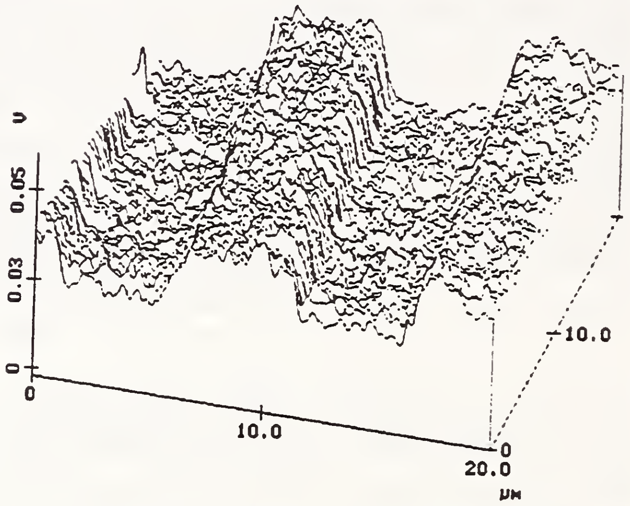

Fig. 2b Corresponding differential SCM image of test pattern.

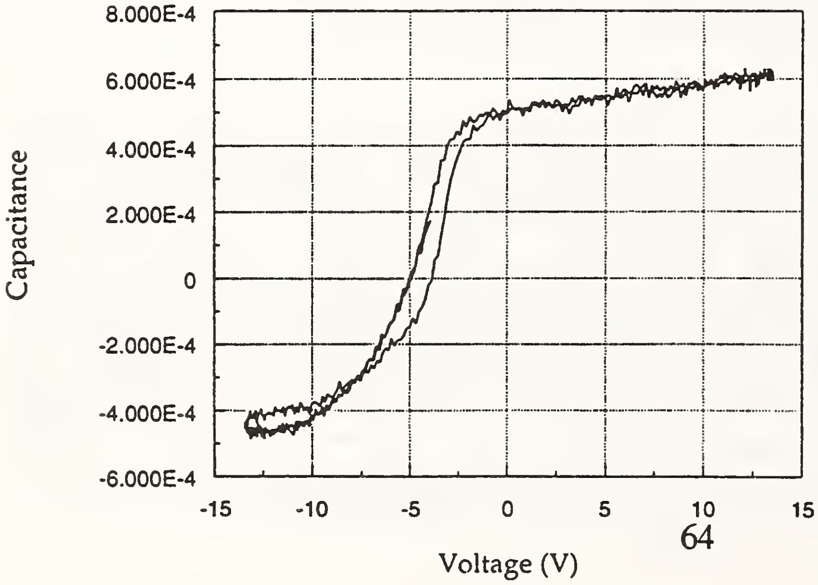

Fig. 3 C-V curve measured with SCM tip over p-type silicon, N ≈ 10^{15} cm^{-3}.

SPREADING RESISTANCE MICROPROBE

R.B. Marcus
Dept. of Elect. Eng., New Jersey Institute of Technology, Newark, NJ 07102
phone: 201-596-8464; fax: 908-464-6936; e-mail: marcus@tesla.njit.edu

I. Introduction

The evolution toward smaller device structures drives a need for diagnostic methods for measuring device properties over increasingly smaller regions. One such need is to measure doping profiles close to sidewalls and across shallow junctions with a spatial resolution in the range of ~10 nm. We need to be able to perform such a measurement at a particular device feature on a wafer or chip "on demand" rather than on specific pre-designed device structures. This means that we need a diagnostic tool that can be applied to a region of interest to measure the doping profile with the required resolution and sensitivity.

Single-point, two-point, and four-point probes have been used for many years for deriving doping levels through measurements of resistance or resistivity. Conventional spreading resistance (SR) methods[1] can provide vertical resolution approaching 1 nm, and recently a single-point probe has been used for resistance measurements with 35 nm resolution[2]. This discussion focuses attention on the proposed development of a high-resolution two-point SR microprobe.

A method for supplying high-resolution resistance measurements requires development of a micromechanical consisting of three main generic parts: a probe tip, a microcompliant member which may or may not contain a microactuator for "self"-actuation, and a stage for supplying the necessary force and motion control. Software and hardware comprise additional components of the microprobe system. The force driving the tip into the surface under test can be supplied either with the AFM-type stage or by a microactuator; in the former case a microcompliant member such as an AFM cantilever is needed for both control and measurement of the applied force.

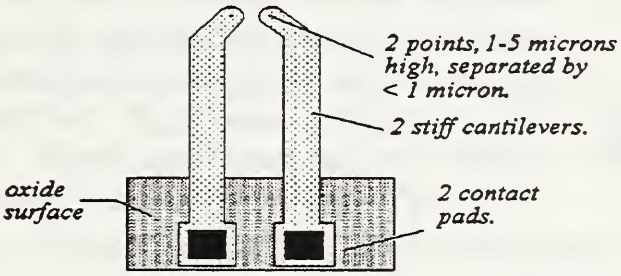

Fig. 1 Illustration of one version of a proposed high-resolution SR microprobe.

II. Spreading resistance microprobe:

One version of a proposed high-resolution SR microprobe is illustrated in **Fig. 1.** The two points are separated by a distance less than 1 µm, and each is mounted on its own cantilever. Either e-beam lithography or focused ion beam etching is needed to make the closely-spaced tips. The dimensions of the cantilever are adjusted to accommodate the applied force through a bending action. The bending action serves three functions: i) supplies better control over the applied force, ii) supplies a means of force measurement by measurment of the displacement of the cantilever, and iii) accommodates small (~10 nm) variations in tip height produced during tip processing.

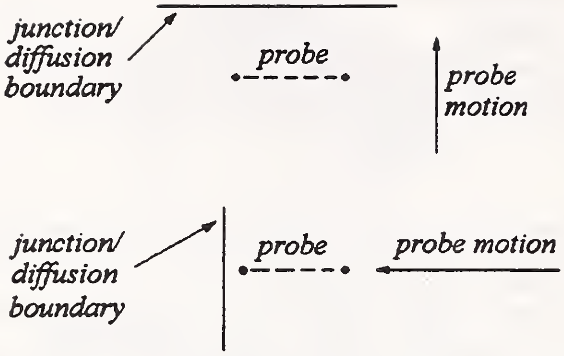

Fig. 2 Two modes of probe operation: parallel (upper) and perpendicular (lower).

The microprobe can be used in two modes. In one mode the probe tips are parallel to the junction, and in the other mode the tips are perpendicular to the junction. The first mode is the "conventional" parallel SR probe arrangement with two probe points moving toward the junction as shown in the upper part of **Fig. 2**. In the other mode of application the points are perpendicular to the junction and move toward the junction as shown in the lower part of **Fig. 2**. It is not clear which of the two modes offer the best spatial resolution and sensitivity to changes in doping level. The parallel mode may offer increased sensitivity but requires careful alignment of probe points with respect to the junction. In the perpendicular mode less uncertainty in probe position is perhaps offset by a loss in sensitivity.

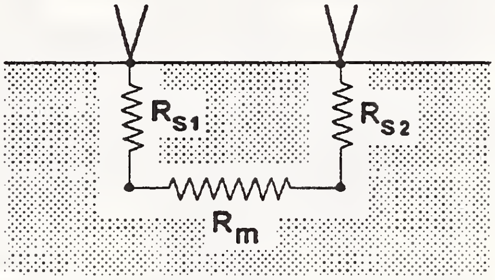

Fig. 3 Equivalent circuit. R_{S1} and R_{S2} are the spreading resistances at the two points; R_M is the bulk resistance.

The main barrier to successful realization of a SR microprobe is based on the need to supply ohmic contact with constant contact resistance. This can be seen by briefly examining a simple model of a spreading resistance measurement described by the equivalent circuit shown in **Fig. 3**, where $\mathbf{R_{S1}}$ and $\mathbf{R_{S2}}$ are the spreading resistances at the two points and $\mathbf{R_M}$ is the "bulk" resistance of the intervening material. The "spreading resistance" of the material $\mathbf{R_S}$ = $\rho/4r$, where ρ is the bulk resistivity and **r** the radius of the disc-shaped contact area. In both parallel and perpendicular modes the measured resistance $R_T = R_{S1} + R_{S2} + R_M$. It is clear that the probe points must be capable of repeated contact to a surface with no significant change in $\mathbf{R_S}$; this requires that probe point penetration into the surface be controlled and that deformation of the probe point be kept within an acceptable limit. The probe tip must be able to "break through" surface oxide layers by a fixed amount upon each application, the applied force must be controlled within the range 10^{-4} N to 10^{-6} N or lower, and the tip must not deform during measurements. Some approaches to solving these problems with atomically-sharp silicon tips are presented.

References

1. S.R. Weinzierl, J.M. Heddleson, R.J. Hillard, P. Rai-Choudhury, R.G. Mazur, C.M. Osburn and Paul Potraj, *Sol. State Tech.* (January, 1993), 31.
2. C. Shafai, D.J. Thomson, M. Simard-Normandin, G. Mattiussi and P.J. Scanion, *Apl. Phys. Lett.* **64** (3), (1994) 342.

Structural Studies of the SiO_2/Si System.

E.P. Gusev, H.C. Lu, T. Gustafsson and E. Garfunkel
Departments of Chemistry and Physics, and
Laboratory for Surface Modification
Rutgers University
Piscataway, NJ 08855-0939.

To understand the properties and reliability of devices which contain ultrathin oxide films, new methods must be developed to address compositional, structural, electronic, and (in some cases) optical properties. The oxidation of silicon is one the most important and widely studied systems in materials science. In this work we present new ways of looking at SiO_2 films on Si substrates using ion scattering methods, and we compare our results with what is obtained by scanned probe and other microscopic methods. We are particularly interested in addressing issues pertaining to film structure (including roughness) and the growth behavior of SiO_2 ultrathin films (<50Å range), precisely the range of interest for critical near-future generation oxides in microelectronics.[1]

Medium energy (100kV) ion scattering spectroscopy (MEIS) is used to determine mechanistic aspects of oxide growth, the interface structure, and roughness of the oxide film and interface. Oxidation is performed on clean Si wafers in the 10^{-3} - 10^{-1} Torr oxygen, and at temperatures of 700-900C. Roughness of the oxide film is examined by an MEIS peak shape analysis. By measuring thickness variations we obtain the sum of surface and interface roughness. The instrumental resolution function, the energy loss due to scattering in the solid, and compositional inhomogeneities must all be accurately modeled before the roughness can be extracted. The utility of this method is compared with other methods. MEIS offers high depth resolution, can measure structural properties of a buried interface, and has elemental specificity.

We also discuss the structure of near-interfacial oxide layers as determined by MEIS channeling and blocking experiments. Angularly dependent blocking dips are observed in the oxygen scattering yield indicating some order in the oxide film at the interface. Finally, mechanistic studies use samples sequentially oxidized in $^{18}O_2$ and $^{16}O_2$ atmospheres. We find both ^{18}O and ^{16}O atoms on the surface of silicon oxide after sequential oxidation, but the distribution of oxygen isotopes in the oxide film is non-uniform. Our results show that several key aspects of the Deal-Grove model[2] (oxygen diffusion to the Si/SiO_2 interface and oxide formation occurring at the interface) are consistent for 50Å oxide films, but inconsistent with results for uiltrathin films. Similar depth distributions for both isotopes in the thinnest films imply isotopic mixing or significant laterally inhomogeneities (e.g. islanding) during the initial stages of growth.

1. E. P. Gusev, H. C. Lu, T. Gustafsson, and E. Garfunkel, MRS Symposium (fall 1993) in press.
2. B. E. Deal and A. S. Grove, J. Appl. Phys. **36**, 3770 (1965).

Feature Placement Accuracy

E. Clayton Teague

National Institute of Standards and Technology

Gaithersburg, Maryland

Acknowledgments:

Steve Nash (IBM), Pat Trocollo (Intel),

Dennis Swyt (NIST), Mike Cresswell (NIST)

Capsule

Assertion: For process control the most important dimensional quantity is mean error of overlay of features formed on the wafer in two consecutive lithography steps.

This talk will present arguments that:
- ONE of dimensional quantities that must be controlled to minimize error of overlay on the wafer is positional accuracy of features on masks/reticles, and
- demands of gigabit & terabit technologies will greatly increase its importance.

"Conventional" Terminology (EOW)

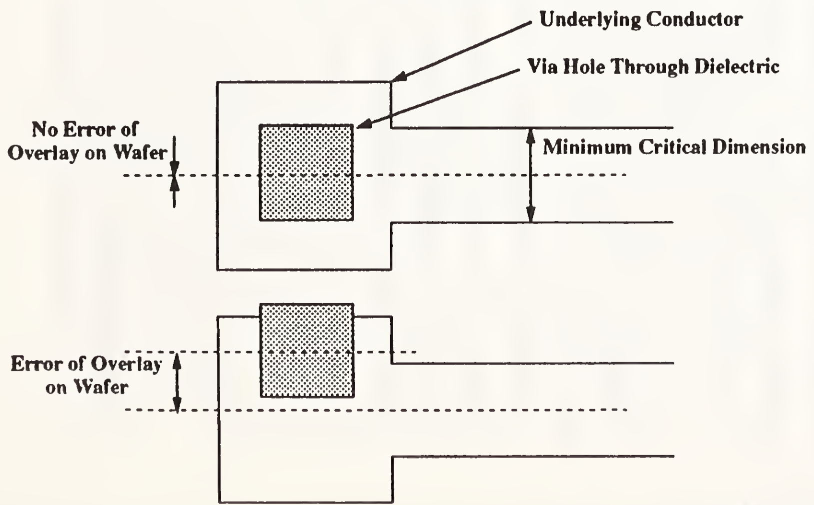
Underlying Conductor
Via Hole Through Dielectric
No Error of Overlay on Wafer
Minimum Critical Dimension
Error of Overlay on Wafer

Error Of Overlay On Wafer Between Two Lithography Steps

(EOW) Determined By:

- * Feature Placement Accuracy of the Two Masks Used For The Steps. (Positional Accuracy of Mask Points Relative to an Absolute Grid) (Differential Positional Error Between Corresponding Features on 2 Masks)
- * Accuracy in Relative Size of Features on the Two Masks and on the Wafer.
- * Alignment/Registration of Second Mask to Exposed Pattern of First Mask
- * Dimensional Changes in the Wafer Resulting From Processing During and Between Two Exposures.

Rules For Combining These Four Components to Obtain The Overall Overlay Error Budget Vary Widely Depending On Devices, Processes, and Manufacturer.

Feature Placement Accuracy

NIST

Relations of Critical Dimensions, Overlay Error, and Required System Accuracies

Minimum Feature Size	Critical Dimension	CD
Overlay on Wafer	Error of Overlay on Wafer	EOW = CD / 2.5
Feature Placement	Feature Placement Accuracy	FPA = EOW / 3 = CD / 7.5
Process Control Metrology	PC Metrology Precision/Repeatability	PCP = FPA / 4 = EOW / 12 = CD / 30
Reference Standard	Reference Standard Accuracy	RSA = PCP / 4 = FPA / 16 = EOW / 48 = CD / 120

E. Clayton Teague

Feature Placement Accuracy

NIST

Lithography Measurement Requirements For Terabit Technology

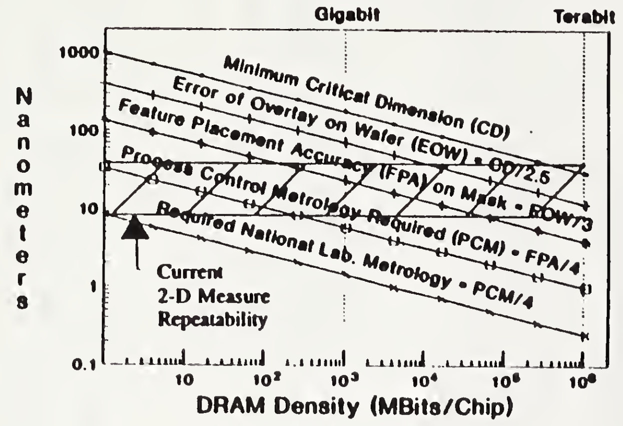

E. Clayton Teague

Feature Placement Accuracy

NIST

Tolerances Imposed On Overlay Error And System Accuracies By Gigabit and Terabit Densities

	1992	2001	2007	2016
Bits Per Chip	16M	1G	16G	1T
Chip Size	20x20 mm	30x30 mm	??	??
Min Feature Size	0.5μm	0.18μm	0.1μm	0.03μm
Error of Overlay	200 nm	90 nm	40 nm	12 nm
Feature Place. Accuracy	67 nm	30 nm	13 nm	4 nm
Process Control Precision	17 nm	7.5 nm	3 nm	1 nm
Ref. Std. Accuracy	4 nm	1.5 nm	0.8 nm	0.25 nm

SIA 1992-2007 Projection Extended

E. Clayton Teague

Feature Placement Accuracy

NIST

Why Feature Placement *Accuracy?*

- ✳ Determine the Distortions Produced by Mounting of Masks In Metrology Systems and During Exposure.
- ✳ Monitor the Temporal Stability of Reference Metrology System.
- ✳ Determine the Temporal Stabilities and Accuracies of More Than One Reference Metrology System.
- ✳ Determine the Accuracy of NX Masks Versus 1X Masks.
- ☛ Temperature Accuracy very important:
  $\Delta T = 0.01K \Rightarrow \Delta S$ of 1 nm / 50 mm for Silicon

E. Clayton Teague

Feature Placement Accuracy

Needs for Absolute Accuracy

- ✳ Part's Function Is Dimensionally Dependent
- ✳ Need for High Confidence Level in Long Term Stability of an Important Dimension.
- ✳ Resolving Differences Between Two or More Traceability Chains.

E. Clayton Teague

Feature Placement Accuracy

Conclusions:

	Gigabit	Terabit
Minimum Feature Size	180 nm	30 nm
Process Control Met. Precision (1/4 Rule)	7.5 nm	1 nm
Ref. Standard Accuracy Reqd. (1/4 Rule)	1.5 nm	0.25 nm

** With Development and Application, SPM Technology Can Contribute to Meeting Needs for Overlay, Feature Placement, CD, and Alignment Metrology of Gigabit Lithography.

** Significant Research and Development Will Be Needed to Meet Requirements of Terabit Lithography.

** Relationships Between Industry Repeatability/Reproducibility Needs and Accuracy Provided By NIST Must be Defined Better.

E. Clayton Teague

Pitch standards via laser-focused deposition

R. Gupta, Z. Jabbour, J.J. McClelland† and R.J. Celotta
Electron Physics Group, National Institute of Standards and Technology
Gaithersburg, MD 20899.

As electronic and magnetic devices continue to become smaller, the need for fabricating structures on the nanometer scale grows larger. We are currently exploring the techniques of atom optics to fabricate structures on the nanometer scale. Atom optics treats neutral atoms, which can have extremely small de Broglie wavelengths, in an analogous way to light beams or charged particle beams. In atom optics, "optical elements" such as lenses, mirrors and beamsplitters are used to manipulate the atoms' trajectories. Optical forces can be either dissipative in nature, in which case they can cool, collimate and/or intensify an atom beam [1], or conservative, in which case they can serve as a lens [2]. Nanostructures created by laser-focusing of atoms possess the potential of being an extremely accurate length standard on the submicron scale.

In our experiments we use the dissipative spontaneous force to collimate a beam of chromium atoms and the conservative dipole force to focus the atoms into an array of lines as they deposit onto a Si substrate [3]. The dipole force arises from the interaction of the induced dipole in an atom with the gradient in the laser intensity. The intensity variation in the standing wave acts as a series of cylindrical lenses, spaced by $\lambda/2$, which can focus atoms in the nodes (antinodes), when the laser frequency is tuned above (below) the atomic resonance. The first demonstration of laser focused atomic deposition was by Timp *et al.*, using sodium [4].

Figure 1 shows the experimental arrangement consisting of an effusive source of chromium atoms, a pre-collimating aperture, a region of optical collimation and a substrate mounted facing the atomic beam. A single-frequency dye laser provides a few hundred mW of laser light for both the optical collimation and the standing wave. The dye laser is tuned 10 MHz below the atomic resonance to collimate the atomic beam and 500 MHz above the atomic resonance for focusing the atoms. The frequency of the dye laser is calibrated against a chromium saturated absorption cell with an accuracy of 1 MHz.

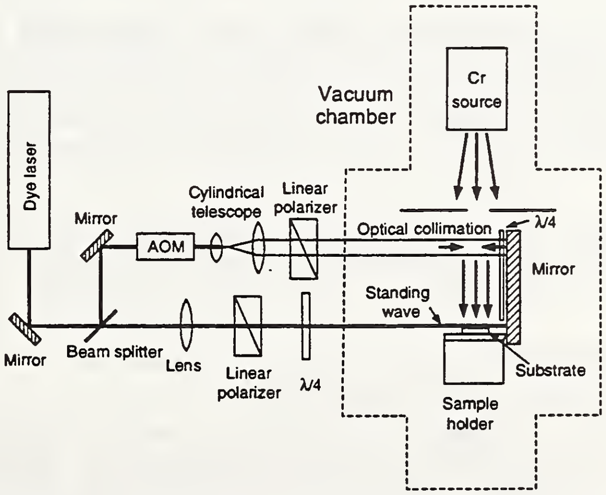

Figure 1. Schematic of laser focused atomic deposition apparatus.

The standing wave laser, with $1/e^2$ diameter 0.4 mm, grazes across the sample so as to generate a half-Gaussian intensity distribution with maximum at the surface of the substrate. Figure 2 shows an atomic force micrograph of a section of the chromium lines created by deposition through the standing wave. The laser wavelength fixes the spacing between the lines at 212.78 nm. Lines extend over the entire region covered by the laser beams. The linewidth is measured to be 65 ± 6 nm and the height of the structures is 34 ± 10 nm.

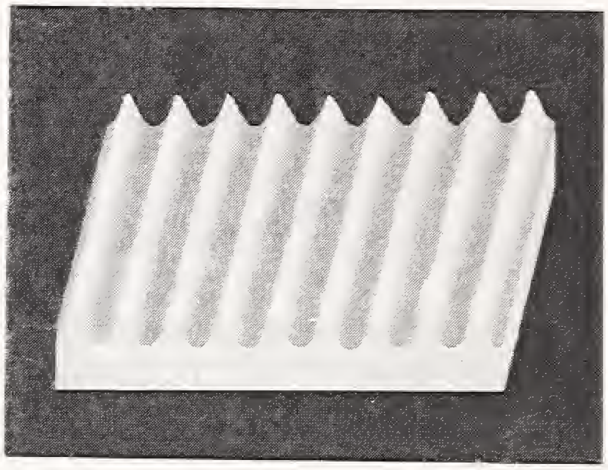

Figure 2. AFM image of Cr lines created by laser focused atomic deposition.

The structures have the potential of being an extremely accurate pitch standard for calibration of microscopes (e.g. AFM and SEM) on the submicron scale since the spacing between the lines is determined solely by the periodicity of the interference pattern created by the laser light. The lines are extremely uniform over 0.2 mm^2 area and therefore they can be used for calibration purposes in a large field of view. The artifacts are made by deposition of Cr and are stable in air and thus portable.

The accuracy of the spacing between the lines is determined by the laser wavelength and the angle between the standing wave mirror and the incident laser light. Since the laser light is provided by a single frequency dye laser locked to an atomic resonance, the wavelength is determined by spectroscopic techniques with a precision of a part in 10^6. The misalignment between the standing wave mirror normal and the incident laser beam is a small perturbation because the pitch changes with the cosine of this angle, which is quadratic near 0°.

We have also done preliminary experiments to generate two dimensional patterns through the superposition of two standing waves at right angles. Such a configuration produces either an array of crossed perpendicular lines or spots depending on the laser frequency and polarization and the spacing is still determined by the interference pattern of the light field.

This work was supported in part by the Technology Administration of the U.S. Dept. of Commerce and NSF Grant #PHY-9312572.

References

† e-mail: jabez@epg.nist.gov

1. V. I. Balykin, V. S. Letokhov, and A. I. Sidorov, JETP Lett. **40**, 1026 (1985); B. Sheehy, S.-Q. Shang, R. Watts, S. Hatamian, and H. Metcalf, J. Opt. Soc. Am. B **6**, 2165 (1989).
2. J. J. McClelland and M. R. Scheinfein, J. Opt. Soc. Am. B **8**, 1974 (1991).
3. J. J. McClelland, R. E. Scholten, E. C. Palm and R. J. Celotta, Science **262**, 877 (1993).
4. G. Timp, R. E. Behringer, D. M. Tennant, J. E. Cunningham, M. Prentiss, and K. K. Berggren, Phys. Rev. Lett. **69**, 1636 (1992).

Sensors and Actuators in Scanned Probe Microscopy

Steven M. Hues
Chemistry Division
Naval Research Laboratory
Washington, D.C. 20375-5342

The advent of scanned probe microscopy has opened a window on a new world of scientific investigations. In order to investigate atomic scale effects, however, it is necessary to displace and sense the displacement of probes on the nanometer level.

Movement of probe components may be divided into two types, coarse and fine. In general, coarse movements are those which are used to bring the tip and sample sufficiently close (~50-100 nm), so that the fine displacement may be performed. Coarse adjustments are made with devices such as screw drives, lever drives, inchworms, or inertial actuators. The main requirement is to bring the tip near the surface, without crashing the tip, such that the remaining separation is within the range of the fine actuator. Fine movements are typically made by applying a voltage to a piezoelectric or electrostrictive ceramic. These ceramics may be made into a variety of structures, one of the most common being a tube. Tubes have the advantage in that, by segmenting the outer electrode, x and y as well as z movement may be obtained by utilizing bending modes of the tube.

The most common piezoelectric material used for nanoscale actuators is lead zirconia titanate (PZT). Typically, "ideal" behavior is assumed where (1) the response (displacement/applied voltage)is linear throughout the entire range, (2) a given applied voltage will always result in a specific displacement, and (3) the entire displacement occurs shortly after the voltage change. However, the true response of PZT actuators is significantly non-ideal. The response is non-linear,and exhibits a high degree of hysteresis and creep. These factors effectively render PZT ceramics poor actuator choices, especially in large displacement applications such as nanoindentation, without an independent means for displacement determination such as a strain gauge. These problems may be significantly reduced by using lead magnesium niobate (PMN) electrostrictive ceramics as actuator materials[1]. In PMN, the displacement is proportional to the square of the applied voltage and is independent of the polarity. While this allows less total displacement than PZT, the PMN devices suffer from no significant hysteresis and much less creep. However, the response of PMN is highly temperature dependent restricting their use in variable temperature applications.

Displacement sensing is another essential requirement of scanned probe microscopy. Displacement sensors may be divided into three classes: tunneling, capacitance, and optical.

Initially, displacement sensing was performed using an STM tip to tunnel into the back of the cantilever. Although this method provides very high sensitivity in DC operation, it suffers from the problems of maintaining a low noise tunneling junction, convolution of cantilever topography into the displacement measurement, and the possibility of tunneling tip/cantilever interaction forces affecting the cantilever spring constant.

Capacitance sensors operate by measuring the capacitance between the cantilever and a fixed plate. As the cantilever moves towards or away from the fixed plate, the capacitance changes with the gap distance. The problem of electrostatic forces associated with the capacitance plates affecting the spring constant of the cantilever is present to an even higher degree than in the tunneling sensor because of the much larger areas involved. DC noise levels[2] of 100 pm have been reported using this method. Capacitance sensing may be affected by such factors as temperature induced drift of the reference capacitor, if a capacitive bridge is used, and the roughness of the cantilever wire, if a rigid plate is not affixed to a wire cantilever.

Optical sensing techniques are based on optical deflection, interferometry, or laser diodes. In optical deflection, a laser beam is reflected off the back of the cantilever onto a position sensitive detector (PSD). A displacement of the cantilever produces a corresponding deflection of the laser spot on the PSD. The major source of noise in this method is shot noise in the detector producing noise values of 100 pm and 3 pm/√Hz for DC[3] and AC[4] operation, respectively. In interferometry, the cantilever displacement is sensed by measuring the interference of a reference laser beam and one that is reflected off the back of the cantilever. Using differential interferometry noise levels of 1 pm (DC) and 0.01 pm/√Hz are achieved[5]. In the laser diode method, advantage is made of the extreme sensitivity of a laser diode to optical feedback of light reflected off the cantilever back into the laser cavity. The sensitivity of the laser diode method is 3 pm/√Hz in the vertical direction[6] and has the advantage of having no optical components other than the laser diode and its integrated photodiode.

References

1. S.M. Hues, C.F. Draper, K.P. Lee, and R.J. Colton, Rev. Sci. Instrum., in press.

2. G. Neubauer, S.R. Cohen, G.M. McClelland, D. Horne, and C.M. Mate, Rev. Sci. Instrum., **61** (1990) 2296.

3. G. Meyer and N.M. Amer, Appl. Phys. Lett., **53** (1988) 1045.

4. G. Meyer and N.M. Amer, Appl. Phys. Lett., **56** (1990) 2100.

5. C. Schönenberger and S.F. Alvarado, Rev. Sci. Instrum., **60** (1989) 3131.

6. D. Sarid, D.A. Iams, J.T. Ingle, V. Weissenberger, J. Vac. Sci. Technol., **A8** (1990) 378.

Probe Microscope Tip Fabrication

Herschel Marchman
AT&T Bell Laboratories, 600 Mountain Ave., Murray Hill, NJ 07974

A common problem encountered in probe microscopy is that of image distortion due to tip shape. Image distortion can be reduced by compensating for the probe shape during data correction. Data correction can be greatly simplified if the geometry of the probe is optimized for the topography being scanned. For example, an ideal probe shape for obtaining line profiles of high aspect ratio rectangular features is that of a perfect right geometric cylinder. The planar endface (oriented perpendicular to the axis of the probe) and sharp 90° corners of the lower portion enable accurate measurements of the feature even at sudden jumps in the surface. The cylindrical probe is ideal for nondestructive wall angle measurements because of its vertical sidewalls and sharp end corners.

In this article, the fabrication of cylindrical probes having diameters as small as 50 nm is described. The fabrication technique involves selectively etching optical fiber segments until their dimensions are reduced to the final values desired. Flared probes for imaging re-entrant (undercut) structures can also be made using a variation of the cylindrical probe fabrication technique. A 500 nm diameter cylindrical and a 250 nm diameter (bottom endface) flared probe are shown in Figure 1 (a) and (b) respectively. In addition, the fabrication of sharp conical tips used in surface roughness and linewidth measurements will also be described. Although precise probe geometries with nanometer-scale dimensions are obtained, the fabrication techniques described in this article are simple and inexpensive; only a Teflon beaker, optical fiber, etching solution, fiber cleaver, and optical microscope are necessary.

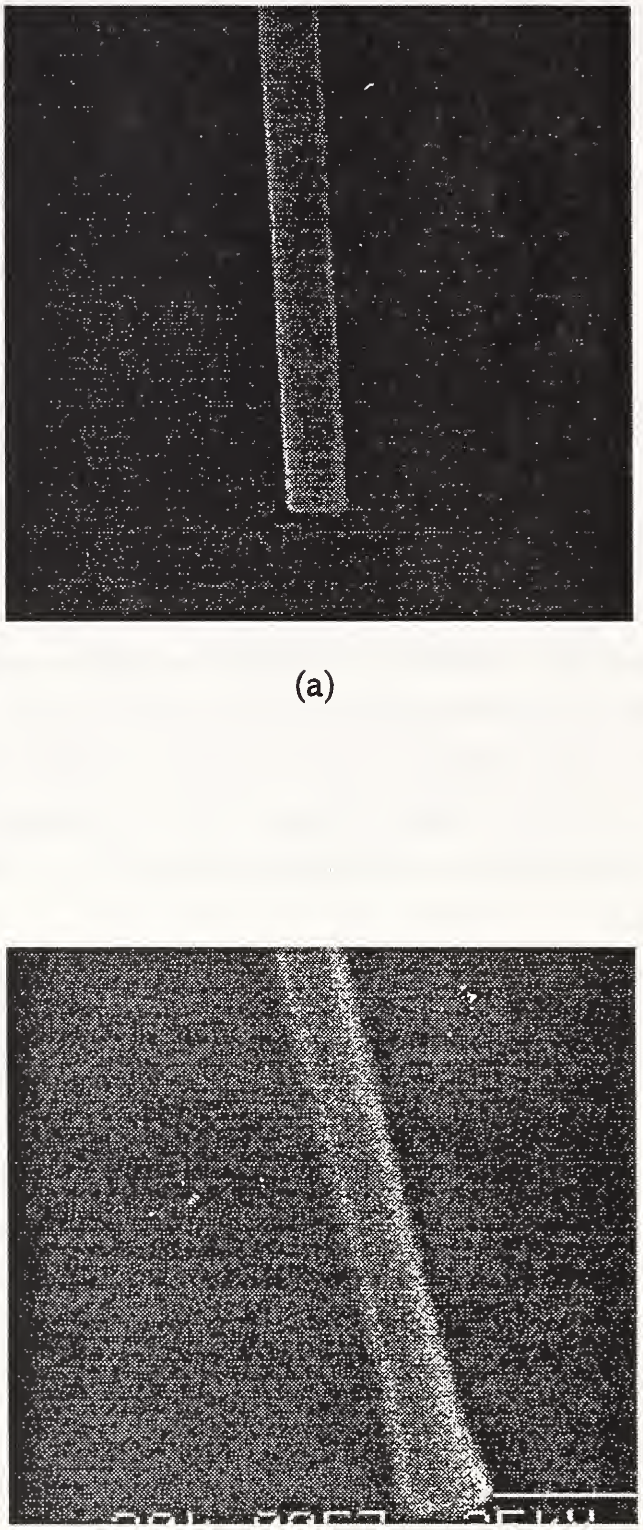

(a)

(b)

Figure 1 - (a) A cylindrical probe with 500 nm diameter,
(b) A flared probe having 250 nm diameter.

Advances in Instrumentation for SPMs used in Dimensional Metrology

Michael Kirk and Lindsey Mitobe
Park Scientific Instruments

Abstract

As commercial SPM's proliferate, there use as industrial process control tools becomes more widely accepted. These industrial applications often involve precision dimensional measurements, which places a premium on accurate, linear, and repeatable scanners used in these instruments. Commercial SPM's use piezoelectric tube or tripod scanners which have several desirable properties like: high resolution and high mechanical resonance in a compact package. Yet, these scanners have undesirable properties such as; hystereses, creep, and nonlinear motion. This paper will describe two closed-loop scanning systems which allow accurate linearized lateral scanning. One system is a commercially available SPM scanner which incorporates a passive vertical sensor with two optical sensors for x-y positioning. The other system was developed at NIST and through a collaboration with PSI.

X-Y Closed loop Scanning

For two years PSI has produced SPM scanner systems which incorporate optical position sensors coupled to servo electronics to drive piezoelectric scanners in an accurate and linear manner (marketed under the trade name ScanMaster^{TM}). Within the scanner housing are an X and Y optical position sensor whose output is fed to a servo controller. This signal is compared to a desired linear ramp signal. From this difference, the controller applies the correct drive voltage to the X and Y piezo elements to produce linear scans and eliminate other scanner artifacts. This system has demonstrated less than 0.5% nonlinear motion for scan ranges from 1-100 micron. Further these detectors have resolution of less than 1 nm. They are simple and inexpensive to build and can be fully contained in a package size of less than 1in.^{3}. A demonstration of this system on a 2-D 1 um grating is shown in Fig. 1. Immediately after taking a larger image a scanner is repositioned and the scan size is reduced. This "Zoom-in" image is shown in image a). This image was acquired without scanner correction and clearly shows the effect of piezoelectric creep. Image b) was acquired under the same conditions as a), but with the X-Y servo system enabled and, therefore, does not show creep.

Because the above system uses position sensitive optical detectors, it does not have a built-in collaboration mechanism. This problem can be solved by replacing these position sensors with an interferometer as was developed at NIST. In this implementation they used a heterodyne plane mirror interferometer (Zygo ZMI-1000 system). This interferometer uses a stabilized HeNe laser and has a resolution of 1.24 nm. PSI produced electronics to read the output from the interferometer, but employed its standard AutoProbe^{TM} control system for the X-Y servo. This controller can produce either a linear or a sinusoidal scan (the later being the preferred operating mode for the actuator used by the group at NIST). This system produced linearity to better than .3% with an RMS jitter of 1.4 nm. Fig. 2 shows a the output from a single 3.2 um sinusoidal scan and the associated residual error.

Z Detection

In every ScanMaster^{TM} scanner from PSI there are 2 passive Z detectors. These detectors do not affect the lateral feedback for the piezo scanner or the probes vertical position. These detectors simply measure the vertical position of the tube as it servos the sample's topography. This independent and linear sensor provides a more accurate image of the surface topography. A schematic of this system is shown in figure 3a. An example data from such a a Z detector is shown in figure 3b. The upper trace is a plot of the signal applied to the Z piezo (this is the traditional signal displayed in SPM's) as a cantilever is scanned over a series of lines and spaces. In this line trace one can see examples of scanner hystereses, creep and overshoot. The trace below is taken from the Z detector. The Z detector measures the Z piezo's physical position as it moves to maintain a constant deflection on the cantilever. Clearly this signal more accurately represents the physical structure of the surface.

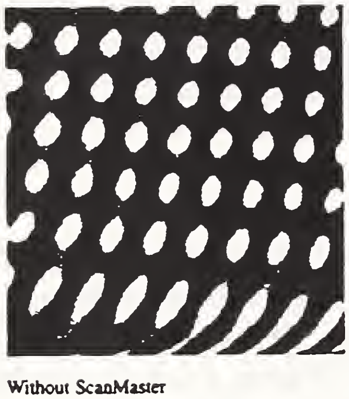

a)

Image a) was acquired without scan correction and after the scanner was "Zoomed-in" and thus shows piezo creep. Image b) was acquired with scan correction.

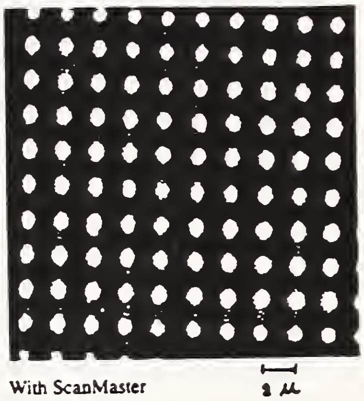

b)

Figure 1.

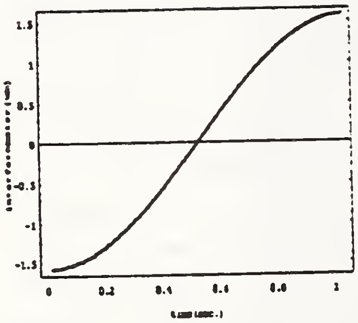

a)

Plot a is interferometer output from a single 3.2 um scan and a least squares best fit sine wave. Plot b) shows the residual error from the best fit and is less than 0.3% of the original scan.

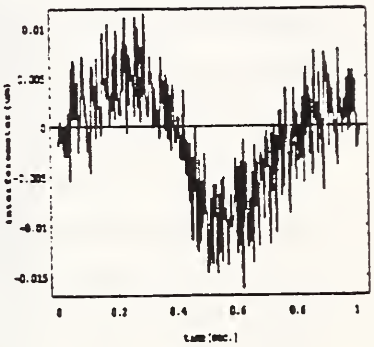

b)

Figure 2.

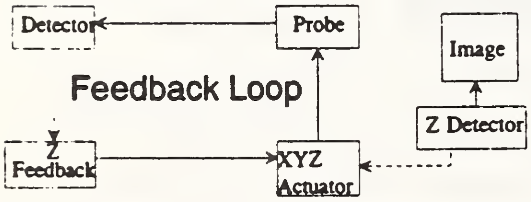

To the left is a schematic of the Z detector used in the ScanMaster system. To the right are two line traces of the same sample. The top trace plots the z-piezo voltage and shows hystereses, creep and overshoot. The lower trace was acquired from the z detector.

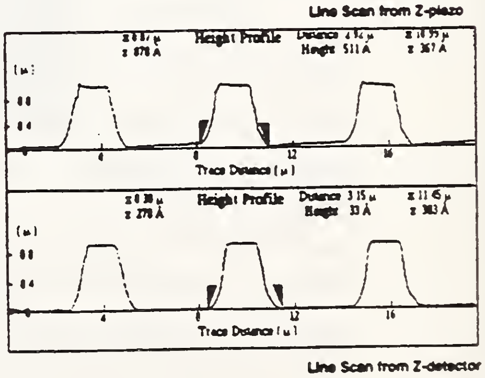

Figure 3.

Park Scientific Instruments
1171 Borregas Ave.
Sunnyvale, CA 94089

Polished Silicon as SPC Sample

Robert H. Brigham, *Charles Evans & Associates*
301 Chesapeake Drive, Redwood City, CA 94063

The advent of TappingMode™ AFM (by Digital Instruments) allows high lateral resolution (5-10nm) AFM to be performed on surfaces with contact forces of only a few Nanonewtons. This has widespread application as a measurement tool for highly polished surfaces, including those routinely produced on silicon wafers for the semiconductor industry.

The reproducibility of microroughness measurements is strongly affected by the quality of the tip. Blunt tips yield images with low resolution and from which deceptively low values of surface roughness are derived. A method of ensuring the quality of the AFM tip, and hence, the roughness analysis, has been investigated that uses a carefully selected piece of silicon as a Statistical Process Control (SPC) sample.

Samples appropriate for SPC use should be uniform, have no blemishes or scratches, and possess a R_q within the range of keenest interest which is less than 1Å. There is no independent technique that can be used to find and certify such a sample. Likely sample candidates must be selected using R_q values obtained from AFM images acquired over many areas of a sample with many tips. The distribution of measured R_q values for a sample appropriate for SPC service should be narrow and can be used to establish a range of acceptable values as well as a cutoff value.

Using this bootstrap method, several samples were found that are uniform, free of blemishes, and possess an appropriate value of R_q. One of these, labelled SPC 4, though not the most uniform of the samples, has been in use for eight months. A plot of the values of surface variance obtained with different tips over this time period is shown in Figure 1. Based on the first 10 values, a cutoff of 0.60Å was provisionally adopted.

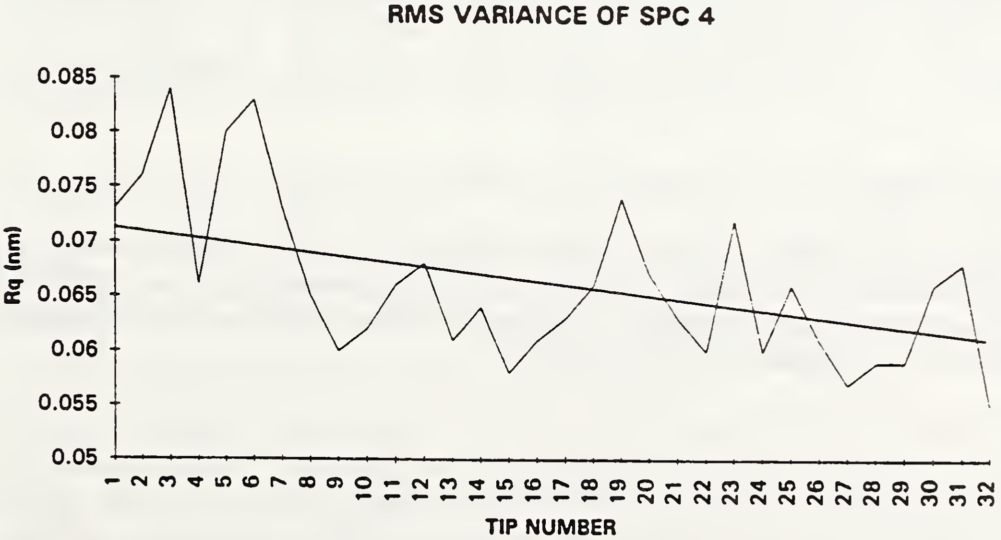

Figure 1. Values of RMS surface variance measured on SPC 4 using tips from a single 4" wafer. This wafer of tips was obtained in January, 1993.

Initially, few tips failed to meet the 0.60Å cutoff, but the number has increased with time. The numerical drop in R_q was matched by a corresponding loss in resolution apparent in the images acquired of this SPC sample. Recently, the point was reached where only a few tips produced high resolution images. An effort was made to determine the source of this apparent lack of resolution. Possible sources are: instrumental (piezo tube) calibration drift, degradation of the tips, fouling of the SPC sample, or a combination of these.

The calibration of the piezoelectric tube was checked. Small corrections were required, but the nature of the shift was opposite to that required to explain the SPC data.

The SPC sample was baked at 100°C for an hour under vacuum to see if any adsorbed contaminants could be driven away. No change in measured R_q values was observed.

However, comparison of R_q values obtained with tips from the original tip wafer (in use for over a year, and used for all measurements in Figure 1) with those from a fresh wafer of tips was revealing. The R_q values obtained with the new tips are all higher than 0.60Å and resemble values obtained from the original tip wafer 6 months ago. As a check, measurements were made using one year old tips from a different wafer. These too yielded images with lower resolution and depressed values of R_q (Figure 2).

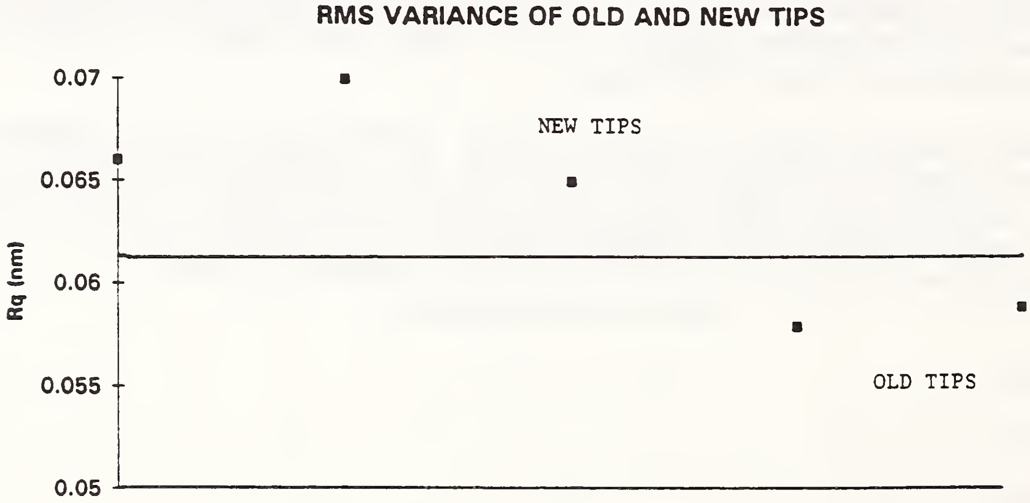

Figure 2. Comparison of RMS surface variance measured on SPC 4 with new tips (tip wafer obtained January 1994) with one year old tips. These old tips are from a different wafer than those used in Figure 1, but yield similar values. Near-horizontal line is extrapolation of regression line of Figure 1.

From these data it appears that etched silicon tips can become blunt with age. The effect is small and only impacts sub-angstrom roughness measurements. However, this effect would have gone unnoticed if Statistical Process Control sample had not been used.

Roughness of Si_xGe_{1-x} films studied by AFM and STM*

M. A. Lutz and R. M. Feenstra
IBM T.J. Watson Research Center
Yorktown Heights, NY 10598

Roughness of strained Si_xGe_{1-x} films grown by ultra-high-vacuum chemical vapor deposition (UHV-CVD) has been studied by atomic force microscopy (AFM) and scanning tunneling microscopy (STM). This roughness is important in determining the electrical properties of the films, as well as affecting processing steps such as photolithography. The AFM work is performed in air, and yields most of the roughness information with the exception of atomic scale roughness. The latter is measured by UHV STM using HF-dipped samples introduced through a load-lock. Films have been grown on both Si substrates and relaxed Si_xGe_{1-x} buffer layers. For films with large mismatch in lattice constant relative to the substrate, very rough surface topography is found. Such "strain-induced" roughness acts to relieve the strain in the film.[1] An example of this is shown in Fig. 1, showing the topography of an 30% Ge film with thickness 600 Å. Large pits, typically 200 nm wide and 50 nm deep, are seen on the surface.

Facetting of the surface occurs, as seen in the gradient analysis of Figs. 2 and 3. Figure 2 shows the component of the surface normal lying along the z-direction (*i.e.* perpendicular to the average surface plane). Dark (steep) features arise from the sidewalls of the pits, and lighter (less steep) features are seen on ridges which form between the pits. The angles of the various facets can be quantitatively measured by plotting a 2-dimensional histogram of values of the surface gradient, $(\partial f/\partial x, \partial f/\partial y)$, as shown in Fig. 3. The axes in that figure correspond to values of $\tan^{-1}(\partial f/\partial x)$ and $\tan^{-1}(\partial f/\partial y)$, each over the range $-90°$ to $+90°$, and the quantity plotted is the number of pixels of Fig. 1 having the particular values of the gradient. We see in Fig. 3 that particular facets are favored: {515} and {112} planes form the sidewalls of the pits, and {103} planes form the ridges between pits. The existence of well defined facets is very significant in terms of growth of smooth films: facetting implies an anisotropic surface free energy, which in turn implies an activation energy for the formation of the facets.[2] Thus, by growing films at conditions below this activation barrier, one can avoid the film roughening and associated undesirable film properties.

We have used spectral analysis to characterize the roughness of a variety of Si_xGe_{1-x} films. Results for the relatively rough film of Fig. 1 are shown by the upper curve in Fig. 4. The Fourier spectrum is flat up to a frequency of about $(200\ \mathrm{nm})^{-1}$, corresponding to the typical lateral dimension of the roughness features, above which it falls off rapidly. In contrast the lower curve in Fig. 4 shows results from a smoother film, containing 15% Ge. Reduced strain in this case allows the film to relax by a different mechanism, giving rise to a cross-hatch pattern of surface undulations, with lateral separation of several μm. Thus, the roughness spectrum displays a falloff starting at this longer wavelength. In addition, we find for wavelengths around 10 nm the occurrence of another component in the roughness. STM investigations identify this component as arising from atomic-scale roughness on the surface.

*in collaboration with J. O. Chu, B. S. Meyerson, P. Mooney, and J. Tersoff

1. W. H. Yang and D. J. Srolovitz, Phys. Rev. Lett. *71*, 1593 (1993).
2. J. Tersoff and F. K. LeGoues, to be published.

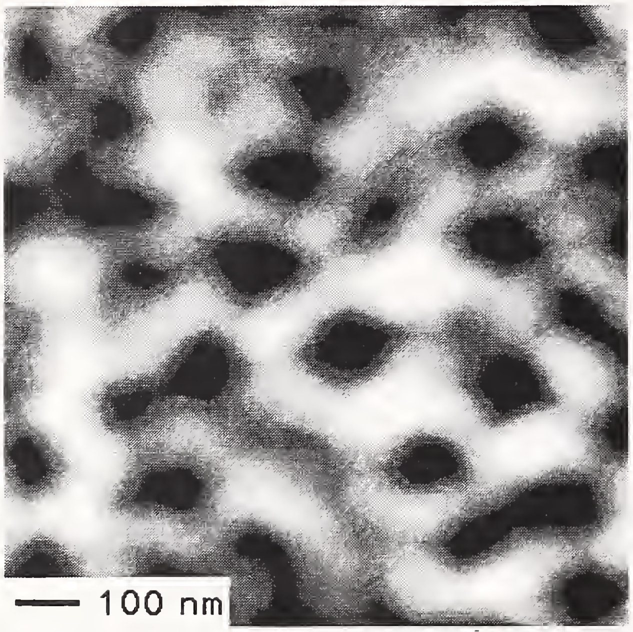

FIG. 1. AFM image of 30% Ge film. Surface topography is given by the grey-scale, with range of 67 nm. Deep pits in the surface are visible.

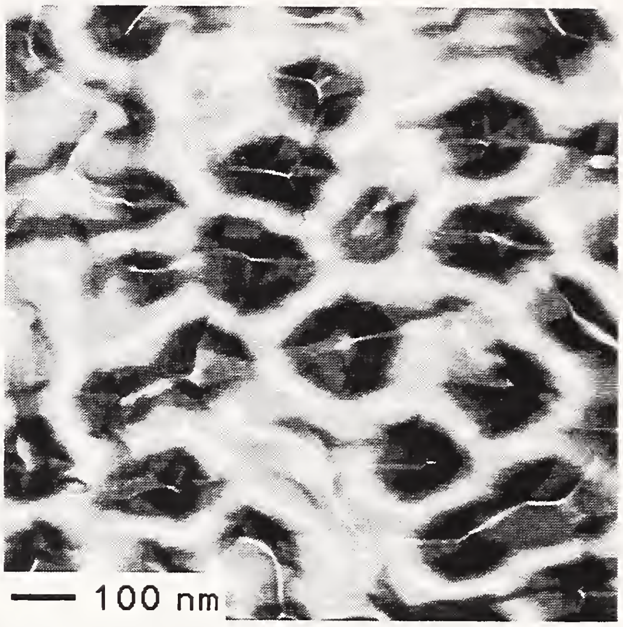

FIG. 2. Gradient image of surface in Fig. 1. The component of the surface normal along the vertical direction is represented by the grey-scale.

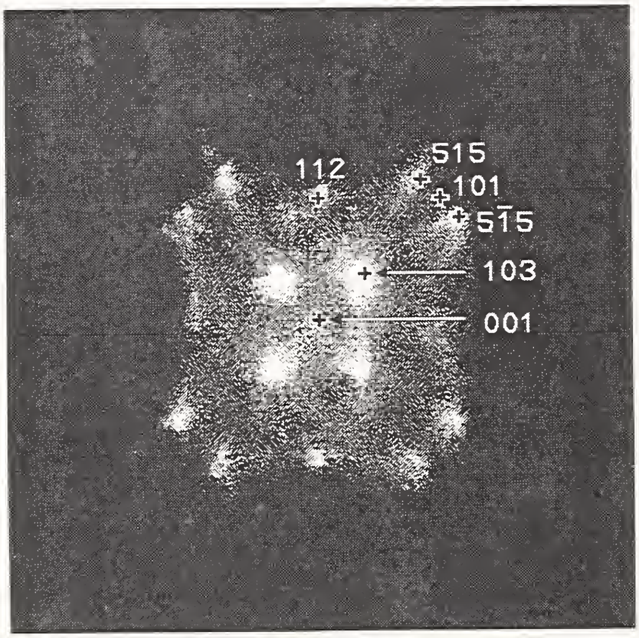

FIG. 3. 2-dimensional histogram of surface gradient values. Crytallographic direction are indicated. Peaks in the histogram correspond to facets in the surface topography.

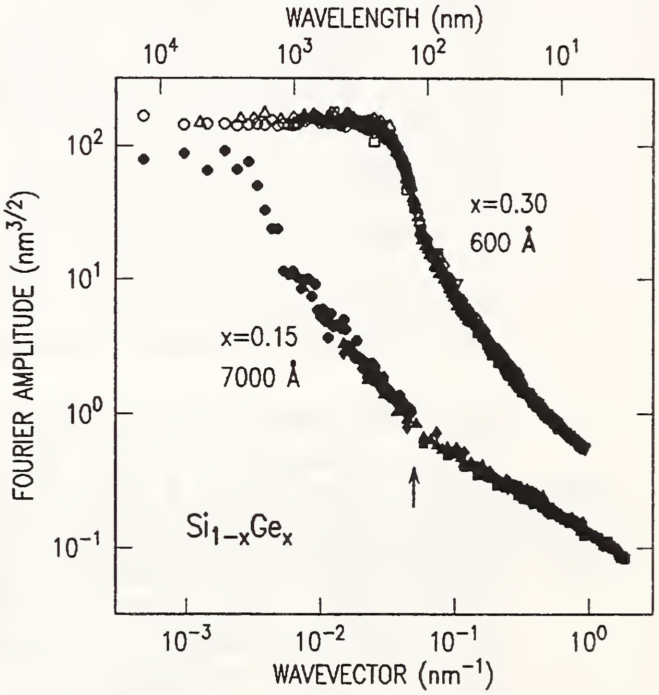

FIG. 4. Roughness spectra, computed from a series of images with varying length scales. Data from different images are represented by different types of data points, and good overlap is found between neighboring spectra.

Evaluation of Wafer Micro-Roughness with Sub Å Resolution on the AFM

Results of an AMD Sponsored Round Robin.

Ruby Raheem & Ercan Adem
Advanced Micro Devices, Sunnyvale, CA

Abstract

As the AFM technique matures it is essential that it is put on a metrological footing as it evolves from a qualitative to a more quantitative technique. This is already happening with AFM machines being used in CD applications to measure submicron geometry in 3-D. The resulting 3-D images are a convolution between the probe tip, sample geometry, external and internal sources of noise and errors. In this paper we describe an AMD initiated round robin investigation of bare Si wafer micro-roughness study on the leading commercial AFM systems being utilized in the laboratories of major semiconductor companies and AFM vendors.

In order to check the absolute value of starting wafer micro-roughness, reproducibility and repeatability of the AFM tools, three test wafers were supplied to 9 participants - control (polished starting silicon wafers), 3 minute BOE etched (Buffered Oxide Etch 40:1 NH_4F:HF) and 15 minute BOE etched Si wafers representing three grades of roughness. For the repeatability study thirty continuous 2μx2μ scans were made at the centre of the control wafer using the same tip and scan area without removing or repositioning the sample or tip . In the reproducibility study each wafer was sequentially scanned twice using a single tip and then repeated with a second tip. Two areas - 3μx3μ and 1μx1μ were scanned.

The repeatability study showed great variability of P/V and RMS micro-roughness values from participant to participant - nearly an order of magnitude. The minimum reported RMS value was 0.2Å and the maximum reported value was 1.5Å as shown in Figure 1. The Relative % Standard Deviation (RSD) ranged from 2% to 12%. The P/V was about 10 times higher than the RMS. In the reproducibility study where the samples were removed and repositioned, the control wafer data ranged from 3.5Å to 20.5Å P/V and 0.2Å to 2.8Å RMS (Figure 2). All participants were able to resolve the three grades of roughness. Figure 3 is a set of top view images of the control wafer scanned by the participants.

The paper will discuss the tip to tip and pass to pass variation, RMS and P/V as a function of scan area, relationship between RMS and P/V as a function of participants, analysis of scatter data as a function of AFM mode of analysis (contact and tapping) and show representative top view and 3-d topographical images.

Figure 1: RMS Micro-roughness versus Participants (2μx2μ area and 30 scans on Control wafer for Repeatability Study)

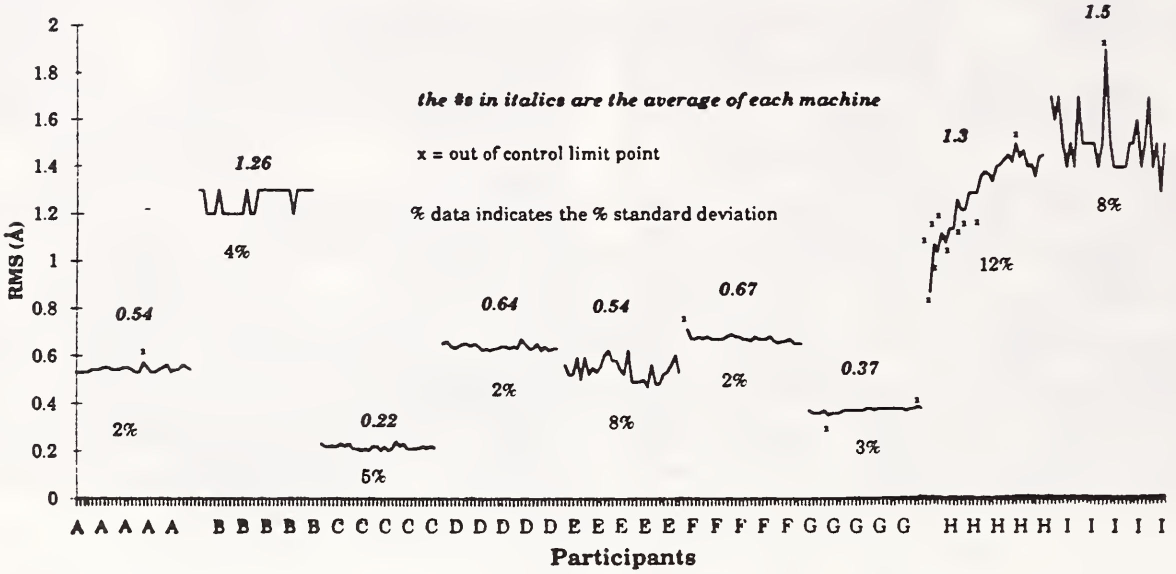

Figure 2: RMS Micro-roughness versus BOE Etch Time for all Participants

(3μx3μ area scans)

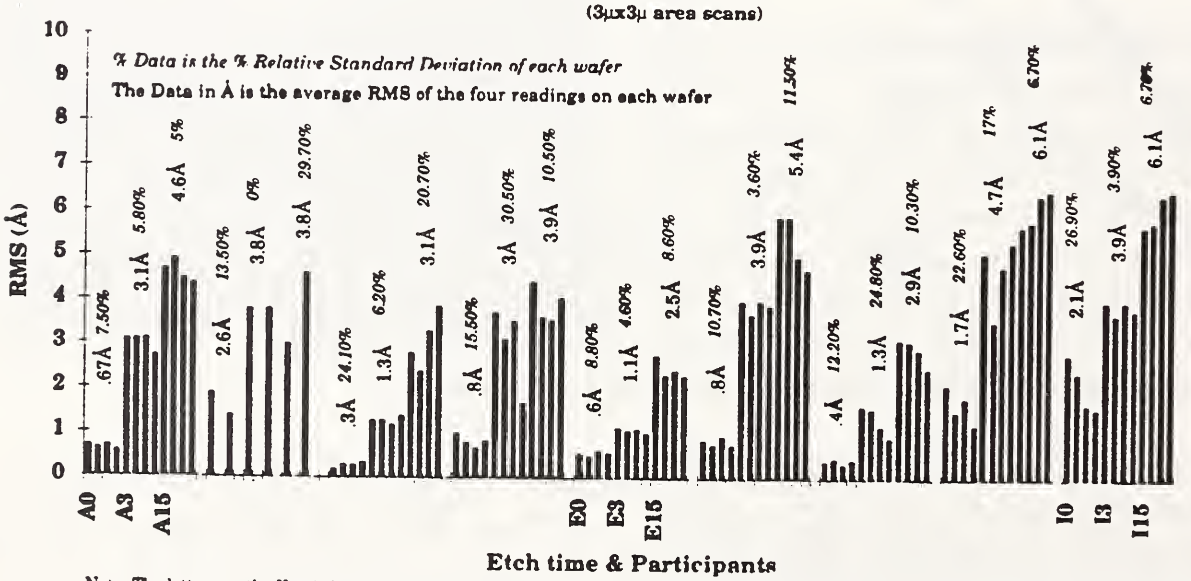

Note: The letters on the X-axis have #s '0', '3' & '15 denoting control, 3min & 15min BOE etch times. There were four scans per wafer with two ti

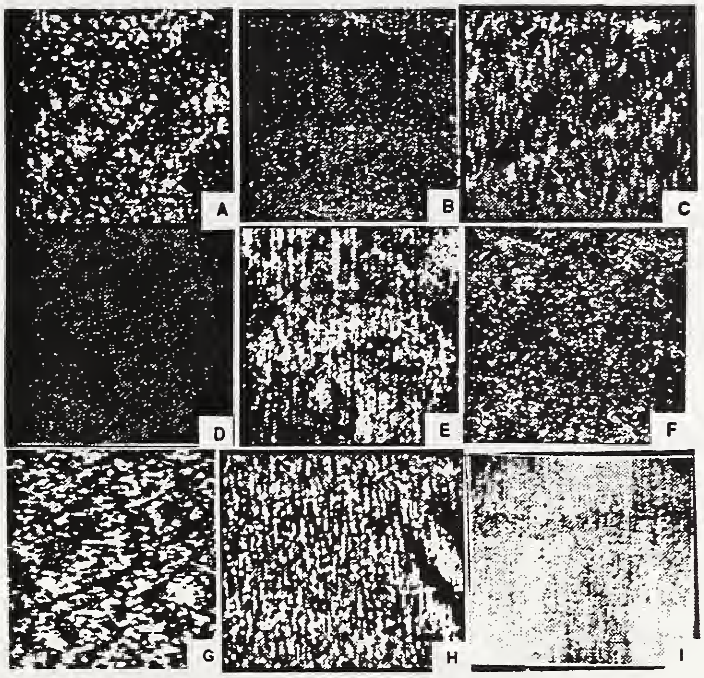

Figure 3 : Top View grey scale images of the control silicon wafer. The polish scratch marks are visible.

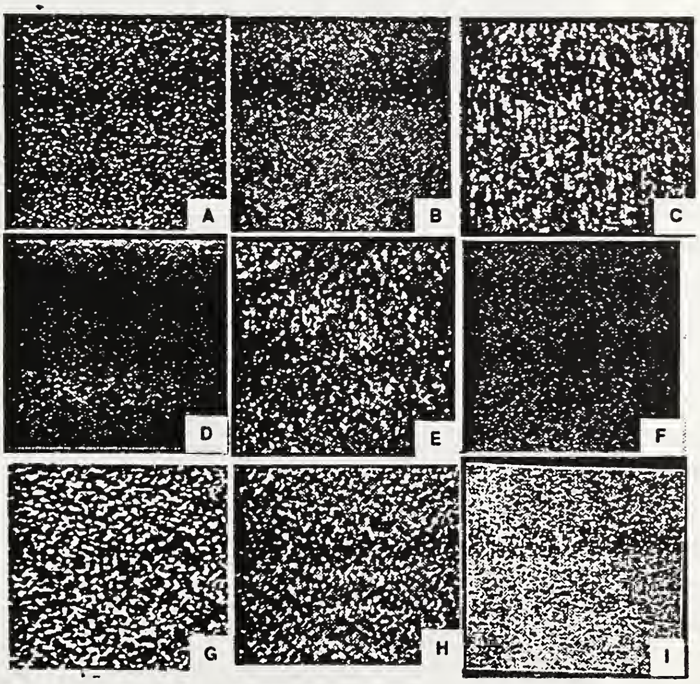

Figure 4 : Top View grey scale images of the 3 minutes BOE etched silicon wafer. No polish scratch marks are visible.

USING CLUSTER MATERIALS FOR HIGH RESOLUTION TOOLS IN AFM.

Donald A. Chernoff, Advanced Surface Microscopy Inc., 6009 Knyghton Rd., Indianapolis, IN 46220-4955, Amar Ramachandra and Ronald Andres, School of Chemical Engineering, Purdue U.

Overview. Image resolution in Atomic Force Microscopy (AFM) is limited by probe tip shape and specimen topography. We have used pre-formed gold clusters (2-5 nm diam.) from the MECS (Multiple Expansion Cluster Source) for vapor phase deposition onto flat substrates (e.g. Si wafers) and standard AFM probe tips. Specimens of gold clusters on Si test tip shape and therefore resolution. We present shape comparisons of several different probe tips; such comparisons can be used to select 'good' tips. Cluster-modified probe tips were much sharper than standard SiN tips: the test cluster specimen image was about 10 nm wide at the contour 1 nm below the summit. Such test specimens and sharper probe tips will aid AFM analysis of polymers, such as DNA and collagen.

Resolution test specimens. Deposition of gold clusters on epitaxial silicon wafers ('epi-Si') resulted in test specimens which were easy to use. Figure 1 is a contact mode AFM image within the masked region of one specimen. The surface is very smooth (rms roughness about 0.15 nm), as expected. This is an important control result, indicating that the specimen topography was unaffected by the general handling involved with cluster deposition. Figure 2 is an image within the unmasked (i.e. cluster-exposed) half of the same specimen. Eleven bumps (the gold clusters) are seen within this 2 μ field of view. The clusters were well-isolated and easily detected (with high contrast) against the smooth substrate surface. We were able to zoom in progressively to examine single clusters. Figures 3 and 4 show typical 1 μ and 125 nm fields of view. Cluster adhesion was satisfactory for testing resolution: high magnification images were stable for at least several frames. We repeatedly examined this specimen over a period of several weeks, at random spots within the cluster-exposed region. The results were similar. The clusters were always sparse and had satisfactory adhesion. Several specimens produced during different deposition runs under similar conditions gave similar results.

Tip Testing. After selecting a suitable resolution test specimen, we mounted different probes in the AFM and used them to image the clusters present on that specimen. Figure 5 shows images of three similar clusters made by three different tips. Because the three clusters are all the same size (8 nm high), we can assess the relative sharpness of the three tips by comparing the width and shape of the height contours. Tip A, a standard silicon nitride pyramid, is elongated parallel to the Y axis. Such blade-like tips are very common. The elongation is always parallel to the X or Y axis and is a result of slightly imprecise microlithography. Tip B, a cluster-exposed pyramid tip, is apparently more symmetric than tip A. Tip C, another cluster-exposed pyramid tip, is the sharpest of the group: it made a cluster image that is round and has narrow contours.

Resolution improvement on other specimens. We used a 'real-world' specimen to make another comparison of probe tips. The specimen was a silicon wafer that had been etched in a fluorine plasma to roughen the surface and then coated with a thin tungsten film. The surface is bumpy all over, with bumps ranging from 5 to 50 nm high. Figure 6 shows images of this specimen made using a standard silicon nitride pyramid and a cluster-exposed pyramid. The image made by the latter is obviously much more clearly resolved.

Acknowledgement. This research was supported in part by NIH SBIR grant # 1-R43-GM47763-01.

Figure 1

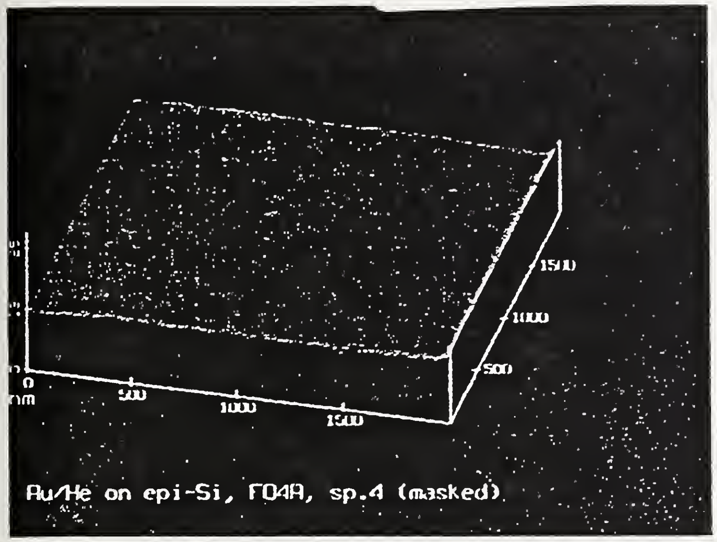

ADVANCED SURFACE MICROSCOPY, INC.

Figure 2

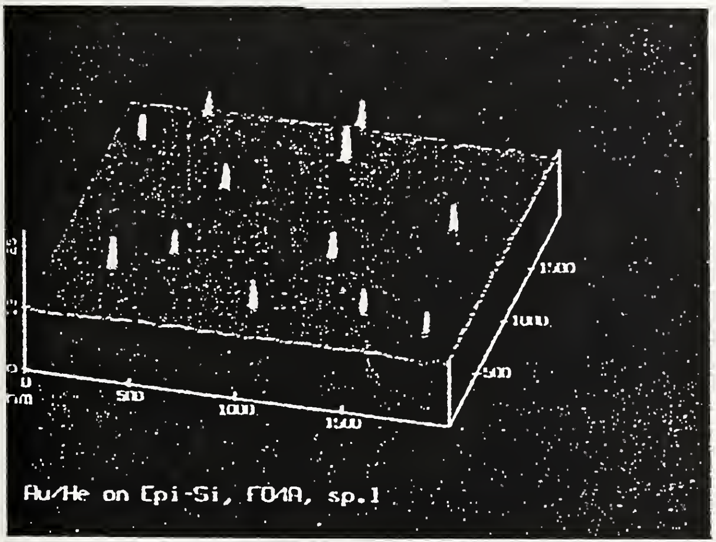

ADVANCED SURFACE MICROSCOPY, INC.

Figure 3

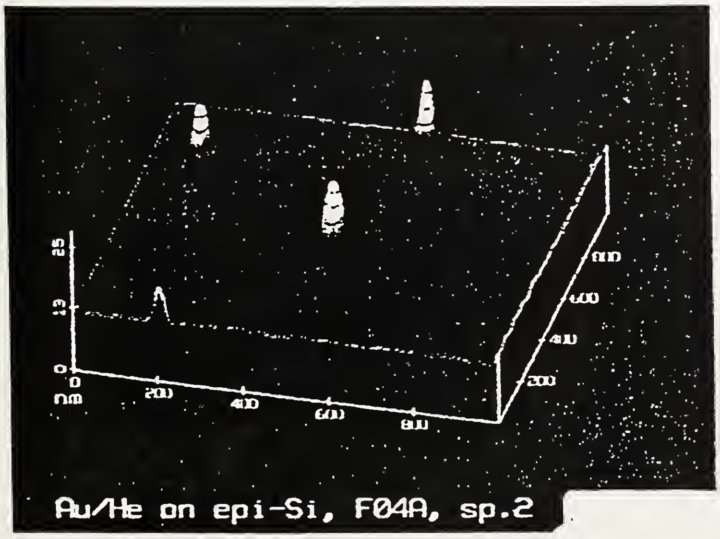

ADVANCED SURFACE MICROSCOPY, INC.

Figure 4

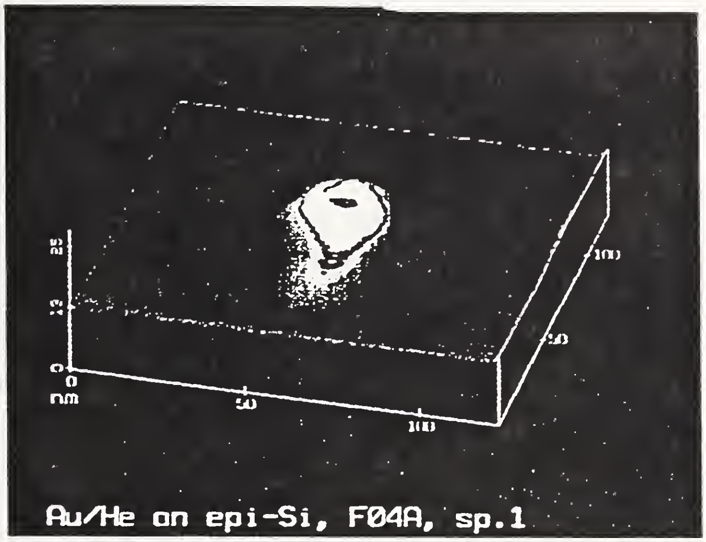

ADVANCED SURFACE MICROSCOPY, INC.

Figure 5

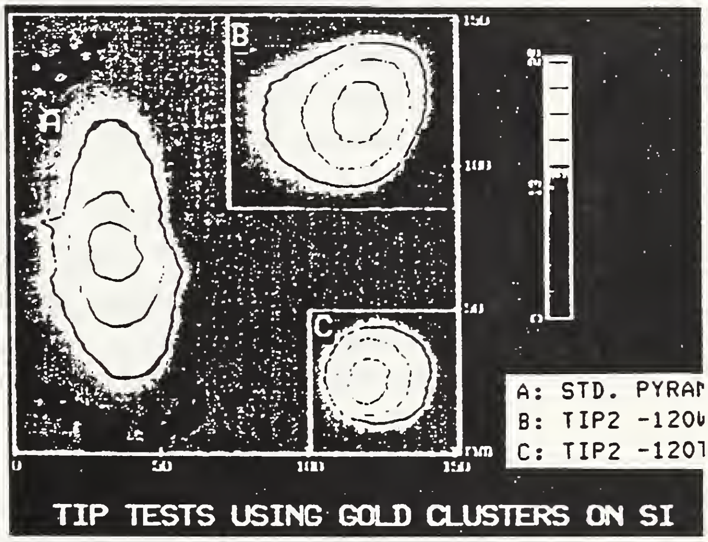

ADVANCED SURFACE MICROSCOPY, INC.

Figure 6

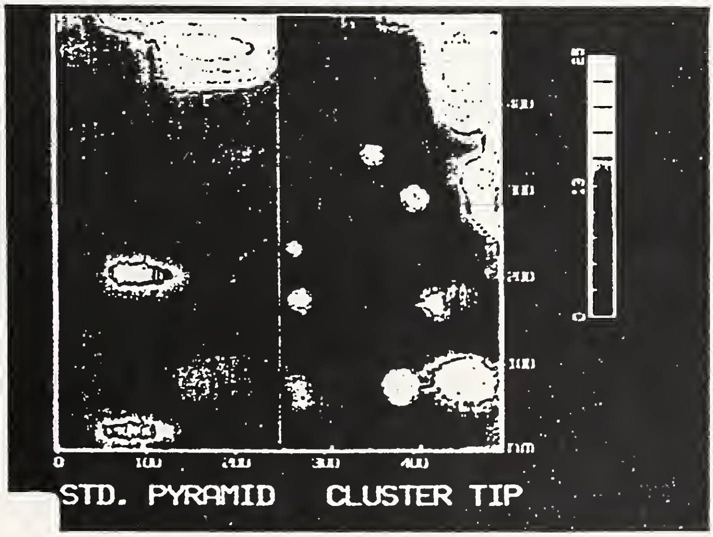

ED SURFACE MICROSCOPY, INC.

ISO Methodology for Determining and Reporting Uncertainty in Measurement for Surface Topography Standards

As of January 1, 1994, VLSI Standards, Inc. has adopted the use of ISO methodology for determining and reporting uncertainties in measurements.[1]

The ISO working group (WG 4) has produced a document that will dramatically improve the transferability of metrology results, interlaboratory consistency and understanding of metrology worldwide. The endorsement of this methodology by NIST essentially completes the internationalization of metrology practices.[2]

VLSI Standards, Inc. is adopting this method for all NIST traceable product calibration and certification, including *Surface Topography Standards.*

Calibrated values (step height, pitch) and *expanded uncertainty* values (at a 95% confidence level) are reported on the Certificate of Calibration. Summaries of measurand input and output quantities, standard uncertainty components, *combined standard uncertainty*, *degrees of freedom*, and expanded uncertainty *coverage factors* are reported in annexes which accompany the certificate of calibration.

Surface Topography Standard (STS) is designed for characterization and calibration of scanned probe microscopes (SPM). The versatile design incorporates features defined in all three spatial directions, allowing correct imaging, measurement standardization, calibration, and monitoring of the instrument's linearity and long term stability. It also offers valuable information about sample alignment as well as probe tip integrity and conditions.

The standard consists of a 12x8 mm silicon die with a precisely fabricated silicon dioxide pitch cluster. The pitch cluster contains 3 distinct grid patterns spaced 100 µm apart. Each grid pattern measures approximately 270x270 µm and consists of an array of alternating bars and spaces, with extremely uniform pitch in both *X* and *Y* directions.
The nominal reference pitches are 3, 10, and 20 µm. STS models are available for nominal reference step heights 18, 44, 100 and 180 nm. The entire die, including the features on the calibration area is coated with a uniform layer of platinum. The precise manufacturing technique ensures a very regular topographic pattern, allowing accurate measurement across the entire working surface of the standard.

The Surface Topography Standard is certified and traceable to NIST for pitch and step height and meets MIL-STD-45662A.

---

[1] ISO/TAG 4/WG 3: June 1992, Guide to the Expression of Uncertainty in Measurement.

[2] NIST Technical Note #1927: January 1993, Guidelines for Evaluating and Expressing the Uncertainty of NIST Measurement Results.

STS TRACEABILITY TO NIST

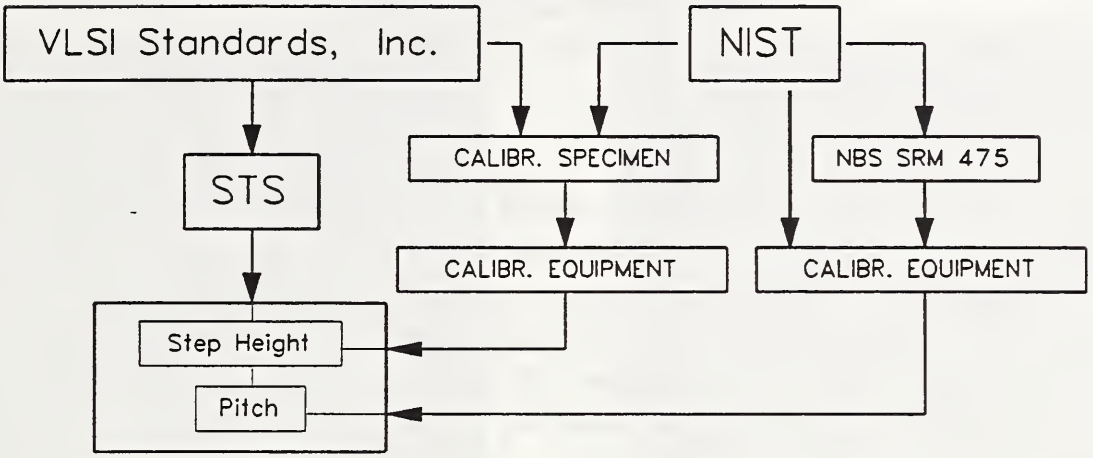
VLSI Standards, Inc.
NIST
STS
CALIBR. SPECIMEN
NBS SRM 475
CALIBR. EQUIPMENT
CALIBR. EQUIPMENT
Step Height
Pitch

VLSI Standards, Inc.

SURFACE TOPOGRAPHY STANDARDS

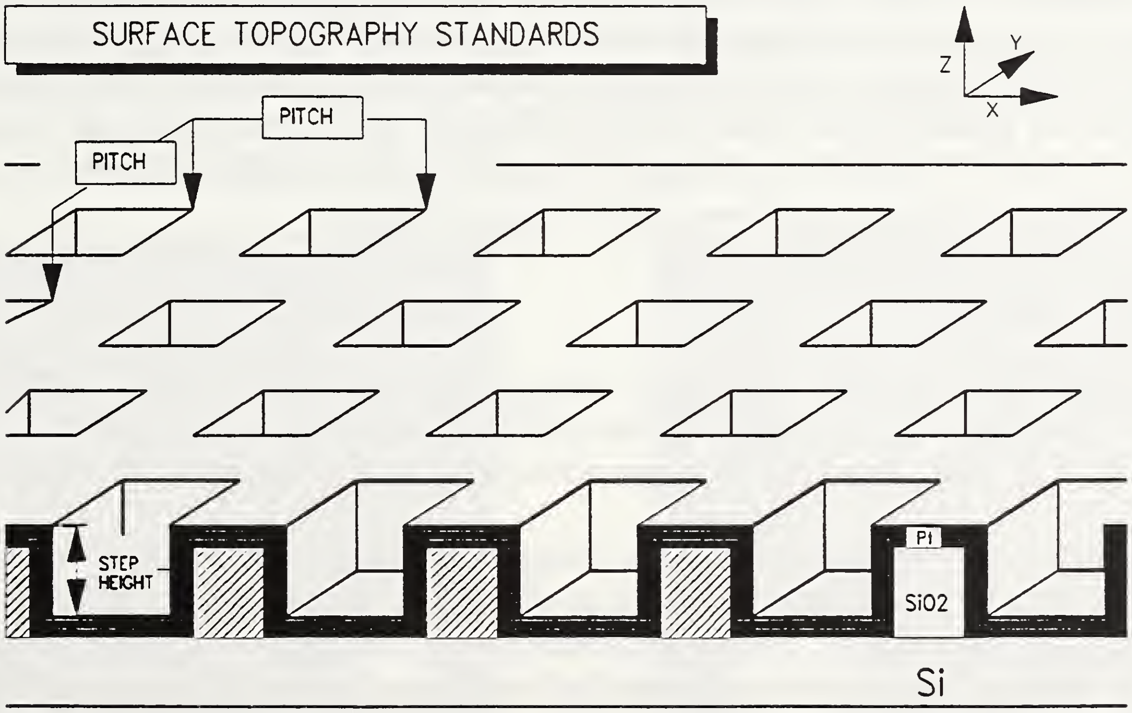
Z
Y
X
PITCH
PITCH
STEP HEIGHT
Pt
SiO2
Si

VLSI Standards, Inc.

USE OF TIP STANDARDS IN THE STUDY OF SILICON SURFACES BY ATOMIC FORCE MICROSCOPY

REBECCA M. RYNDERS, JAMES R. STETS, and ANDREW G. GILICINSKI*
Corporate Research Services Department
Air Products and Chemicals, Inc.
Allentown, PA 18195

ABSTRACT

Progress is reported in the development of a reliable methodology for imaging silicon surfaces with the atomic force microscope (AFM). A key to our methodology is the use of tip standards for checking AFM probe tips. Colloidal gold spheres have been used to fabricate tip characterization standards, and AFM images of the spheres are used to report tip size and symmetry. The use of these standards is now being extended to other industrial probe microscopy studies, including the study of particle coalescence in polymer coatings by AFM and carbon films by scanning tunneling microscopy using platinum coated standards.

INTRODUCTION

Surface roughness measurements of silicon surfaces are critical to a number of technologies in semiconductor device manufacturing. Light scattering or interferometric methods have been used to determine roughness at the micron scale. The AFM allows access to lateral dimensions at the nanometer scale. We have found that differences in AFM tip size and shape can have a significant effect on the roughness values obtained in AFM measurements. However, until recently, tip characterization standards and procedures have not been generally available. In the course of studies at Air Products aimed at developing new chemical vapor cleaning processes for silicon wafers, we have developed a methodology for characterizing AFM tips and reporting values of approximate tip diameter and symmetry with roughness values.

EXPERIMENTAL

AFM experiments were done in air using a Digital Instruments NanoScope III MultiMode AFM using "oxide sharpened" Si_3N_4 tips for contact-mode AFM or etched single crystal silicon tips for tapping-mode AFM. Device quality p-type silicon (100) wafers were used in the studies.

Tip characterization was done in two ways. Uncoated tips were imaged in a JEOL 6300 field emission scanning electron microscope with an accelerating voltage of 2 kV, which allowed magnification up to 50,000x. For key measurements, tips were analyzed before and after AFM imaging to determine whether gross damage had occurred and to estimate tip diameter. In addition, a tip characterization standard was prepared using colloidal gold spheres (Ted Pella) deposited on mica with l-lysine. This standard consisted of a dispersion of three diameters of gold spheres (about 7, 14, and 28 nm diameter), with diameters determined from heights in AFM images.

RESULTS

Field emission SEM was used to obtain a macroscopic view of tip size and shape. Examples from imaging tapping mode tips are shown below. A damaged tip with debris attached is seen in (a), while an image of a good tip is shown in (b) (slightly distorted by charging effects).

(a)

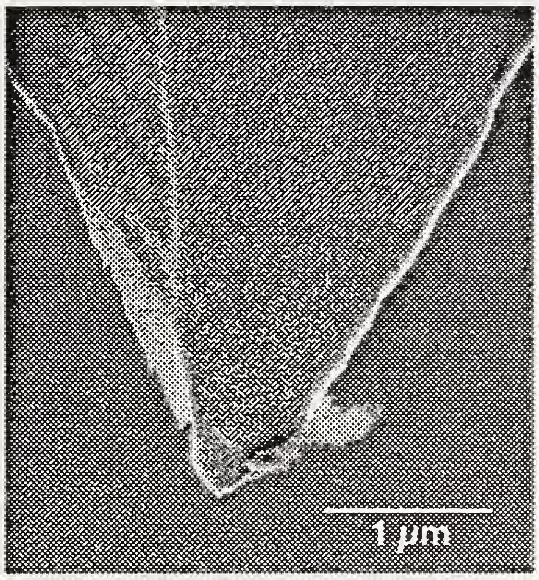

(b)

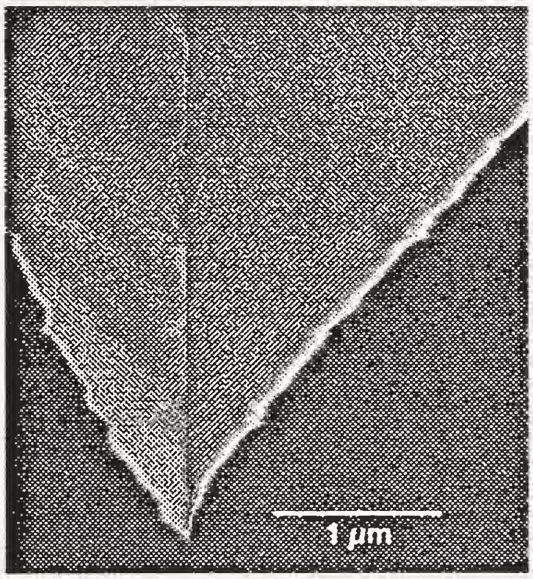

Tips were also characterized by AFM imaging of gold spheres on mica. AFM images (c) and (d) were obtained on the same sample using tips (a) and (b), respectively. Triangular images of 7 and 14 nm gold spheres are seen for tip (a), while tip (b) revealed uniform 7 and 28 nm spheres. Tip diameters were estimated to be 50 and 20 nm for (a) and (b), respectively, by geometric analysis of AFM data. Roughness values for silicon surfaces were found to vary based on the diameter of the tip used, and tip characterization by field-emission SEM and AFM was found to be critical to allowing a quantitative comparison of silicon surface roughness from different AFM experiments.

(c)

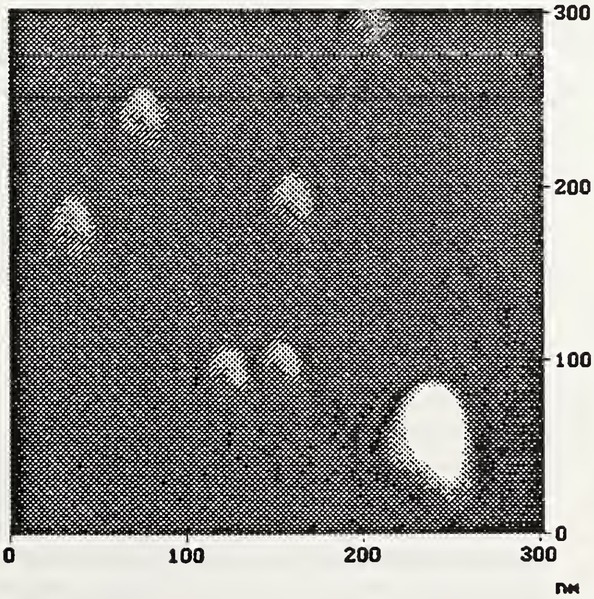

(d)

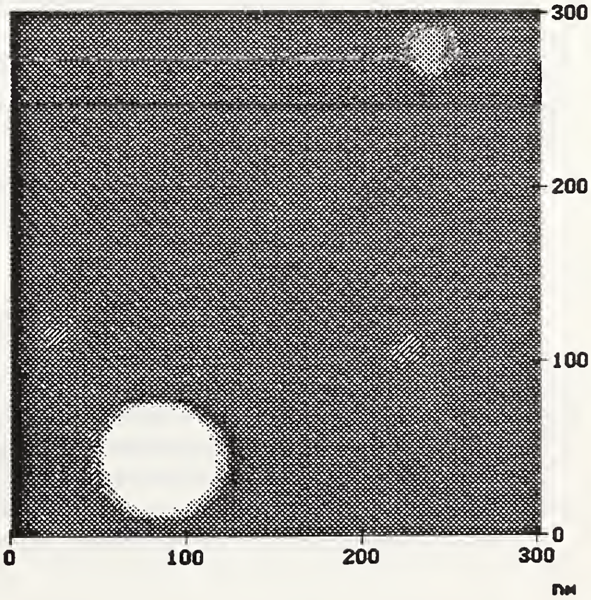

The Effect of AFM Tip Radius on Imaging of Thin Film Surfaces

K. L. Westra and D. J. Thomson, Department of Electrical and Computer Engineering, University of Manitoba, Winnipeg, Manitoba, Canada R3T 5V6

Abstract

Distortion of AFM images by the size of the AFM tip is a significant artifact in imaging of columnar thin films. A 2-D numerical simulation of AFM tips scanning columnar thin films was used to study the accuracy of AFM images. We show that for the distortion AFM images of columnar thin films to be small enough to be undetectable by eye, the radius of features in the AFM image must be 10 times larger than the radius of the tip. However, if the radius of features in the AFM image was less than twice the radius of the AFM tip, the images are severely distorted and not representative of the surface of the thin film.

1.0 Introduction

The atomic force microscope is closely related to the surface profilometer. In both instruments, a stylus is used to probe the topography of the surface. In surface profilometry, it is well known that the surface profiles are distorted by the size of the stylus [1,2]. Similar distortion of AFM images by the finite size of the AFM tip has also been recognized [3,4]. In this paper, we study a special case, the AFM imaging of columnar thin films and describe a simple technique for determining accuracy of the AFM image.

2.0 Distortion of AFM Images of Thin Films

The microstructure of thin films tends to be columnar. This columnar microstructure is well known in thin films deposited by sputtering, evaporation, electrodeposition, and occasionally chemical vapour deposition (CVD) [5]. A simulation of the spherical apex of an AFM tip scanning a columnar thin film is shown in figure 1. The AFM profiles for two different tip radii are shown in this figure. This figure shows the distortion of the AFM profile caused by the finite radius of the tip. The distortion causes the features to appear wider and the spaces between the features become smaller. As the distortion increases, smaller features on the surface are no longer imaged, and the AFM profile no longer reflects the distribution of features in the real surface. Unfortunately, the distorted profiles shown in figure 1 have the expected shape of a columnar thin film. There are no visual clues that mark these profiles as distorted. This makes identifying distorted AFM images of columnar thin films, difficult.

We showed previously that severely distorted AFM images can be found by measuring the radius of curvature of the features in an image [3]. The radius of curvature of a feature can be determined from the feature's cross section. An approximate radius of curvature of a feature in an AFM image can be found by calculating the radius of a truncated sphere with the same height and width as the feature. This radius is given by;

$$R_{AFM} = \frac{h^2 + \left(\frac{w}{2}\right)^2}{2h}$$

where w is the width of the feature and h, its height. The cross section must be taken through the highest point in the image or the radius of curvature is not valid.

3.0 Accuracy of AFM Images

The delineation between acceptable and unacceptable distortion in AFM images is arbitrary, since the amount of acceptable distortion in an image depends on how the data is used. In our work, we are interested in imaging the surface structures of thin films. For this application, distorted images are acceptable if most of the features in the orginal surface are reflected in the AFM image. A numerical simulation was used to study how the distortion of the image varies as the relative size of the tip and the surface changes.

Our numerical simulation is similar to that used to study surface profilometry [1]. The simulation is two dimensional and the interaction between the surface and the tip is geometric. It is also assumed that only the spherical apex of the tip is in contact with the surface. The AFM profile is determined by numerically determining the trajectory of the apex of the AFM tip, as the tip scanned over the surface. Using the simulation, three categories of tip distortion were defined; visually accurate AFM images, non representative AFM images, and distorted images.

3.1 Visually Accurate Images

AFM images are often used as micrographs or pictures of the surface. If the distortion of an AFM image by the finite size of the tip is very small, the distortion will not be visible to the eye. We consider such images visually accurate. For the distortion in an image not to be visible, the difference between the

AFM profile and the actual surface must be less than what can be perceived by the eye. In a grey scale image, the human eye can perceive approximately 50 grey levels [6]. If the distortion at each pixel in an image is less than one of these 50 grey levels, the eye will not perceive any distortion. We have shown using simulations of tip scanning over trial surfaces, that for AFM images of columnar thin films to be visually accurate that the radius of curvature of the features in the AFM image must be greater than 10 times the tip radius ($R_{AFM}/R_{tip} > 10$) [7].

3.2 Non Representative Images

If AFM images are to be used to study the surface features of columnar thin films, then some distortion of the image is acceptable. However, if the AFM images are distorted to the extent where smaller features are no longer imaged, then the AFM profile does not reflect the distribution of features in the actual surface. We call images that do not reflect the actual surface of the thin film, non representative. We found using the simulations that AFM images of columnar thin films are non representative of the actual thin film surface when radius of curvature of the features in the AFM image are less than twice radius of the AFM tip ($R_{AFM}/R_{tip} < 2$) [7].

3.3 Distorted AFM Images

Between films visually accurate and non representative AFM images, are distorted AFM images. These AFM images are visibly distorted, but still reflect the general shape of the film surface. These distorted AFM images, which have AFM features with radii between 2 and 10 times the tip radius, must be carefully interpreted.

4.0 Implications

To determine the extent of tip shape induced distortion in AFM imaging of thin films, a study of the radius of curvature of 23 different columnar thin films was performed [3, 7]. For this set of films, the AFM images of only 6 films were visually accurate, while for 7 films, the AFM images were non representaive. The AFM images of a majority of the films (10 of the 23) were in the third category, distorted. The results of this study suggest that distortion of AFM images of thin films is a significant artifact and must be accounted for when interpreting AFM images of thin films.

5.0 Conclusions

The distortion of AFM images by the finite size of the tip can be a difficult to detect artifact in AFM imaging of thin films. However, the extent of the distortion in an image can be determined using a simple technique, the ratio of the radius of the features in an AFM image to the radius of the tip (R_{AFM}/R_{tip}). The accuracy of AFM images was studied using a numerical simulation. Using the results of the simulation and an AFM study of the surfaces of thin films, we found that the distortion of AFM images by the finite size of the tip is a significant artifact. AFM images of 17 of the 23 films were distorted by this artifact, with 7 of these distorted images were severely distorted.

Acknowledgments

The authors wish to thank the Natural Sciences and Engineering Research Council and the Micronet Network of Centres of Excellence (Canada) for their financial support.

References

1) V. Radharkrishnan, Tribology Int., April, p 101 (1977)
2) W. Hillmann, O. Kranz, and K. Eckolt, Wear **97**, 27 (1984)
3) K. L. Westra, A. W. Mitchell, and D. J. Thomson, J. Appl. Phys. **74**, 3608 (1993)
4) J. E. Griffith and D. A. Grigg, J. Appl. Phys. **74**, R83 (1993)
5) K. G. Sheppard and S. Nakahara, Processing of Advanced Materials **1**, 27 (1991)
6) R. C. Gonzalez and P. Wintz, 'Digital Imaging Processing' (Addison-Wesley, Reading Mass. 1977)
7) K. L. Westra and D. J. Thomson, to be published

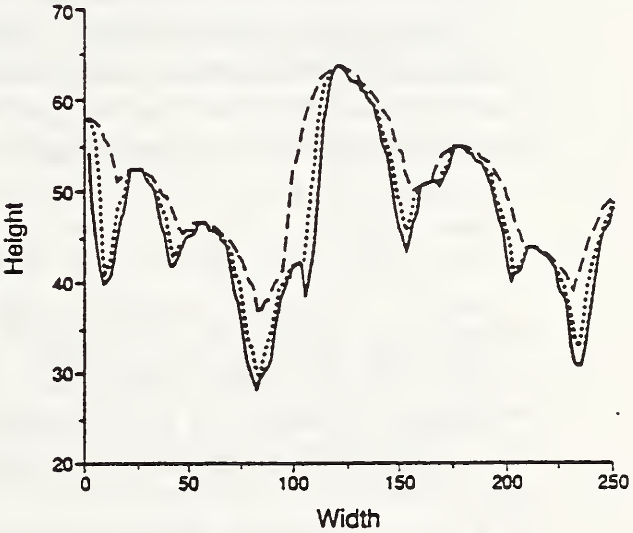

Figure 1. Numerical simulation of the AFM tip scanning over the cross section of a Al-Cu thin film. The ratio of the AFM feature radius to the tip radius is 4.4 for the dashed and 1.7 for the dotted line. The dashed profile is a distorted image of the surface, while the dotted profile is a non representative image of the surface.

Electrical Characterization of Semiconductors by STM: Tip-induced Band Bending and Pinned vs. Unpinned Surfaces

R. M. Feenstra and M. A. Lutz
IBM T.J. Watson Research Center
Yorktown Heights, NY 10598

Spectroscopic studies of semiconductor surfaces using the scanning tunneling microscope (STM) yield information on both surface state features and bulk band derived features. The latter are dominant in studies of passivated surfaces such as GaAs(110):S or Si(111):H, and also dominate for cleaved GaAs(110) which is "self-passivated". Tunneling spectroscopy of such surfaces yield significantly different results between n- and p-type material due to the shift in Fermi-level position in the two cases.[1] Also, it is found for a given doping type that the observed tunnel current depends strongly on the doping concentration in the semiconductor.[2] The mechanism for this dependence is tip-induced band bending in the semiconductor, which leads to an attenuation of the current for lower doping densities (this same band bending is the basis for the application of scanning capacitance microscopy to doping determination). The attenuation factor which is important here is the tunneling probability of carriers through the depletion region of the semiconductor.[1] A more complete understanding of this factor will potentially lead to practical application of the STM for doping determination.

The authors have performed extensive STM spectroscopic studies on a wide range of semiconductor materials and structures, which illustrate the above points concerning doping dependence. Studies of UHV cleaved GaAs, comparing results from flat cleaves with those from stepped cleaves, are useful in understanding the effects of Fermi-level pinning due to residual surface states.[3] Such effects are the same as occur in comparing UHV prepared surfaces with passivated surfaces prepared in air.[4] The residual surface states partially pin the surface Fermi-level near midgap, and also screen the electric field from the STM tip. Such effects have also been observed on H-terminated Si surfaces, prepared in a variety of ways. For ideal surfaces, doping determination can be performed simply by counting the number of dopant atoms,[5] but for nonideal surfaces (which occur in practice) the above dependence of the tunnel current on doping concentration through tip-induced band bending must be employed. Experimental results, and computer simulations, of this dependence will be presented.

1. R. M. Feenstra and J. A. Stroscio, J. Vac. Sci. Technol. B 5, 923 (1987).
2. R. Maboudian et al., Surf. Sci. Lett. *275*, L662 (1992).
3. R. M. Feenstra, A. Vaterlaus, J. M. Woodall, and G. D. Pettit, Appl. Phys. Lett. *63*, 2528 (1993).
4. S. Gwo, K.-J. Chao, and C. K. Shih, Appl. Phys. Lett. *64*, 493 (1994).
5. M. B. Johnson, O. Albrektsen, R. M. Feenstra, and H. W. M. Salemink, Appl. Phys. Lett. *63*, 2923 (1993).

Cross-Sectional Scanning Probe Microscopy of Semiconductor Structures

M.B. Johnson, H.W.M. Salemink, and E. Druet*

IBM Research Division, Zurich Research Laboratory,
CH-8803 Rüschlikon, Switzerland
*IBM France, Service 1807-31U,PB 58
F-91105 Corbeil-Essonnes, France

The on-going down-scaling of semiconductor structures for device applications requires novel analysis tools. Ultimately, chemical and structural properties on an atomic scale, as well as electronic and optical properties on a near-atomic-scale are needed in both the lateral and depth dimensions. Conventional techniques can measure such quantities, unfortunately, they spatially average over several nanometers in one or more dimensions. In contrast, various scanning probe microscopies (SPMs) are sensitive to such properties on a near-atomic or atomic scale in all dimensions. Such microscopies have usually been applied to planar surfaces. However, interface layers and buried interfaces that make up semiconductor structures, can be accessed by using suitable cross-sectional surfaces (i.e surfaces through which bulk properties can be sensed). Such cross-sectional scanning probe microscopies (XSPMs) are ideally suited to the analysis of semiconductor structures. Already, their applications are becoming important and this will increase in the future.

In this work, we discuss our applications of several XSPMs to three distinct types of semiconductor structures. These structures include, in order of decreasing maturity: A) III-V nanostructures, B) group IV heterostructures, and C) real Si CMOS FET devices. The differences in the level of success to date are the result of differences in material properties – namely the success at generating a suitable cross-sectional surface, rather their industrial impact.

A) III-V Nanostructures

Conventional III-V (001)-oriented materials easily cleave producing an essentially atomically-smooth cross-sectional (110) surface. This cleaved surface has been used in two ways: *ex-situ* cleave and $S(NH_4)_2$ etch to produce an electronically-passivated surface; and direct UHV-cleave to produce a 1x1 reconstructed, unpinned, surface. The former allows access of electronic properties of the structure and is not discussed here (see Ref. [1]). The latter provides a remarkable surface which allows the group-III and -V sublattices to be separately imaged. We discuss our results using this surface. These include: 1) Atomic-scale chemical sensitivity within the group-III sublattice, which allows the assessment of interface roughness, as well as alloy clustering and ordering in various heterostructure system [2]; 2) Imaging of individual dopants, which allows the measurement of doping profiles in modulation-doped structures with atomic precision [3]; and 3) These abilities are then applied to quantum wire nanostructures [4]. In 3) a new technique called scanning tunneling-induced luminescence (STL) is also used. This technique allows the measurement of the luminescence efficiencies of nanostructures.

B) Group IV Heterostructures

Cleaving technologically-useful Si(001) is not as simple as that for GaAs(001). Both (110) and (111) type cleavage faces are possible, however, neither are as well behaved as the GaAs(110) cleaved surface. The (111) face is difficult to achieve from the (001) growth geometry and has not been studied in this context. The in-situ UHV-cleaved (110) surface is disordered and pinned, and so far the *ex-situ* HF-dipped (110) surface is partially pinned and contaminated. In this work we discuss results on the HF-dipped (110) surface including: Si p/n structures, where variations in electronic properties over 5 nm have been achieved; and Si/SiGe modulation-doped structures where the interfaces are identified and electronic properties across these are observed [5].

C) CMOS FET Devices

Realistic CMOS FET device structures consist of heterogeneous mixture of semiconductor, metallic, and insulator layers. This has profound effects on the cross-sectional surface preparation as well as the SPM techniques that can be employed. Regarding the former: cleaving will not work, instead polishing -analogous to that used in TEM- must be used. Regarding the latter: the probe technique must be able to cope with insulators, so that atomic force microscopy (AFM) and scanning capacitance microscopy (SCM) are the leading candidates. In this work, we discuss AFM on cross-sectionally polished ULSI DRAM cells [6]. Success has been achieved in imaging the gate oxide and capacitor insulator with remarkable detail. Outstanding problems are the chemical identification of the materials under study and the assessment of two-dimensional doping profiles within these device structures.

References

1. C.K. Shih et al. in this proceedings.
2. M.B. Johnson, U. Maier, H.P. Meier and H.W.M. Salemink, Appl. Phys. Lett. **63**, 1273 (1993).
3. M.B. Johnson, R.M. Feenstra, O. Albrektsen and H.W.M. Salemink, Appl. Phys. Lett. **63**, 2923 (1993).
4. M. Pfister, M.B. Johnson, S.F. Alvarado, H.W.M. Salemink, U. Mari, D. Martin, F. Morier-Genoud and F.K. Reinhart, submitted to Appl. Phys. Lett.
5. E.T. Yu, M.B. Johnson and J.M. Halbout Appl. Phys. Lett. **61**, 201 (1992).
6. P.H. Albarede and E. Druet, Proc. 2nd European Symp. on Reliability of Electron Devices, ESRED '91, Vol.2, 747 (1991), and unpublished.

16/03 '94 21:15 ☎01 724 08 09 IBM RESEARCH CH 003

AIR AND VACUUM STM/S OF BULK-DOPED GaAs AND pn JUNCTIONS

R. M. Silver (a), J. A. Dagata, and W. Tseng
National Institute of Standards and Technology
Gaithersburg MD 20899

Characterization of local electronic properties and topography of semiconductor device structures is of increasing importance as critical dimensions are scaled down. Techniques must be developed to allow improved measurements of doping homogeneity, surface-state energy distributions and defect densities. The new class of scanned probe instruments, the scanning tunneling microscope (STM) in particular, makes possible non-destructive electronic measurements on the sub-nanometer scale with unparalleled resolution. Mapping the density of states of an individual defect, three-dimensional images of isolated dopants, and atomically resolved interfaces are only a few of the advances. Although these examples show the potential of the STM it remains a challenge to make accurate, quantitative electrical measurements on real surfaces encountered in device fabrication since these surfaces have a substantial number of surface states or lack of atomic order.

The intent of this study is to provide the basis for a comprehensive understanding of STM/S measurements of non-ideal semiconductor surfaces and device structures. This knowledge base is directly useful to the electronics industry and to the development of new scanned probes such as the scanned resistance and capacitance microscopes. The key to facilitating scanned probe microscopy as a reliable quantitative measurement tool is the development of a systematic understanding of tip-sample interactions to enable the accurate interpretation of the data. A necessary step in this process is the application of STM techniques to well-characterized samples with known dimensions and controlled surface-state densities. Bulk-doped GaAs and MBE-grown heterostructures provide this model system, allowing the complete study of passivated surfaces in air and UHV and a detailed comparison with UHV cleaved surfaces.

The format used in the work presented here is to first collect a substantial imaging and spectroscopic database from cleaved, passivated bulk-doped GaAs in air and UHV [1]. n- and p-type bulk-doped samples of various doping densities and surface terminations were used to provide a complete sample spectrum: The different surface terminations, sulfur (GaAs:S) and oxygen (GaAs:O), yield different surface-state distributions and zero-bias bandbending, Φ_{bo}, while the different doping densities change the Fermi level within the semiconductor creating different surface-state occupations and Φ_{bo} [2]. The spectroscopic and imaging results are then modeled by adapting the planar metal-insulator-semiconductor (MIS) theory to account for the variable tip-sample separation in STM, the different interfacial layers (vacuum, air) and tip geometry [3]. To accurately account for surface state distributions in the theoretical simulations, independent optical photoreflectance measurements were used. The experimental STM results in conjunction with photoreflectance data, Hall resistivity measurements etc. impose the necessary external constraints to develop a model which explains all of the fundamental experimental observations. These calculations also show the usefulness of making spectroscopic measurements at different tip-sample separations, s, in understanding the complex exponential dependence of the current on s and sample voltage, V.

With a detailed understanding of STM measurements on passivated bulk GaAs surfaces we then performed an in-depth set of spectroscopic and imaging measurements on the simplest and best understood device, a pn junction [4]. With a substantial experimental database obtained in air and UHV from symmetric and asymmetric pn junctions with varying depletion widths we modeled the STM tip-pn junction system with a more complex application of the MIS theory incorporating surface-state- and tip-induced bandbending effects as well as the space-charge component due to the pn junction [5]. The key experimental observations explained in this work are the bias dependent junction locations, the change in relative height of the p and n regions under different imaging conditions, and the effects of surface terminations.

The successful application and verification of a quantitative two-dimensional model to the STM results is essential, since experimentally observed tip-induced effects can be significant, moving the apparent junction location by as much as 100 nm. There is consistent agreement within the bandbending model from the data obtained in air and UHV. The dielectric nature of adsorbates present during STM/S in air has been taken into account in the model and is responsible for the different data acquisition parameters and the dramatic effects observed when comparing air and UHV results. The combined experimental and theoretical effort demonstrates that the STM is an effective tool for analysis of surface-state distributions and dopant profiling on the local scale. The proper systematic treatment of surface-state- and tip-induced bandbending make the STM a quantitative measurement tool for semiconductor device structures on the nanometer scale.

(a) Supported through a grant from the Office of Naval Research

[1] J.A. Dagata, W. Tseng, and R. M. Silver, J. Vac. Sci. Technol., **A11** 1070 (1993).
[2] J.A. Dagata, W. Tseng, J. Bennett, J. Schneir, and H.H. Harary, Appl. Phys. Lett., **59** 3288 (1991).
[3] R.M. Silver, J.A. Dagata, and W. Tseng, Submitted to J. of Appl. Phys., (1994).
[4] W. Tseng, J.A. Dagata, R.M. Silver, J. Fu, J.R. Lowney, J. Vac. Sci. Technol. **B12** 373 (1994).
[5] R. M. Silver, J.A. Dagata, and W. Tseng, Submitted to Appl. Phys. Lett., (1994).

PROGRESS TOWARDS CONTACT MODE POTENTIOMETRY

John Moreland
National Institute of Standards and Technology, Boulder, CO

Craig Prater
Digital Instruments, Santa Barbara, CA

One of the first adaptations of scanning tunneling microscopy (STM) was scanning tunneling potentiometry (STP).[1,2] The proximity between the STM tip and sample afforded by the tunneling feedback mechanism leads to the nanoscopic spatial resolution of STP. Further, at a given point on the sample, with the feedback off, it has been shown that the voltage measurements can be made with a resolution of 100 nV using a tunneling current nulling scheme. STP works well on conductive samples where a reasonable tunneling contact can be maintained during scanning.

More recently, the atomic force microscope (AFM) has been adapted for scanning potentiometry.[3] The advantage of AFM is that parts of the sample being scanned can be insulating. The likely superiority of an AFM potentiometry over STP becomes evident when one considers potentiometry imaging of submicron structures like the interconnects or contact vias of ULSI circuitry. In such cases it will be difficult to land a STM tip on the sample without crashing.

The question is what mode of operation is the best for AFM potentiometry? Requirements to be considered for industrial applications include nanoscopic spatial resolution, submillivolt voltage resolution, reasonable scan times, calibratibilty, simplicity of operation, and operating cost. AFM potentiometry can be divided into two general categories - contact or noncontact. In contact modes the tip and sample are in physical contact whereas in noncontact modes electric field-forces between tip and the sample are used to deduce voltage variations along the sample surface. Contact-mode potentiometry has the advantage of high spatial and voltage resolution if measurable electrical contact can be maintained while scanning. This can be difficult, as discussed below, due to surface contamination between the tip and the sample. This is not a problem in noncontact mode. However, since electric-field forces between the tip and the sample are long range, spatial resolution is limited. Further, the tip-sample force interaction has to be modeled or calibrated in some way in order to determine an accurate potential.

The high compliance of an AFM cantilever compared to the STM tip of STP is a source of difficulty when performing contact-mode AFM potentiometry. Both the cantilever tip and sample may have a fluid surface contamination layer. In addition, the cantilever and sample may be oxidized or corroded in some way. During STP the rigid STM tip pushes the fluid layers away and breaks through any thin oxide in order to establish tunneling contact to the sample. The movement of a AFM cantilever tip on the other hand is dominated by fluid meniscus forces and the presence of surface oxides.[4] Fluid forces can dominate the tip sample interaction preventing electrical contact even between a Au coated tip and a Au sample as reported by Meepagala, *et al.*[5]

Even if fluid and oxide effects could be minimized the area of the contact is presumably quite small. In the Sharvin limit[6] where the mean free path, l, is much larger than the radius of the contact, a, $R_{contact} = 4/3\pi \bullet \rho l/a^2$. $\rho l = 5 \bullet 10^{-12}\ \Omega\text{-cm}^2$ for most metals. Assuming an atomic sized contact of 0.1 nm radius contact, $R_{contact} = 21\ \text{K}\Omega$. Note that this is for the ideal case of clean point contact. Typical AFM contacts have resistances above 1 MΩ. Such high resistances make direct voltage measurements difficult. Thus, a current nulling scheme similar to those applied in STP should be used.[3] Current sensitivity should be better than 100 pA in order for voltage sensitivity below 1 mV. A current sensitive preamplifier located close the cantilever is required. Recently, we have been experimenting with miniature preamps built into the cantilever holder.

We have been trying to develop a process for making highly conductive cantilever tips. In one method micromachined Si cantilevers (which are readily available commercially) have been coated with 100 nm of Au. The Si based technology lends itself to well established batch microfabrication processing. We have found the same results as Meepagala, *et al.* when making a static AFM contact in air. The main conclusion is that one has to push very hard (10 to 100 nN) on the sample to make contact. This force level would be damaging to the tip and sample in a scanning mode. Also, we found if one maintains static contact at lower force levels, eventually, over many seconds or minutes, the cantilever tip will drift into contact. This time scale is so long that it would lead to image frame rates of many days.

Au coated cantilevers are susceptible to abrasion. So, we are now looking into ways of treating the Si tips so that the bare Si or a very thin durable coating on bare Si will be used for contact. The Si should be highly doped to reduce Shottkey barrier effects. Preliminary measurements indicate that n-type Si tips with a resistivity around 0.02 Ω-cm work roughly as well as the Au coated tips in static contact tests in air after the Si was etched in buffered HF or 10:1 HF. Very, recently we have experimented with B and P thermal diffusion sources in order to increase doping at the surface of the tips. B doping may have the additional advantage because during this process a tough, thin, highly conductive SiB diffusion layer forms on the surface of the Si.[7]

At this juncture we feel the main problem with contact mode AFM potentiometry is that it is difficult to make measurable electrical contact in air without physically disturbing the tip or the sample at the atomic level. The primary problem is the fluid layer between the tip and the sample in air. We believe that the effects of oxide corrosion can be minimized by cleaning the sample prior to imaging. We are now considering operation in a desiccated, high-vacuum, or fluid-cell conditions. However, we feel that for certain samples with hard surfaces high resolution contact-mode AFM potentiometry in air is possible.

[1.] P. Muralt and D. W. Pohl, Appl. Phys. Lett. 48, 514 (1986).

[2.] J. R. Kirtley, S. Washburn, and M. J. Bradey, Phys. Rev. Lett. 60, 414 (1988).

[3.] M. Anders, M. Mück, C. Heiden, J. Vac. Sci. Tech. A8, 394 (1990).

[4.] H. G. Hansma, J. Vesenka, C. Siegerist, G. Kelderman, H. Morrett, R. L. Sinsheimer, V. Elings, C. Bustamante, and P. K. Hansma, Science 256, 1180 (1992).

[5.] S.C. Meepagala, F. Real, and C. B. Reyes, J. Vac. Sci. Technol. B9, 1340 (1991).

[6.] Yu. V. Sharvin, Sov. phys. JETP 21, 655 (1965).

[7.] private communication, M. P. Czyz, Carborundum Co.

Two-dimensional Delineation Of Semiconductor Doping by Scanning Resistance Microscopy

C. Shafai and D. J. Thomson
Department of Electrical Engineering, University of Manitoba, Winnipeg, Manitoba,
Canada, R3T 2N2

M. Simard-Normandin
Northern Telecom Limited, Ottawa, Ontario, Canada, K1Y 4H7

Introduction

To meet the challenge of producing ULSI circuits, there is a need for the development of techniques for the two-dimensional delineation of P-N junctions with high spatial resolution. We will be describing a new technique for junction delineation using a Scanning Resistance Microscope (SRM). In this technique, a sharp conducting probe is used to perform localized resistance measurements over a semiconductor surface. These measurements are used to delineate between regions of different doping type and concentration. The SRM was constructed from a modified Park Scientific Instruments Scanning Force Microscope (SFM), which was operated from custom electronics. The SRM probe was fabricated from a metal wire of diameter 250 µm. Both tungsten and molybdenum wires were used successfully. In order to produce sharp probe tips, the probe tips were electrochemically etched in 1.27 M KOH solution. The probe was mounted as a cantilevered beam 2 cm in length, and the free end of the probe beam was used to probe the sample under test. Resistance measurements were performed as follows. The SRM probe was placed in contact with the sample. With the p- and n-type regions of the sample electrically grounded, a bias voltage was applied to the probe and the current flowing between the probe and the sample was measured. The resistance of the probe-surface contact was then obtained. Two dimensional resistance measurements were performed by moving the sample in a raster pattern beneath the probe. A piezoelectric scanner capable of three dimensional motion was used to displace the sample.

The ultimate spacial resolution of SRM measurements is determined in part by the mechanical contact area between the SRM probe and the sample. As shown by Weihs et. al. in [1], the contact radius between a hemispherical tip and an elastic surface is given by:

$$\text{Contact Radius} = (3PR/4E^*)^{1/3} \qquad (1)$$

where P is the applied force, R is the tip radius, $E^* = [(1-\nu_1^2)/E_1 + (1-\nu_2^2)/E_2]^{-1}$ and E_1, ν_1 and E_2, ν_2 are Young's modulus and Poisson's ratio of the tip and sample respectively. Equation (1) shows that in order to achieve high spacial resolution, the radius of curvature of the SRM probe tip and the probe-sample contact force must be minimized.

A low contact force along with the small radius of curvature of the probe tip, resulted in a probe-surface contact radius estimated, using (1), to be 30 nm. In order to insure a constant probe-surface contact area during measurements, the force controller of the Park Scientific SFM was used to maintain a constant contact force.

One dimensional resistance profiles were performed across a cleaved P-N junction sample [2]. Figure 1a shows the result of an SRM conductivity scan across the junction.

Figure 1b shows the junction dopant profile as obtained by spreading resistance profiling [3]. In order to compare these two profiles, the sample surface (located at 0.0 µm in the two figures) was used as a topographical point of reference.

In Figure 1a we see the following. Between 0.0 and 0.32 µm the p-type region is highly conductive. This region corresponds to the highly doped p-type region near the sample surface. Between 0.32 and 1.0 µm the p-type region possesses a lower conductivity. Between 1.0 and 1.05 µm we see a change in the measured conductivity as the SRM probe crosses from the p-type region to the n-type region. Figure 1a clearly shows the SRM's ability to distinguish between regions of high and low dopant concentration, and between regions of different dopant type. The spacial resolution of this measurement was estimated by determining the distance it took the current to rise from 10% to 90% of its value in the n-type region. This distance is labeled δ in Figure 1a and is measured to be 35 nm. This represents an upper bound on the spacial resolution of the SRM and is in reasonable agreement with the contact area.

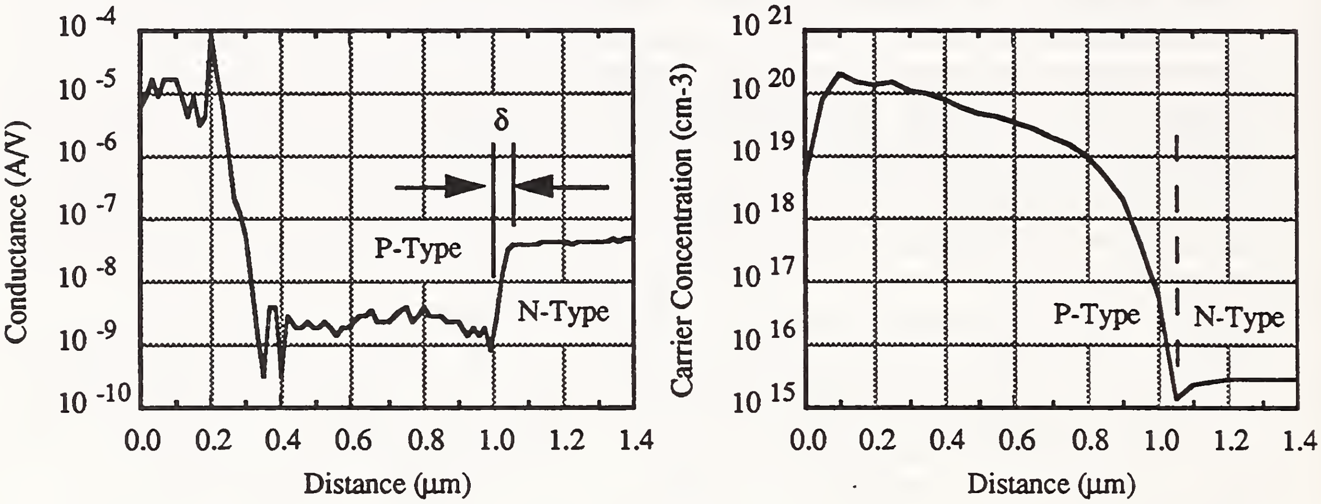

(a) (b)

Figure 1: Result of a one dimensional SRM profile across a P-N junction performed by a molybdenum SRM probe biased to 0.2 V. (a) is the SRM measured probe-surface conductivity. (b) is the junction doping profile as measured by spreading resistance.

We will also be presenting two-dimensional resistance images of 1 µm diameter p-type islands on an implanted n-type layer.

In conclusion, we have outlined a new technique for P-N junction delineation based on scanning resistance microscopy. This technique is capable of P-N junction delineation with less than 35 nm spacial resolution. The SRM has shown capable of distinguishing between regions of different doping type and concentration. The SRM has also shown to be capable of performing simultaneous conductivity and topography measurements.

The authors also thank the Natural Sciences and Engineering Research Council of Canada and Micronet for financial support.

REFERENCES

1. Appl. Phys. Lett., **59**, 3536 (1991).
2. Sample supplied by Y. Loke, Alberta Microelectronics Center, Edmonton, Canada.
3. Spreading resistance profiles by Solecon Laboratories Inc., San Jose, California.

A Calibrated Atomic Force Microscope

Thomas H. McWaid and Jason Schneir

Abstract

Atomic force microscopy (AFM) is a rapidly emerging measurement technology. As the technology develops, it is being incorporated into industrial research and development, and manufacturing facilities. At present there are no sub-micrometer pitch or sub-ten nanometer height standards suitable for calibrating AFMs. University- and industry-based researchers are developing suitable calibration artifacts. We are developing an AFM capable of calibrating these artifacts.

Introduction

Advances in the manufacture of integrated circuits, x-ray optics, magnetic read-write heads, optical data storage media, film, etc. require advances in ultraprecision metrology. Each of these industries is currently investigating the use of AFM to improve the precision and accuracy of their manufacturing process control measurements. AFM is one of only a very few techniques that have the potential to make measurements at the required level of resolution.

One roadblock to the use of the AFM is the lack of NIST-traceable sub-micrometer pitch standards and sub-ten nanometer height standards suitable for calibrating commercial AFMs. Researchers are developing specimens with artifacts of this size that may prove suitable for the calibration of AFMs; however, NIST does not yet have the capability of performing calibrations at the required level of accuracy. We are developing a Calibrated AFM (C-AFM) in order to overcome this limitation.

Apparatus

The basic design goal of this project is to combine commercially-available components/sub-assemblies into an AFM-based metrology system meeting the following performance specifications: (1) Measurements are to be made in air in order to maximize throughput; (2) A scan range of a least 100 μm; (3) A lateral resolution of 2 nm; (4) A lateral measurement uncertainty of 3 nm; (5) A vertical resolution of 0.1 nm; (6) A vertical measurement uncertainty of 1 nm.

We use a Wye Creek[1] flexure stage driven by Physik Instrumente piezoelectric (PZT) actuators for scanning; Kepco high voltage amplifiers to drive the PZT actuators; Zygo heterodyne interferometers to measure the X-Y displacement of the sample; a Queensgate PZT actuator with integral capacitance sensor to generate and measure z-motion; and a Park Scientific Instruments control system. The interferometers are mounted on an invar metrology frame; the z-stage is fastened to the invar flexure stage.

---

[1] Certain commercial equipment, instruments, or materials are identified in this paper in order to specify adequately certain experimental procedures. Such identification does not imply recommendation or endorsement by the National Institute of Standards and Technology nor does it imply that the materials or equipment are necessarily the best available for the purpose.

The precision and accuracy of commercial metrology equipment has improved considerably over the last five years. We expect the requirements of ultraprecision metrology to continue to drive this trend. Our use of commercial equipment will allow us to upgrade the C-AFM as improvements are made.

Preliminary Measurements

The C-AFM is presently in a preliminary configuration. We have conducted several experiments with the instrument in an effort to characterize the performance of various sub-systems, including the interferometers, the control electronics and software, and the flexure stage. Fig. 1 presents a plot of 1000 data points that were obtained over one second while the stage was held at a fixed position (based on the x-axis interferometer reading) under active control. The individual bits (corresponding to 1.24 nm each) of the interferometer are apparent. Using these data, the RMS jitter was found to be 1.4 nm, and the linear drift was determined from a least squares fit of the interferometer data to be less than 0.02 nm/s. In contrast, the drift with the feedback loop open was measured to be 7 nm/s. Fig. 2 presents data from a 0.32 μm peak-to-peak sinusoidal scan. The RMS value of the residuals after subtracting out the best fit sine function is 2.1 nm.

Fig. 1 X-Axis Jitter

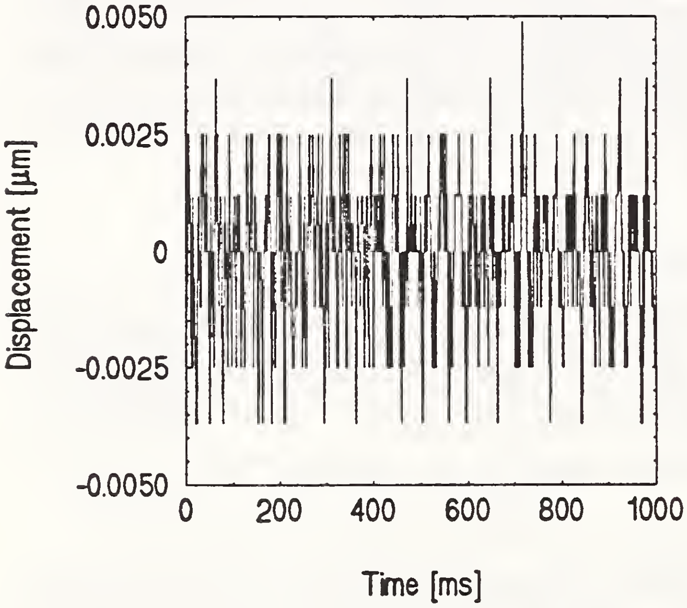

Fig. 2 Sinusoidal Scan

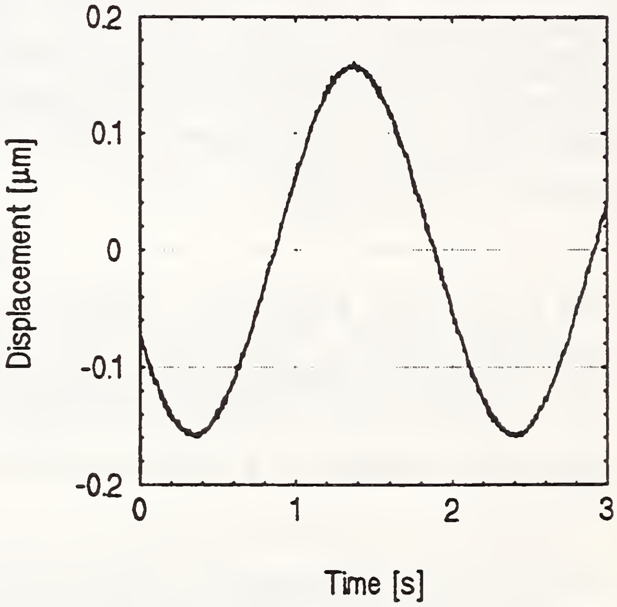

Summary

The National Institute of Standards and Technology has initiated the development of a calibrated AFM that will be used to perform highly-resolved measurements that are directly traceable to the wavelength of light in all three axes of motion. The C-AFM will be used to measure artifacts that can be purchased by industry. These reference artifacts will enable customers to calibrate their own AFMs with traceability to NIST.

Effect of Overlayer Thickness on the Nanoindentation of SiO_2/Si

Charles F. Draper[1], Richard J. Colton[2], and Steven M. Hues[2]

[1] Department of Mechanical Engineering, Vanderbilt University, Nashville, TN, USA 37205

[2]Code 6170, Naval Research Laboratory, Washington, D.C., USA 20375-5342

A main forte of the atomic force microscope (AFM) as a nanoindentor is its ability to measure mechanical properties of thin films down to one monolayer. The properties measured, however, are composite properties that reflect not only the intrinsic properties of the film, but also the underlying substrate. Upon tip/surface contact, a stress field is generated which penetrates into the sample. The magnitude of the composite modulus is determined by the relative distribution of the stress and strain fields between the layer and substrate.

Amorphous SiO_2 layers were grown on Si (100) single crystals by dry thermal oxidation. Oxide thickness was measured by ellipsometry. A blank sample which was subjected to the same cleaning procedure as the thermally processed samples served as an additional sample with a native oxide of 1-2 nm. Nanoindentation was performed with an AFM, described in detail elsewhere(1). All nanoindentation measurements were performed under identical conditions using the same indentor tip with the instrument in a thermally isolated dry-nitrogen glove box.

Simulations of the force - penetration depth relations were performed using finite element analysis (FEA) on a Cray YMP-EL computer using the ABAQUS FEA code(2). Using symmetry, only one quarter of the specimen and one half of the indentor needed to be modeled to simulate the indentation. The finite element mesh for the semi-infinite sample was discretized into 1162 axis-symmetric, four-noded elements with 1318 nodes. In microindentation experiments the shape of the loading curve signifies the geometry of the indentor. Because the shape of the AFM indentation curves is linear, the indentor in the simulation was modeled as a rigid flat punch of 40 nm diameter.

Several significant features may be seen in the force curves of the thin oxide layers, Figure 1. Firstly, there is an initial contact region seen in the native oxide data associated with a low elastic modulus surface hydrocarbon layer. In the thermally-grown oxide samples a much sharper jump-to-contact region is observed which is presumably obscuring the hydrocarbon layer. The increased surface forces responsible for the jump-to-contact may be due to some intrinsic property of the thermally-grown oxide or due to differences in surface energy. Secondly, with increasing

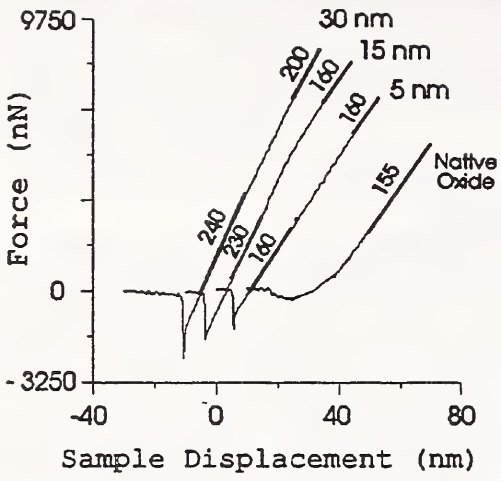

Figure 1: Force curves of thin oxide layers on Si.

penetration the slope, which is directly proportional to elastic modulus (3), is seen to increase as the stress field encounters the stiffer oxide layer, this we will refer to as the "oxide" region. A third region is then seen as the stress zone encounters an increasing fraction of the more compliant underlying Si substrate, the "bulk" region. Mean values for the slope of the curves for each of these regions are shown. The slope in the region primarily attributed to the oxide layer is also seen to increase with oxide thickness. This may be explained by the increasing contribution of the stiffer oxide layer to the sample volume containing the stress gradient. This effect is also seen in the steeper slope of the "bulk" region in the 30 nm oxide sample.

The results of the FEA modeling of the loading portion of the force curves shows good qualitative agreement with the experimental data. As the oxide layer thickness increases from 0 to ∞ (bulk oxide) the slope of the curve also increases, similar to the effect seen in the "oxide" portion of the experimental curves. Although there is a qualitative agreement between the model and experiment, quantitative agreement would be entirely fortuitous at this time for several reasons. The first is that we do not know the actual nature of the tip/sample contact. In the model we presume that it is a flat punch. Secondly, two of the inputs required for the FEA model are the elastic modulus and the Poisson's ratio of the material. For the current FEA results, the bulk modulus of Si and SiO_2 were used. However, it has been documented in the literature(4,5) that the nanoscale mechanical properties of materials can be quite different than the bulk properties. We hope to be able to model the smaller scale contacts by developing model systems and systematically vary the contact area.

References

1. N.A. Burnham and R.J. Colton, J. Vac. Sci. Technol. **A7**, 2906 (1989).
2. ABAQUS finite element program, ver. 5.3 (1993), HKS Inc. Providence, RI, USA.
3. G.M. Pharr, W.C. Oliver, and F.R. Brotzen, J. Mater. Res., **7**, 613 (1992).
4. T.E. Schlesinger, R.C. Cammarata, A. Garvin, J.Q. Xiao, C.L. Chien, M.K. Ferber, and C. Hayzelden, J. Appl. Phys. **70**, 3275 (1991).
5. J.B. Pethica, R. Hutchings, and W.C. Oliver, Philos. Mag., 48 (1983) 593.

Scanning Near Field Optical Microscopy for Genetic Mapping and Information Storage

Raúl Fainchtein
Applied Physics Laboratory, Johns Hopkins University
Laurel, Maryland 20723-6099

The scanning near field optical microscope is capable of imaging objects with a resolution in the range of 50 nm. This overcomes the fundamental resolution limitation of conventional optical microscopy realized more than 100 years ago by Ernest Abbe. Namely, that diffraction would impose a resolution limit of the order $\lambda/2$ where λ is the wavelength of the radiation used to probe the specimen. We are applying scanning near field optical microscopy to problems in the areas of medicine and information storage.

In the area of medicine we are attempting to identify areas on human chromosomes that may be involved in cancer initiation. In order to asses and develop a technique to detect genetic predisposition to cancer, it is necessary to isolate the genetic region believed to be responsible for this condition. Mapping of particular areas of a chromosome depend in large part on the ability to hybridize and localize cosmid probes to G-banded chromosomes. Current mapping techniques are ultimately limited by resolution under light microscopy. In addition, molecular techniques including YAC cloning, and cosmid cloning allow definition of higher resolution maps. Much of the time consumed in current mapping techniques is spent in the arrangement of different clones in a specific order to obtain the fine resolution map. We are using scanning near field optical microscopy to improve resolution for in situ hybridization. Furthermore, the ability to hybridize specific probes to a large human genomic fragment or YAC may allow physical ordering without molecular techniques. These new techniques may improve the resolution of physical mapping and reduce the time needed to order probes across a large genomic region.

In the area of information storage we intend to increase the density and speed of erasable storage materials by the application of scanned near field optical techniques to excite and deexcite photochromic materials including metallorganic nanoparticles that display bistable optical behavior. With near field optical techniques we expect to optically switch detect and erase photochromic materials with a resolution in the 50 nm range. This will be particularly interesting in particles with nm diameter in which nonlinear effects could enhance a multilevel behavior and therefore multilevel storage (more than two levels per storage site) may be achieved.

MEASURING BIOMOLECULAR RECOGNITION INTERACTIONS WITH THE ATOMIC FORCE MICROSCOPE

G. U Lee, D. A. Kidwell, R. J. Colton
Code 6177, Surface Chemistry Branch, Naval Research Laboratory, Washington, DC 20375-5320, U.S.A.

The strategies that living organisms employ for replication, regulation and assembly are based upon macromolecules capable of molecular recognition. Although molecular recognition bond energies are accessible through kinetic studies, the forces of interaction have not been accessible up to this time. We have exploited the capacity of the AFM for measuring forces on the order of a single atomic bond, i.e., forces of 10^{-12} Newton magnitude over displacements of 0.01 nm, to study molecular recognition interactions.

In this presentation we will discuss the specific interactions and nonspecific surface forces measured between surfaces functionalized with the complimentary components of two systems: 1.) a model receptor-ligand complex (i.e., streptavidin-biotin) and 2.) double-stranded DNA. We will demonstrate that the form and magnitude of the adhesive force resulting from the molecular recognition interaction may be measured for *individual* intermolecular interactions through the control of environmental conditions, the area of contact and density of molecules on the surfaces. Further, the influence of the physical chemistry of the surfaces, the environmental conditions and the manner in which the bonds are stressed can be correlated with the properties of the observed interaction.

Phases of alkanethiol self-assembled monolayers on Au(111): The c(4x2), px$\sqrt{3}$, and the 2-D liquid phase

G. E. Poirier, H. E. Rushmeier, and M. J. Tarlov
National Institute of Standards and Technology
Gaithersburg Md 20899

Abstract:

We report ultrahigh vacuum scanning tunneling microscopy (STM) of *n*-alkanethiol $[CH_3(CH_2)_{n-1}SH]$ (C_n) monolayers self-assembled on Au(111) single-crystal surfaces. The STM images show that the saturation coverage self-assembled monolayer (SAM) unit cell measures 0.86 x 1.0 nm and contains four thiolate molecules (see graphic right). The observed unit cell is consistent with results from recent x-ray, electron, and helium diffraction studies. This unit cell corresponds to a c(4x2) superlattice of a basic ($\sqrt{3}$x$\sqrt{3}$)R30 dense-packed monolayer. The domain size is 5.0 to 15 nm with domains separated by molecular-width rotational boundaries and stacking faults. SAMs composed of longer chain thiols (C_8 and C_{10}) were stable in vacuum for over 40 days. Short-chain homologues (C_4 and C_6) exhibited a 2-D liquid phase at room temperature. Ordered domains having a unit cell of px$\sqrt{3}$ ($p \approx 9$) nucleate homogeneously on the Au terraces and grow. This ordering transition was observed in real time using STM. Facile mass transport of surface gold atoms was observed in the presence of the liquid phase. This mass transport was shut-off as the ordering transition went to completion. No such 2-D liquid phase was observed for longer chain homologues (C_8 and C_{10}).

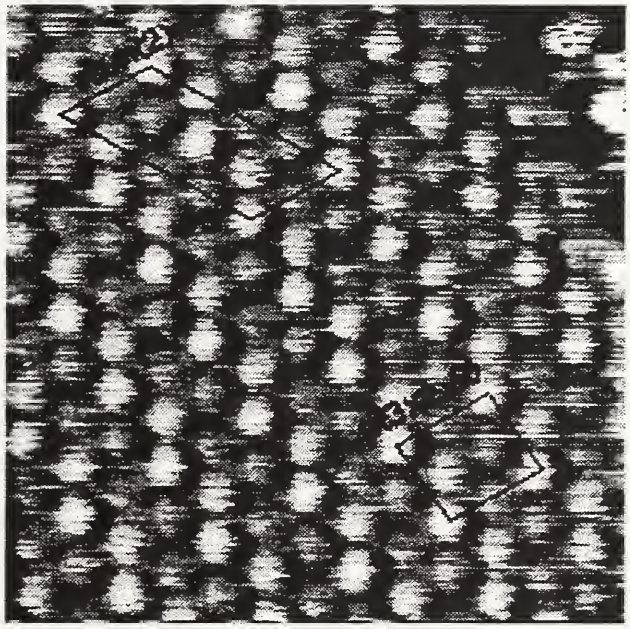

March 3, 1994

3-D Chemical Profiling of Sub-surface Semiconductor Structures by Magnetic Resonance Force Microscopy

P.C. Hammel and G.J. Moore, Los Alamos National Lab, Los Alamos, NM 87545
and
M.L. Roukes, Condensed Matter Physics, Caltech, Pasadena, CA

As dimensions of semiconductor devices become smaller, the details of the sub-surface electronic, structural and chemical properties become increasingly important in determining the behavior of the device. Thus there is a critical need for high resolution scanning microscopies capable of probing *sub-surface* properties of semiconductor devices. We are currently developing a Magnetic Resonance Force Microscopy (MRFM) instrument which may allow for direct visualization of sub-surface structure and electronic behavior in semiconductors. In particular, this technology will be capable of direct 3-D imaging in semiconductors from depths of several tenths of a micron to a few microns below the surface depending on the resolution desired. Ultimately, we expect to be able to obtain chemical-specific images of dopant density, to study *individual* donor/acceptor cores, and to image impurities with single electron spin sensitivity.

Recently published work has shown that any magnetic resonance observed using conventional inductive techniques, can also be detected using microscale mechanical resonators and the technology of force microscopy. The very exciting aspect of MRFM is that, through emerging capabilities in surface micromachining, mechanical detection can offer greatly increased sensitivity and enable extremely high resolution imaging. While current inductive detection limits are on the order of $\sim 10^{15}$ nuclear spins, the theoretical limit for mechanical detection is a *single* nuclear spin. In the first experiment nuclear magnetic resonance (NMR) signals have been successfully detected with a sensitivity of $\sim 10^{13}$ nuclear spins by mechanical means. We are currently building an instrument capable of detecting nuclear magnetic resonance signals. We believe that this technique presents a promising approach for the design of a nanoscale imaging instrument. We expect after two years to have an instrument with sufficient sensitivity in an NMR experiment detecting ^{29}Si (5% abundant) nuclear spins to reduce the measurement volume to less than $(100\ \text{Å})^3$. A dopant density of $\sim 10^{18}/\text{cm}^3$ means a volume of $(100\ \text{Å})^3$ per dopant. Thus single dopant sensitivity will be necessary to achieve resolution of 100 Å. We expect to be approaching single electron spin sensitivity in electron spin resonance with this same instrument. This will allow us to determine the distribution of dopants in the semiconductor as well as study the properties of the dopants.

A key advantage of MRFM over other high resolution microscopies is the ability to probe deeply beneath the surface. In one potential configuration a permanent magnet (e.g. a lithographically patterned thin magnetic film) which produces a highly inhomogeneous field will be deposited a on a micromechanical resonator. The field gradient ∇B of the magnet provides the coupling between the (nuclear or electron) spin magnetization, $\mathbf{m}$, of a volume element deep within the semiconductor and the micromechanical resonator: $\mathbf{F} = (\mathbf{m} \bullet \nabla)\mathbf{B}$. A time varying nuclear or electronic spin magnetization then produces a force which drives the mechanical resonator. The magnetization is caused to vary at the characteristic frequency of the mechanical resonator. The variation in the resonator's oscillation amplitude is detected using laser interferometry. The factor which determines the depth of the volume element being probed is the range of the inhomogeneous field of the small magnet. Because the oscillation frequency of the cantilever is small the penetration depth of this field into conducting material is many microns. However, the resolution is determined by the magnitude of the field gradient; because this decreases with distance from the magnet, the spatial resolution decreases as probe depth increases.

Our MRFM efforts will focus on obtaining spin density images for both electron and nuclear spins by exploiting electron spin resonance (ESR) and NMR force microscopy. The advantage of ESR force microscopy compared to NMR is that ESR will allow us to achieve much higher sensitivities and resolutions due to the thousand fold larger magnetic moment of the electron in comparison to the nuclear moment. Using NMR force microscopy we will apply these well established and understood and chemical-specific NMR techniques to microscopic, sub-surface volumes. As an example, the potential for microscopic measurement of the spatial variation of the density of electronic states at the Fermi energy exists. Our initial efforts detecting NMR will have resolution on the order of a micron and will focus on developing the techniques necessary for acquisition, analysis and interpretation of mechanically detected magnetic resonance in electronic systems. Within two years we expect to obtain ~100 Å resolution in NMR using this technology. Using the same MRFM instrument we expect to have a sensitivity in ESR approaching a single electronic spin. The successful development of this instrument will enable detailed structural and electronic and chemical studies of sub-surface structure in semiconductor devices.

The key to obtaining great increases in sensitivity is the *miniaturization* of the resonant mechanical element, which forms the heart of the MRFM. This miniaturization is possible with advanced techniques of nanofabrication. We have developed new methods of surface *nano*-machining which have enabled us to fabricate mechanical resonators with masses less than one picogram and cross-sections below 100 *nm*. (We expect to press toward even smaller dimensions and sub-femtogram resonators in the near future.) Employing nanostructures such as these to build a magnetic resonance force microscope presents formidable technological challenges, and will require specific innovations in displacement readout and overall instrument design. Nonetheless, we believe the goal of instruments yielding atomic scale resolution is achievable.

We give here a brief description of how NMR imaging of, for example, the density of boron dopants in silicon might work (assuming the development of appropriate deconvolution algorithms). The resonant frequency of a boron nuclear spin is proportional to the magnetic field it experiences: $\omega_o = 2\pi\gamma B$ where B is magnetic field, and γ is the gyromagnetic ratio. Thus we can differentiate boron from silicon spins by this field/frequency relationship. Further, if the applied field varies spatially, then the correspondence between applied field and resonant frequency translates into a correspondence between spatial location and frequency. Thus only the boron nuclei in a small volume satisfy the field/frequency relationship. The enhanced sensitivity of MRFM allows one to reduce the volume of the sample isolated for study, and thus to improve the resolution of the microscopic study while maintaining adequate signal to noise ratios. An analogous discussion applies for electron spin resonance (ESR) imaging of the donor/acceptor cores or impurities in semiconductors. The greater sensitivity to electronic spins will provide greater resolution.

In addition to the ability to provide information about sub-surface features, MRFM has other advantages over other technologies used for characterization of semiconductors (Scanning Tunneling Microscopy and Atomic Force Microscopy), namely: the imaging is non-contacting and nondestructive, in NMR the imaging is chemical species-specific, and the theory of magnetic resonance interactions is sufficiently well developed and validated that it provides a reliable basis for the design and implementation of imaging techniques.

We believe that two years of work will set the stage for unprecedented investigations of sub-surface features of semiconductors. This work will exploit NMR resolution of ~100 Å, and the ability to conduct ESR experiments on *single* donor/acceptor cores in doped regions of semiconductors. The unique power of the NMR technique for studying electronic systems and semiconductors in particular has been demonstrated repeatedly. MRFM offers the possibility of carrying out these same experiments with nm-scale resolution. The potential MRFM offers for new insight into the physical nature of semiconductors is unprecedented.

DC MAGNETIC FORCE MICROSCOPY OF THIN FILM RECORDING HEADS

Paul Rice and John Moreland
Electromagnetic Technology Division
National Institute of Standards and Technology, Boulder, CO, 80303

We have used a recently developed DC-MFM operating technique to image thin-film recording heads.[1] This DC technique is preformed by first taking a line scan using atomic force microscopy (AFM) in contact mode. The topographical and slope information is stored. The tip is then lifted and scanned using the stored topography and slope information to position the tip from the surface. On this second scan the deflection of the tip is recorded as the magnetic signal. This allows for accurate tracking of the sample surface during the magnetic scan since the tip is away from the surface for only one scan line, thus minimizing error due to piezo drift. This also allows for simultaneous imaging of topography and magnetic force.

Two thin-film heads were measured. These were standard thin-film heads with two pole pieces that were approximately 9 μm × 3 μm as measured by the AFM. The separation of the poles (gap length), also measured with the AFM, varies from 300 nm to 500 nm. The nonuniform gap length can be attributed to polishing. On one of the heads imaged, the pole pieces were vertically offset by 200 nm. This was visible in the optical microscope and appeared to be a fracture. Although apparently flawed, the head still wrote magnetic bit patterns and produced a strong magnetic field as measured by the MFM. Separation between disk and head, or flying height, is typically between 50 nm and 100 nm. Saturation current for these heads was reportedly 40 mA. The heads were removed from the flexures and mounted in the MFM with the trailing edge of the slider to the left, relative to the images presented. The head was driven with a DC current source. The tips for these measurements were standard 100 μm Si_3N_4 microfabricated cantilevers.

Figures 1(a) and 1(b) are top-view images of the unfractured head. The tip was coated with 10 nm Fe base layer and a 10 nm Au cap layer with a spring constant of 0.58 N/m. The Au coating was to minimize oxidation of the Fe. It was calculated that the change in spring constant due to these coatings was less that 5 percent. Figure 1(a) image is magnetic and the Fig. 1(b) is topographic. In the magnetic image, attractive forces are indicated by dark contrast. The current to the head was 10 mA DC. The gap in the magnetic image can be seen as a bright line accented by the dark contrast of the pole pieces. For the magnetic image, the tip was scanned 100 nm above the surface. The maximum tip deflection is 30 nm. Multiplying this by 0.58 N/m gives a force of 17.4×10^{-9} N.

Decreasing the tip height above the sample increases the magnetic contrast due to the increasing field gradient. Pole recession of 20 nm caused by polishing can be seen in Fig. 1(b). Comparing the magnetic image to the topographical image shows that the magnetic contrast trails off, shadowing the edge of the pole piece. These fields compare closely with calculations of thin-film head field profiles by J. Zhu et al..[2]

Figure 2 is a line scan of the magnetic image taken with the tip height at 100 nm and a head drive current of 30 mA. The magnetic gap is more clearly visible in the line scan image, as is the attraction due to the pole pieces. Varying the head drive current increased tip deflection linearly with current. Tip displacement for this image is 85 nm with a corresponding force of 5×10^{-8} N. With the tip-to-head spacing again at 100 nm and the head current increased to 100 mA, the tip continually snapped onto the sample. This is attributed to the soft spring constant of the cantilever.

Figure 3 is and MFM image of a glass substrate disk. The bits were written with a thin-film head similar to the ones measured in this paper.

Figure 4 is a single scan line across the head. The arrows point to two small depressions which are the edges of the pole pieces where the field diverges most rapidly. Below the scan line, the pole pieces are indicated as blocks. This image shows that the tip is magnetically soft, since it is attracted to the pole pieces regardless of polarity. A magnetically soft tip minimizes force variations due to domain switching that can occur in high coercivity (magnetically hard) tips. In the gap the magnetic field gradient is low and deflects the tip less. The asymmetry of the image is likely due to the pole recession. Scanning direction and tip angle can also make the image asymmetrical. In this case the offset seems to be comparable to the pole recession height.

As measured in air, the tip-to-head spacing for good magnetic imaging appears to be a function of surface roughness and tip spring constant. If the surface is rough or the cantilever is very flexible, the tip snaps onto the surface often. This is attributed to the difficulty of maintaining the head-to-tip separation as force deflections cannot be anticipated during the AFM scan. With proper selection of cantilever spring constants and magnetic tip coatings, rough surfaces with large magnetic fields can be imaged. Figure 5(a) shows a topographical surface view of the head with the 200 nm vertical offset defect. The trailing pole piece is 200 nm higher than the leading one, as measured by the AFM. Figure 5(b) is a line scan display of the magnetic force image, taken with a tip-to-head separation of 187 nm. When the tip was closer than this it would contact the surface and van der Wals or meniscus forces would keep the tip in contact with the surface.

Using the DC operated magnetic force microscope allows us to study the fringing fields above thin-film heads at different driving currents and tip-to-head separations.[3] Comparison of surface topography and magnetic forces has shown there are magnetic fields associated with the ends of the pole pieces. These fields could possibly contribute to off-track failures of the drive if they are strong enough. Simultaneous imaging of surface topography and magnetic force can also pinpoint problems in head manufacture. A further advantage is that the tip-to-sample separation can be more accurately monitored, allowing much rougher samples to be imaged. We are currently studying the field profiles of thin-film heads and their corresponding bit pattern as written the disk. This should help hard drive manufacturers understand some of the head-disk readback signals.

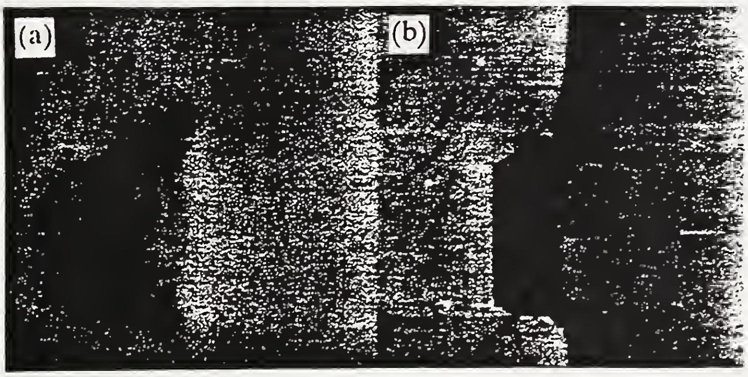

Fig. 1 (a) Magnetic force image of the air bearing surface of a thin-film head. (b) Corresponding AFM topography of the head. (20 μm × 20 μm)

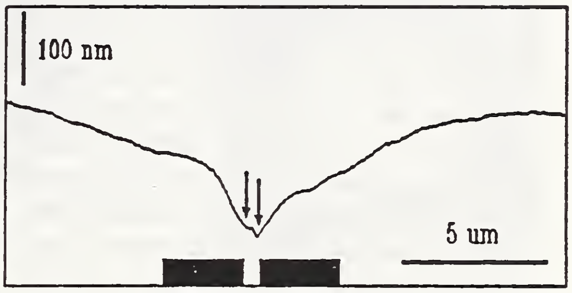

Fig. 4 An individual MFM scan line taken through the center of the head.

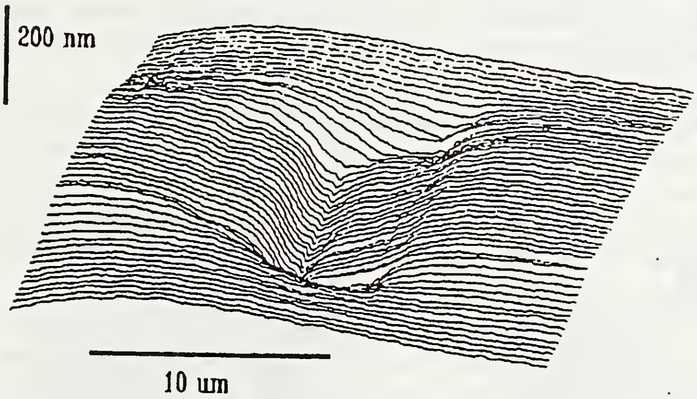

Fig. 2 Magnetic force image line scan taken of the head as it was driven with a current of 30 mA.

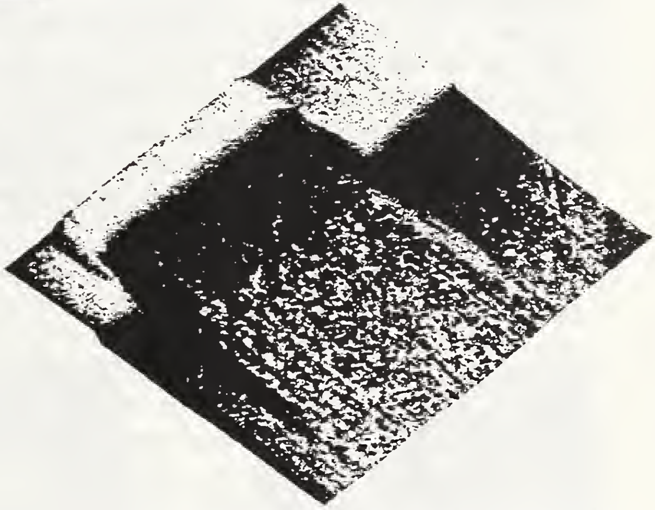

Fig. 5 (a) AFM topography of a flawed thin-film head. (15 μm × 15 μm)

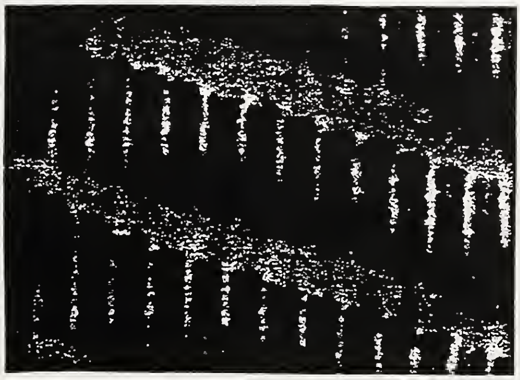

Fig. 3 DC-MFM image of glass substrate hard disk. (30 μm × 20 μm)

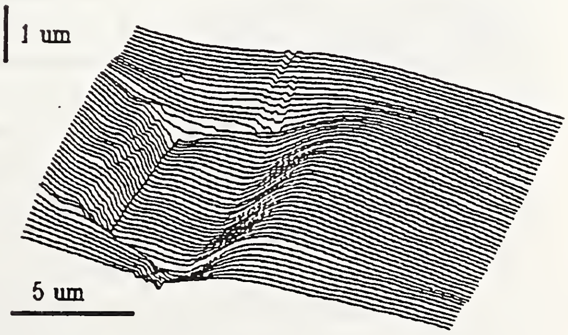

Fig. 5 (b) Corresponding MFM image of flawed thin-film head.

---

[1] R. Giles, J. P. Cleveland, S. Manne, P. K. Hansma, B. Drake, P. Maivald, C. Boles, J. Gurley, and V. Elings, Appl. Phys. Lett., Vol. 63, 617 (1993).

[2] J. Zhu, X. Ye, and T. C. Arnoldussen, IEEE Trans. Magn., Vol. 28, 2716 (1992).

[3] P. Rice, J. Moreland, and A. Wadas, J. Appl. Phys. to be published.

Surface Modification of $YBa_2Cu_3O_{7-\delta}$ Thin Films Using the Scanning Tunneling Microscope

R.E.Thomson, John Moreland and A. Roshko
Electromagnetic Technology Division, National Institute of Standards and Technology,
Boulder, Colorado 80303

Abstract

We have investigated using the scanning tunneling microscope (STM) as a tool for surface modification of $YBa_2Cu_3O_{7-\delta}$ (YBCO) thin films and have developed five distinct methods whereby the STM tip can modify the superconductor surface. The first of these we have called milling. For this method the tunneling resistance of the STM is lowered below about 2000 MΩ while the tip is being scanned. The result of milling a square area 200 nm on a side can be seen in Fig. 1. This area was milled for eight passes with a tunneling resistance of 100 MΩ. Our investigations show that this method works by mechanically scratching the surface. We find that lowering the tunneling resistance even further increases the milling rate. However, finer features can be produced by milling slower for longer periods of time.

The second method we have developed is illustrated in Fig. 2. This is an examples of a "NIST Boulder" logo we wrote with the STM using a bias voltage of 5 V and a tunneling current of 0.20 nA. In addition to the tunneling conditions, for this method the tip velocity is also an important parameter. In the case of the logo shown in Fig. 2, the tip velocity was 1 µm/s. An atomic force microscope (AFM) image of part of the logo is shown in Fig. 2(b). From the cross-section shown in Fig. 2(c) we find that the height of the letters formed by the STM is about 200 nm. We used scanning Auger spectroscopy to determine that there was no material deposited off of the tip in an area where we had written using this technique. We think that this technique damages the YBCO with the tunneling current, and so have called it electron beam damage.

Figure 3 shows an example of the third technique we developed. This technique, which we call vaporization, removes the entire film down to the insulating substrate. In order for vaporization to occur the tunneling current must be above 1 nA while the bias voltage is above 5 V. In Fig. 3, the white bar in the optical microscope image [Fig 3(a)] is the vaporized area which shows up as a deep trench in the AFM image[Fig. 3(b)]. This area was scanned at 10 V bias voltage and 20 nA tunneling current. The remainder of the square in this image was made by using the electron beam damage technique.

The fourth method we developed we call electrochemical etching because it only works when the STM is in a humid atmosphere with a high percentage of carbon dioxide. Figure 4 shows a square 500 nm on a side that was etched using this technique. In this case the tunneling current was 0.25 nA and the bias voltage was 1.0 V and the square was scanned for 33 passes. These are the same parameters we routinely use for imaging YBCO in air where we do not observe any changes in the YBCO image even after imaging up to four hours. An example of a line made using electrochemical etching is shown in Fig. 5. This line was made by 3500 translations of the STM tip using the same tunneling parameters as for the square in Fig. 4. This line is about 10 nm across at the top and is 5-15 nm deep.

The final technique we have investigated we call oxygen electromigration. This technique has proven to be very difficult to reproduce. On two occasions after scanning with the STM using our normal imaging parameters we observed that the scanned area had turned dark black in the optical microscope image. An example of this effect is shown in Fig. 6(a). The dark square started to fade within a few hours and was almost invisible 24 hours after it was first made. The same area as was shown in Fig. 6(a) after the square had faded is shown in Fig. 6(b).

We are currently attempting to use several of these techniques to create a Josephson junction in a YBCO bridge. Because of the precise control possible with the STM tip, it may be possible to create extremely small superconducting structures with these techniques.

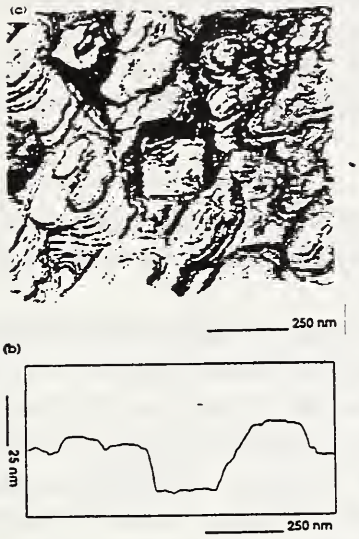

Figure 1: (a) STM image of area milled for 10 passes at a tunneling resistance of 100 MΩ. (b) Cross-section of (a).

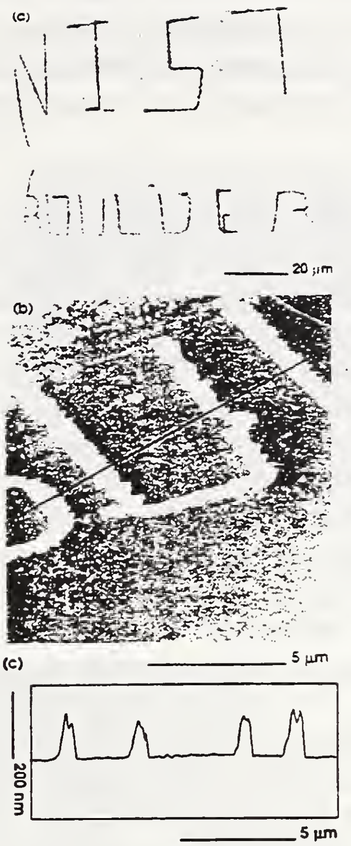

Figure 2. (a) Optical microscope image of logo written with electron beam damage method using a bias voltage of 4 V. (b) AfM image of a portion of logo. (c) Cross-section of (b).

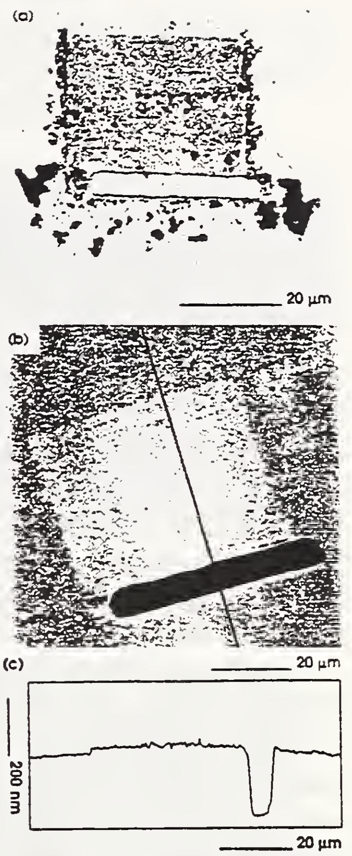

Figure 3. (a) Optical microscope image of square where the tunneling current was reduced from 20 nA to 1 nA about 1/8 of the way up the square. (b) AFM image of same area shown in (a). (c) Cross-section of (b).

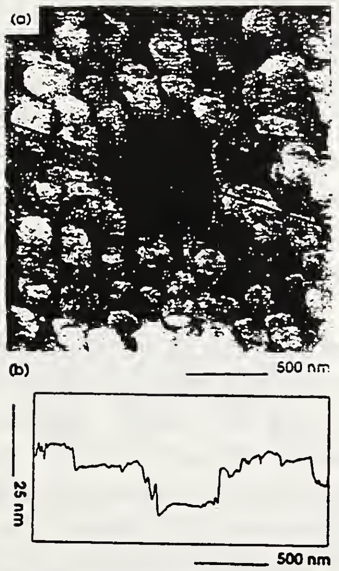

Figure 4: (a) STM image of square etched for 33 passes at 0.25 nA and 1.0 V in a wet carbon dioxide atmosphere. (b) Cross-section of (a).

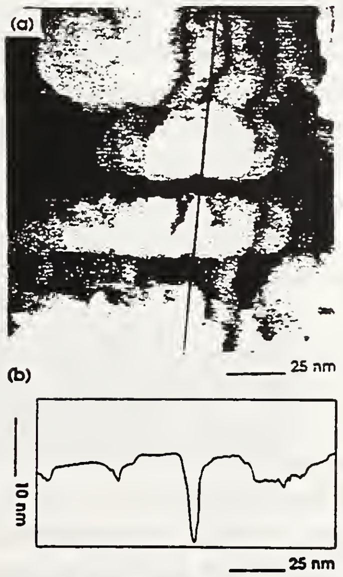

Figure 5: (a) STM image of line etched for 3500 passes at 0.25 nA and 1.0 V in a wet carbon dioxide atmosphere. (b) Cross-section of (a).

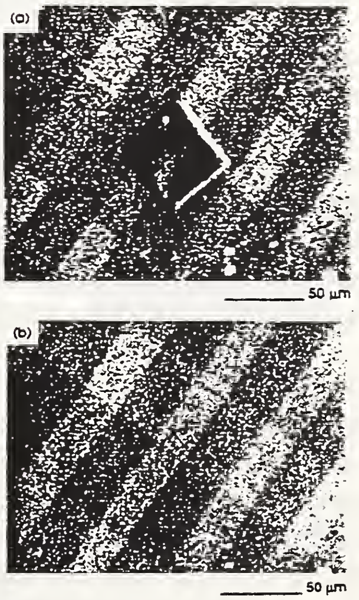

Figure 6: (a) Optical microscope image of square imaged by the STM for 5 passes at 0.25 nA and 1.0 V (b) Image of the same area after the square had faded.

SPM IMAGING OF THIN FILMS MORPHOLOGIES

Alexana Roshko
Electromagnetic Technology Division
National Institute of Standards and Technology, Boulder, CO, 80303

Most applications of thin films have stringent requirements for the film microstructure and topography. We have found that scanning tunneling microscopy (STM) and atomic force microscopy (AFM) are excellent tools for examining the morphologies of thin films.

We have examined thin films of many different materials for a variety of applications including optical, magnetic, superconductor and insulator. Each of the applications has different requirements and, therefore, different aspects of the film morphologies are of interest. For all of the films the grain size and orientation is important for properties. Most of the applications require essentially single crystalline material, however, for magnetic recording small isolated grains are desired. In addition surface roughness is an important parameter. For optical applications roughness can cause loss, for magnetic storage applications surface roughness can cause recording/reading heads to crash, and for thin film multilayer structures roughness can cause shorts between layers. In addition we have examined step edges that are important for devices and contact vias in multilayer film processing.

There are several different aspects of optical materials where the information obtained by scanned probe microscopy (SPM) is useful. We have examined wave guides formed by cation diffusion into $LiNbO_3$ single crystals and into phosphate glasses. The AFM images reveal both changes in the surface roughness and also buckling of the surfaces due to strain caused by the diffusion (fig. 1); both of these can contribute to increased losses in the guides. We have also imaged $KNbO_3$ films deposited by ion beam sputtering and solid source MOCVD. Depending on the growth conditions, the microstructures varied from large grained and rough to smooth with holes or small particles in the surfaces (fig. 2a).

Similar variations were found in the morphologies of magnetic films for recording media deposited under different conditions. Some films are fine grained with smooth surfaces while larger grained materials tend to have rougher surfaces. Frequently large protrusions were observed in the films (fig. 2b). Identifying and understanding the source of these so that they can be eliminated is of particular interest, since they can cause the magnetic heads to crash.

One of the most impressive examples of SPM studies of surfaces is that of ceramic superconductor films. Due to the conductive nature of the these materials it is possible to image them with STM as well as with AFM. We have examined thin films of $YBa_2Cu_3O_{7-\delta}$ (YBCO) deposited by sputtering, laser ablation, coevaporation and sol gel processing. Both c-axis and a-axis growth features have been observed, and the c-axis films are found to grow by both screw dislocation growth and island nucleation and growth (fig. 3). Examination of the films with the AFM does not reveal the detail found in the STM images, probably due to a reacted layer on the film surfaces which is not conductive. While the STM tunnels through this layer to image the conductive material beneath, the AFM reveals the true topography of the film surface.

We have obtained especially interesting results on yttria stabilized zirconia (YSZ) films grown on (001) Si wafers. These films are of interest as buffer layers for growing other oxide materials on Si for integration with Si technology. Films grown on Si surfaces which were stripped in situ prior to deposition gave RHEED patterns corresponding to single crystalline material. However, AFM images of these same films revealed that they had large holes, $\sim 1\ \mu m$ in diameter, that made them unsuitable for multilayer processing (fig. 4). Images of YSZ films grown on Si surfaces with a thin layer of native oxide show uniform coverage; X-ray and TEM analyses of these films revealed that they are epitaxial.

AFM is also useful for obtaining detailed information about the quality of step edges in films and substrates for multilayer devices. We have examined steps in many different oxide materials and found that the angle, height and uniformity of the edges can all vary a great deal from what was expected based on the processing parameters (fig. 5).

We have found that the high resolution of the SPM techniques allows detailed examination of thin film surfaces at a level that is very useful for understanding and controlling thin film processing for applications.

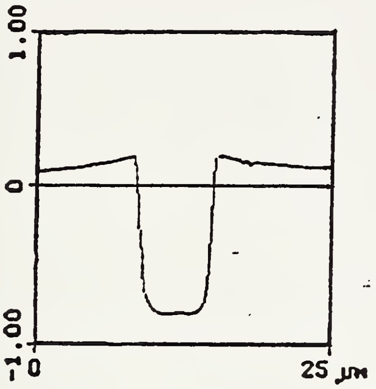

Fig. 1 Cross section from AFM image of a wavequide in P-glass.

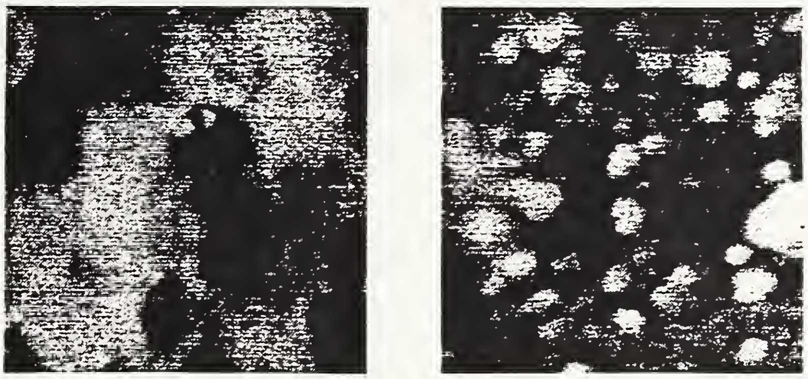

Fig. 2 AFM images of rough (a) $KNbO_3$ and (b) CoPtCr thin films. The images are 1 μm square and the gray scale is 30 nm.

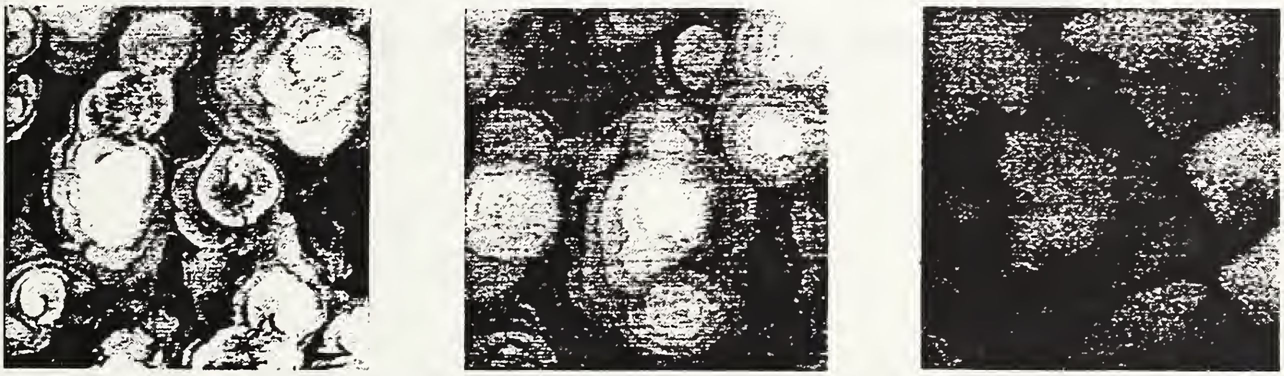

Fig. 3 STM images of YBCO films: (a) screw dislocation growth spirals in a film grown at a slow rate (6 nm/sec), (b) island growth features in a film grown at an intermediate rate (60 nm/sec), C) a-axis growth features in a film grown under supersaturated conditions. The images are 500 nm square and the gray scale is 30 nm.

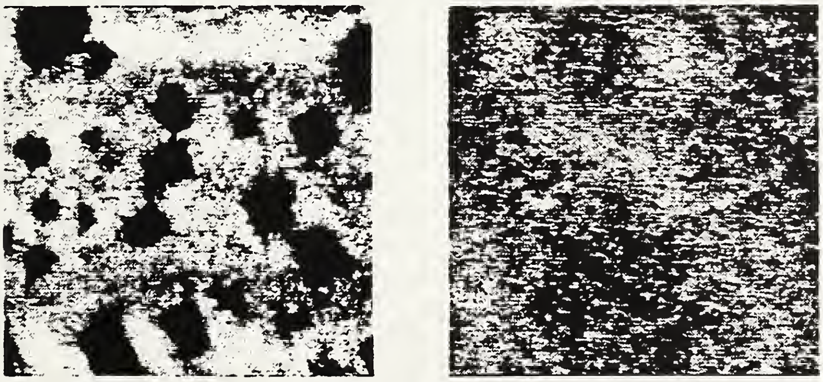

Fig. 4 AFM images of YSZ films grown on Si wafers: (a) with native oxide, (b) stripped in situ. The images are 1 μm square and the gray scales are 25 and 10 nm respectively.

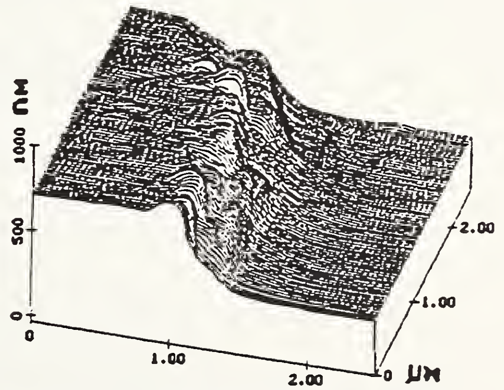

Fig. 5 AFM topography of a step ion milled into $SrTiO_3$, showing unexpected ledge in step.

Acknowledgements: Films were obtained from Stephen Russek, Steve Sanders, David Rudman, Joe Rice, Norman Sanford, Andy Aust, Pat Morris, Tom Graettinger, Thao Nguyen, Jim Speck, and Eric Tarsa. Kathleen Trott and John Moreland assisted with the SPM.

VI. WORKSHOP PARTICIPANTS

FINAL PARTICIPANTS LIST

Workshop on Industrial Applications of Scanned Probe Microscopy

March 24 - 25, 1994

Phillip Abel
NASA-Lewis Research Ctr.
21000 Brookpark Rd.
MS 23-2
Cleveland, OH 44135
USA

Winthrop Baylies
Baytech Group
30 Winsor Way
Weston, MA 02193
USA

Jeanne Beacham
Tencor Instruments

Greg Blackman
DuPont
Experimental Station
E323/110B
Wilmington, DE 19880-0323
USA

Robert Brigham
Charles Evans & Assoc.
301 Chesapeake Dr.
Redwood City, CA 94063
USA

Dan Brower
Optex Communications Group
2 Research Ct.
Rockville, MD 20850
USA

Juan Carrejo
Motorola, Inc.
2200 W. Broadway
M360
Mesa, AZ 85202
USA

Richard Chapman
Motorola
6501 William Cannan Dr. W.
MD: OE214
Austin, TX 78735-8598
USA

Donald Chernoff
Advanced Surface Microscopy, Inc.
6009 Knyghton Rd.
Indianapolis, IN 46220-4955
USA

Richard Colton
Naval Research Lab.
Code 6177
Washington, DC 20375-5342
USA

John Dagata
NIST
Bldg. 220, Rm. A107
Gaithersburg, MD 20899
USA

David Denley
Shell Development Co.
P.O. Box 1380
Houston, TX 77251
USA

Ankur Desai
MEMC Elect. Materials Inc.
501 Pear Dr.
MZ 33
St. Peters, MO 63376
USA

Alain Diebold
SEMATECH
2706 Montopolis
Austin, TX 78741
USA

Charles Draper
Vanderbilt University
Code 6170
Naval Research Lab.
Washington, DC 20375-5342
USA

Virgil Elings
Digital Instruments, Inc.
520 E. Montecito St.
Santa Barbara, CA 93103
USA

Raul Fainchtein
Johns Hopkins University
Applied Physics Lab.
Johns Hopkins Rd.
Laurel, MD 20723-6099
USA

Randall Feenstra
IBM Research
P.O. Box 218
Yorktown Heights, NY 10598
USA

Leigh Ann Files-Sesler
Texas Instruments
P.O. Box 655930
MS 147
Dallas, TX 75265
USA

Joseph Fine
NIST
Bldg. 248, Rm. 222
Gaithersburg, MD 20899
USA

Wayne Ford
Intel Corp.
AL3-15
5200 N.E. Elam Young Pkwy.
Hillsboro, OR
USA

Thomas Francis
IBM France
224 blvd. John Kennedy
Corbeil, Essonnes
91105 France

Rick Garfunkel
Rutgers University
Dept. of Chemistry
P.O. Box 939
Piscataway, NJ 08855
USA

Andrew Gilicinski
Air Prod. & Chemicals Inc.
7201 Hamilton Blvd.
Allentown, PA 18195
USA

Anthony Gonzales
Motorola SPS
2200 W. Broadway Rd.
Mesa, AZ 85202
USA

Joseph Griffith
AT&T Bell Labs
Rm. 6F225
Murray Hill, NJ 07974-0636
USA

P. Chris Hammel
Los Alamos National Lab.
MTL-10 MS K764
Los Alamos, NM 87545
USA

Douglas Hansen
MOYTEK
452 W. 1260 N.
Orem, UT 84057
USA

Karl Harris
Topometrix
5403 Betsy Ross Dr.
Santa Barbara, CA 95054
USA

Rama Hegde
Motorola Inc.
3501 Ed Bluestein Blvd.
P.O. Box 6000
Austin, TX 78762
USA

Lou Ann Heimbrook
AT&T Bell Labs
2525 N. 12th St.
Rm. 30-1-Ma9
Reading, PA 19612-3566
USA

David Henderson
Burleigh Instruments, Inc.
Burleigh Park
Fishers, NY 14453
USA

Rob Hershey
SEMATECH/Motorola Inc.
2708 Montopolis Dr.
Austin, TX 78741-6499
USA

Dan Hirleman
Arizona State University
College of Eng. and Applied Science
Tempe, AZ 85287
USA

J. E. Houston
Sandia National Labs
Org. 1114
P.O. Box 5800
Albuquerque, NM 87185-0344
USA

Steve Hues
NRL
Code 6170
4555 Overlook Ave., S.W.
Washington, DC 20375-5000
USA

Howard Huff
SEMATECH
2706 Montopolis Dr.
Austin, TX 78741
USA

Thomas Jay
Veeco Instruments Inc.
Terminal Dr.
Plainview, NY 11803
USA

Mathew Johnson
IBM Forschungslab Zurich
Saumerstrasse 4
8803 Ruschlikon
Switzerland

Ronald Kee
Hewlett Packard
ICBD
1050 N.E. Circle Blvd.
Corvallis, OR 97330-4299
USA

David Keller
University of New Mexico
Dept. of Chemistry
Albuquerque, NM 87131
USA

Michael Kirk
Park Scientific Instruments
1171 Borregas Ave.
Sunnyvale, CA 94089
USA

Daniel Koleske
NRL
Code 6177
Washington, DC 20375-5342
USA

Joseph Kopanski
NIST
Bldg. 225, Rm. A305
Gaithersburg, MD 20899
USA

Mark Lagerquist
IBM Burlington
D/B57 B/967-1
1000 River Rd.
Essex Jct., VT 05452-4299
USA

Larry Larson
SEMATECH
2706 Montopolis Dr.
Austin, TX 78741-6499
USA

Eric Liu
The Gillette Company
One Gillette Park
Boston, MA 02127
USA

Henry Luftman
AT&T Bell Labs
9999 Hamilton Blvd.
Bremigsville, PA 18031
USA

Phillipe Maillot
SEMATECH
2706 Montopolis Dr.
Austin, TX 78703
USA

Igor Malik
MEMC Elect. Materials Inc.
MZ 33, P.O. Box 8
501 Pearl Dr.
St. Peters, MO 63376
USA

David Mansur
Optra, Inc.
461 Boston St.
Topsfield, MA 01983
USA

Herschel Marchman
AT&T Bell Labs
Rm. 7E-411
600 Mountain Ave.
Murray Hill, NJ 07974
USA

R. B. Marcus
New Jersey Inst. of Tech.
Dept. of Elect. Eng.
University Heights
Newark, NJ 07101
USA

Dave Martin
University of Michigan
Dept. of MS & E
H.H. Dow Bldg., Rm. 2022
Ann Arbor, MI 48109-2136
USA

Yves Martin
IBM Yorktown
Thomas J. Watson Ctr.
P.O. Box 218
Yorktown Heights, NY 10598
USA

Thomas McWaid
NIST
Bldg. 220, Rm. A117
Gaithersburg, MD 20899
USA

Gregory Meyers
Dow Chemical Company
Analytical Sciences
1897F Bldg.
Midland, MI 48667
USA

John Moreland
NIST
Supercond. & Mag. Meas.
325 Broadway
Boulder, CO 80303
USA

Thomas Neal
MRL/DOD
9231 Rumsey Rd.
Columbia, MD 21045
USA

Gabi Neubauer
Intel Corp.
SC2-24 P.O. Box 58119
3065 Bowers Ave.
Santa Clara, CA 95052-8119
USA

Sang-il Park
Park Scientific Instruments
1171 Borregas Ave.
Sunnyvale, CA 94089
USA

Gopal Pingali
University of Michigan
1101 Beal Ave.
Ann Arbor, MI 48109-2110
USA

Greg Poirer
NIST
Bldg. 222, Rm. A313
Gaithersburg, MD 20899
USA

Cedric Powell
NIST
Bldg. 222, Rm. B248
Gaithersburg, MD 20899
USA

J. Jerry Prochazka
VLSI Standards, Inc.
2660 Marine Way
Mountain View, CA 94043
USA

Ruby Raheem
Advanced Micro Devices
MS 32, One AMD Pl.
P.O. Box 3453
Sunnyvale, CA 94086
USA

Tom Remmel
Motorola, Inc.
MD M350
2200 W. Broadway
Mesa, AZ 85202
USA

Robert Reway
Optex Communications Corp.
2 Research Ct.
Rockville, MD 20850
USA

Paul Rice
NIST
MS 814.05
325 Broadway
Boulder, CO 80303
USA

Alexana Roshko
NIST
MS 814.05
325 Broadway
Boulder, CO 80309
USA

Rebecca Rynders
Air Prod. & Chemicals, Inc.
7201 Hamilton Blvd.
Allentown, PA 18195-1501
USA

Huub Saleminck
IBM Forschungslab Zurich
Saumerstrasse 4
8803 Ruschlikon
Switzerland

Amin Samsavar
Burleigh Instruments, Inc.
Burleigh Park
Fishers, NY 14453
USA

Joyce Sapjeta
AT&T Bell Labs
Rm. 1A-142
600 Mountain Ave.
Murray Hill, NJ 07974
USA

Jason Schneir
NIST
Bldg. 220, Rm. A107
Gaithersburg, MD 20899
USA

Gerry Scilla
IBM
D324, 967-2
Essex Junction, VT 05452
USA

David Seiler
NIST
Bldg. 225, Rm. A305
Gaithersburg, MD 20899
USA

C. K. Shih
Univ. of Texas - Austin
Dept. of Physics
RLM 5.208
Austin, TX 78712
USA

Rick Silver
NIST
Bldg. 220, Rm. A107
Gaithersburg, MD 20899
USA

Bhamwar Singh
Advanced Micro Devices
M/S 79
901 Thompson Pl.
Sunnyvale, CA 94088
USA

T. S. Sriram
Digital Equipment Corp.
77 Reed Rd.
MS HL02-3/J9
Hudson, MA 01749
USA

Yale Strausser
Digital Instruments, Inc.
520 E. Montecito St.
Santa Barbara, CA 93103
USA

Timothy Stultz
Veeco Instruments
1323 Martin Ave.
San Jose, CA 95126
USA

Dennis Swyt
NIST
Bldg. 220, Rm. A107
Gaithersburg, MD 20899
USA

Clayton Teague
NIST
Bldg. 220, Rm. A119
Gaithersburg, MD 20899
USA

D. J. Thomson
University of Manitoba
Dept. of Elect. and Comp. Engineering
Winnipeg, Manitoba R3T 5V6
Canada

Ruth Ellen Thomson
NIST
Div 814.05
325 Broadway
Boulder, CO 80303
USA

Steven Weinziero
Solid State Measure, Inc.
110 Technology Dr.
Pittsburgh, PA 15275
USA

Paul West
Topometrix

K. L. Westra
University of Manitoba
Dept. of Elect. and Comp. Engineering
Winnipeg, Manitoba, R3T 5V6
USA

Robb White
Columbia University
530 W. 120th St.
Rm. 1001
New York, NY 10027-6601
USA

Clayton Williams
University of Utah
Dept. of Physics
302 JFB
Salt Lake City, UT 84112
USA

Li Zhou
Topometrix
5403 Betsy Ross Dr.
Santa Clara, CA 95054
USA